
UNIVERSITÀ DEGLI STUDI DI MILANO

***Scuola di Dottorato in Scienze Biologiche e Molecolari***

XXVIII Ciclo

# Vessel associated progenitor cells as a cell-based approach to treat Cystic Fibrosis disease

**C. Vezzali**

PhD Thesis

**Scientific tutor: Prof.ssa Graziella Messina**

Academic year: 2014-2015

SSD: [BIO/10; BIO/11]

Thesis performed at the Department of Biosciences of Università degli Studi di Milano and at the Section of Respiratory Medicine of the Department of Pedriatics of Yale University, School of Medicine.

# CONTENTS

# PART I

During the first year of my PhD I contributed to a work that I started in the internship of my Master of Science, about the role of the transcription factor Nfix in muscle regeneration. The results of this project have been recently published on Cell Reports. This work addressed the role of the transcription factor Nfix during muscle regeneration upon injury. Indeed, we demonstrated that Nfix regulates the proper temporal progression of muscle regeneration through the modulation of Myostatin, a well-known inhibitor of muscle growth and regeneration (Rossi et al. 2016, Part II).

In the meantime, I started to work on my PhD project about the possible use of Mesoangioblasts as a therapeutic tool to cure Cystic Fibrosis disease. The data obtained are now collected in a manuscript in preparation (Vezzali et al., in preparation, Part III).

## ABSTRACT

Cystic Fibrosis (CF) is the most common autosomal recessive genetic disorder in Caucasian population. It is caused by mutations in the gene that encodes for the cystic fibrosis transmembrane conductance regulator (CFTR) protein, which functions mainly as anion channel and is primarily expressed in the apical membrane of secretory epithelia. Lung disease, characterized by airway obstruction, inflammation and bacterial infection is the leading cause of death. At variance with some pharmacological approaches, no efficacious gene and cell therapy have been proved to date. Advances in the application of stem cells have generated hope that, by the use of this new potential tool, it will be possible to provide therapeutic treatments for CF, where current therapies are still inadequate. Our laboratory worked for several years on mesoangioblasts (MABs), blood vessel-associated progenitor cells that can differentiate into different mesoderm cell types. When delivered in the arterial circulation, MABs cross the vessel wall and participate to skeletal muscle regeneration, ameliorating signs of Muscular Dystrophies in different pre-clinical animal models. For these reasons they have been used in a trial in human patients that definitely demonstrated that the transplantation of donor MABs in humans is feasible and safe. During studies on MABs isolated from adult mouse skeletal muscle (mMABs) we observed that, when systemically transplanted in healthy, wild type mouse model, mMABs surprisingly engraft lung, tracheal and intestinal epithelium up to one month from a single transplantation trough the caudal vein. Due to this striking evidence, included MAB capability to express CFTR, we proposed to investigate on a possible use of MABs as a therapeutic tool for CF disease. In this work we present strong evidence that the transplantation of mMABs in two different CF mouse models leads to a rescue of CF phenotype. We demonstrated that mMABs engraft the respiratory and the intestinal epithelium in CF mice up to six months from their single transplantation, leading to a functional rescue of CFTR-dependent chloride current. Notably, once engrafted in the epithelium, mMABs express typical epithelial markers, revealing an unexpected and powerful relevant ability of MABs to differentiate into epithelial cells, thus contributing to airways and intestine homeostasis and biology. Overall, these data demonstrate that MABs are eligible for a cell-based therapy of CF.

# STATE OF THE ART

## 2.1 Cystic Fibrosis

Cystic fibrosis (CF), caused by mutations in the *cystic fibrosis transmembrane conductance regulator* (*CFTR*) gene, is a multi-organ disease that affects the upper and lower airways, gastrointestinal and reproductive tracts and the endocrine system (Davis 2006; Riordan et al. 1989; Cutting 2015; Rowe et al. 2005). CF is one of the most common lethal autosomal-recessive disorders in Caucasian population (Welsh et al., 2001); it is also well described, albeit at lower frequencies, in African American, Hispanic, and Middle Eastern ethnicities (WHO/ECFTN 2004). The prevalence for CF is approximately 1 in 30 in the United States, with a birth rate of approximately 1 in 3,500 and 1 in 2500 in the European Union (Farrell 2008; R.S. Pettit; C. Fellner 2014). Globally, more than 70,000 people are currently affected by CF, with the widest number of identified patients in the United States (≈ 30,000 in 2012) and Europe (≈ 32,000 in 2010) (Anon 2014; Zolin et al. 2014).

The *CFTR* gene encodes for a cAMP-dependent chloride ($Cl^-$) channel expressed in secretory epithelia of the body and, at lower levels, in other cell types such as alveolar type II cells (Bove et al. 2010), immune cells (Bruscia et al. 2009; Sorio et al. 2011), smooth and skeletal muscle cells (Divangahi et al. 2009; Vandebrouck et al. 2006) and neurons (Niu et al. 2009). Although CFTR functions mainly as a chloride ion channel, it has numerous other regulatory roles, including the inhibition of sodium transport through the epithelial sodium channel (ENaC), the regulation of the externally rectifying chloride channels, the acidification of intracellular organelles, the regulation of ATP channels and of intracellular vesicle transport and the inhibition of endogenous calcium-activated chloride channels (Reisin et al. 1994; Schwiebert et al. 1995; Stutts et al. 1995; Vankeerberghen et al. 2002; Mehta 2005); moreover, CFTR is also involved in bicarbonate–chloride exchange that is important for the correct solubility of luminal mucins (Quinton 2008).

Lack of functional CFTR expression at the apical membrane of secretory epithelia leads to defective chloride and bicarbonate secretion, associated to enhanced sodium absorption and mucus secretion, which in airway epithelia provokes dehydration and acidification of the airway surface liquid (Tarran et al. 2001; Derichs et al. 2011; Chen 2010; Pezzulo 2012). As a consequence, impaired mucociliary clearance causes continuous infection and uncontrolled inflammation culminating in

lung failure, which is the primary cause of morbidity and mortality in CF (Ratjen & Döring 2003; Boucher 2007).

The clinical features of CF were first described by Dorothy Andersen in 1938 (Andersen 1938), and the term Cystic Fibrosis was chosen to describe the fibrotic aspect of the cystic dilatations that characterize the pancreas of affected individuals. Although ten years later it was clear that the pathology was caused by a single gene defect because of its autosomic recessive inheritance, the high mortality did not allow genetic studies. Moreover, it was also difficult to understand which was the most affected tissue, since CF is a multi-organ disease. Recognition of other symptoms characteristic of CF and their connection to mortality was also well reported before the twentieth century. Efforts to isolate the involved gene, localized it to chromosome 7 by the mid-1980s (Rommens et al. 1988) and the *CFTR* gene was finally sequenced in 1989 (Kerem et al. 1989; Riordan et al. 1989; Rommens et al. 1989). Afterwards, the identification of CFTR mutations has been extensive, with 2,006 known mutations described to date, both disease causing and benign (http://www.genet.sickkids.on.ca). For many of the identified mutations, the disease cause is unknown, but efforts are under way to assess their functional consequence and pathological severity (www.cftr2.org; Sosnay et al. 2014). The Clinical and Functional Translation of CFTR (CFTR2) project had collated data of common and uncommon mutation and phenotype from 88,664 patients as of August 2015 (www.cftr2.org).

CFTR is member of the ATP-binding cassette subfamily C (ABCC7) (Kerr 2002) and consists of two homologous halves, each containing a hexa-helical transmembrane domain (TMD1 and TMD2) and a nucleotide-binding domain (NBD1 and NBD2) that are connected by an unstructured regulatory domain (R domain) (Figure 1) (Riordan 1993; Riordan et al. 1989; Vankeerberghen et al. 2002).

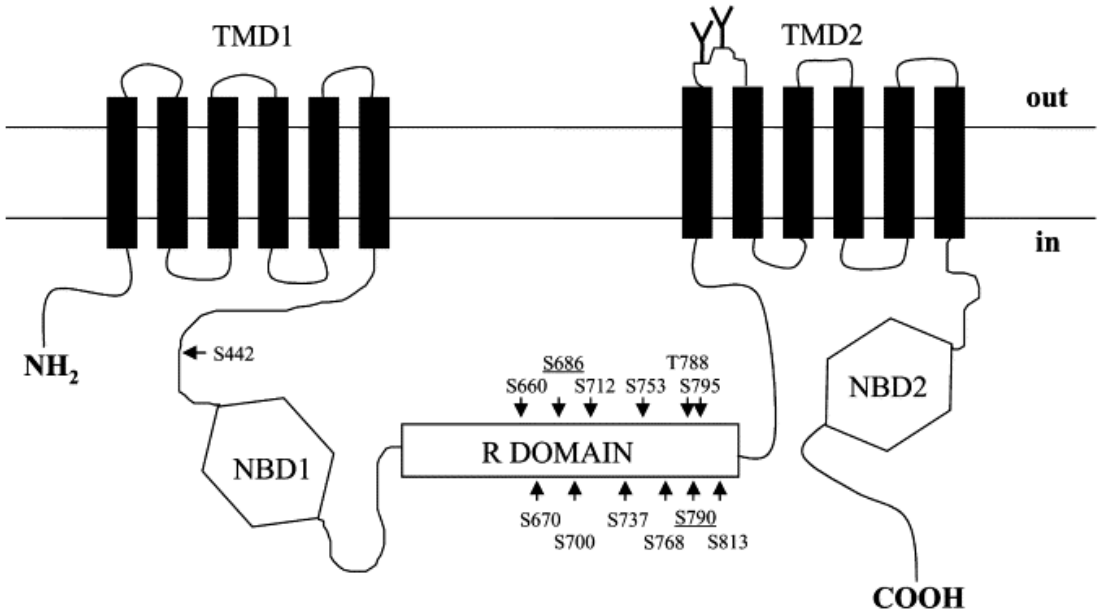


**Figure 1: Schematic representation of the CFTR channel (from Vankeerberghen et al. 2002).** The different domains, transmembrane domain 1 (TMD1) and 2 (TMD2), nucleotide binding domain 1 (NBD1) and 2 (NBD2), the regulatory domain (R), the N-terminal ($NH_2$) and C-terminal (COOH) ends, the PKA (arrowhead) and PKC (arrowhead and underlined) consensus sites and the glycosylation sites present on the fourth extracellular loop are highlighted.

CF wide range of disease severity is even influenced by modifier genes (Joseph M. Collaco & Cutting 2008; Cutting 2010) and also by the environmental and socioeconomic status of affected individuals (Schechter et al. 2001; Barr et al. 2011; Kopp et al. 2015). The identification of modifier-gene polymorphisms might lead to more precise prediction of the course of disease: the gene products could become therapeutic targets. Welsh and Smith proposed the first classification of CF mutations into four classes, according to their primary biological consequence, in 1993 (Welsh & Smith 1993). To date, six major classes are distinguished (Zielenski & Tsui 1995) (Figure 2).

Class I encloses frameshift, splicing, or nonsense mutations that introduce premature stop codons, resulting in seriously reduced or absent CFTR expression.

Class II mutations provoke misfolding, premature degradation by the endoplasmic reticulum (ER) quality-control system, and impaired protein transduction, sorely reducing the number of CFTR molecules that reach the cell membrane.

Class III mutations damage the regulation of the CFTR channel, resulting in abnormal gating characterized by a reduced open chance.

Class IV mutations impair the channel conductance by impeding the ion conduction pore, causing a reduced conductance (Sheppard et al. 1993; Hammerle et al. 2001).

Class V mutations do not change the conformation of the protein but alter its abundance by introducing promoter or splicing abnormalities (Highsmith et al. 1997; Zielenski & Tsui 1995).

Class VI mutations reduce CFTR conformational stability by destabilizing the channel in post-ER compartments and/or at the plasma membrane level. This results in accelerated turnover and reduced protein expression (Haardt et al. 1999; Silvis et al. 2003).

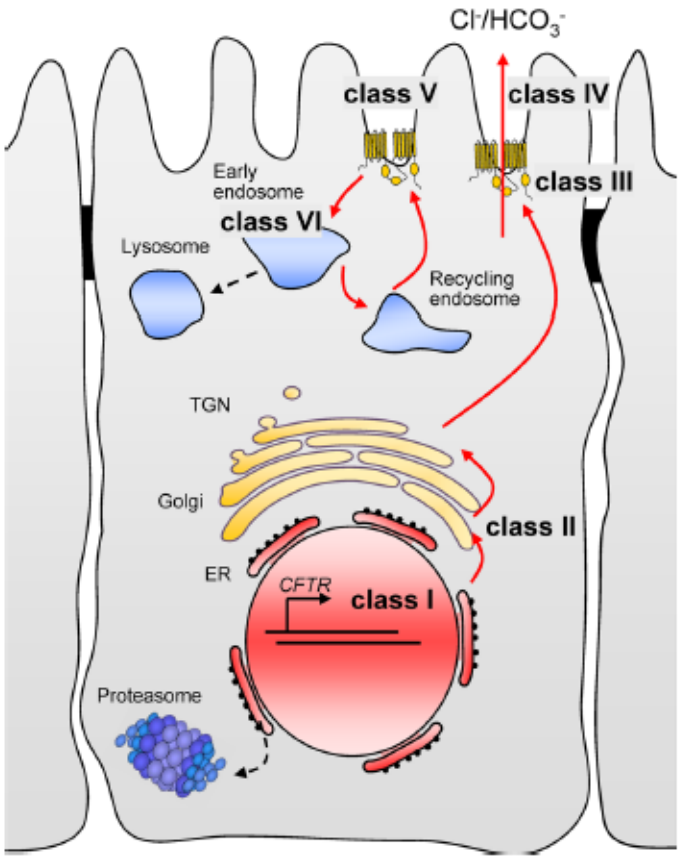


**Figure 2: Traditional classification of CF mutations based on their cellular phenotype (from Veit et al. 2016).** Class I: protein synthesis defect; class II: maturation defect; class III: gating defect; class IV: conductance defect; class V: reduced quantity and class VI: reduced stability (ER, endoplasmic reticulum; TGN, trans-Golgi network).

The most common mutation is the *F508del (Phe508del)* that occurs in about 70-90% of CF patients in Northern Europe and North America (Bobadilla et al. 2002). This mutation belongs to class II and is due to a deletion of the three nucleotides that comprise the codon for phenylalanine (F) at position 508. *F508del* impairs CFTR conformational maturation and causes its targeting for premature ER-associated degradation (Cheng et al. 1990; Cyr 2005; Kim & Skach 2012; Lukacs et al. 1994). However, *F508del-CFTR* proteins that either constitutively or following rescue procedures evade the ER quality control and accumulate at the plasma membrane (PM) exhibit a channel-gating impairment, which is a characteristic of class III mutations (Dalemans et al. 1991), as well as accelerated turnover in post ER compartments and at the PM, a class VI mutation hallmark (Lukacs et al. 1993). Unless the folding and conformation of the rescued *F508del-CFTR* are fully restored to that of the wild type protein by pharmacological therapy, this mutation remains partially defective and requires correction of its gating and/or stability impairment. In conclusion, the most common mutant has multiple defects that extend beyond the characteristics of a class II mutation. The observed pleiotropic molecular defects caused by single mutations led to the suggestion of a modification of the traditional classification scheme (Veit et al. 2016). This expanded classification of the major mechanistic categories (Welsh & Smith 1993) holds the unusually complex, combinatorial molecular/cellular phenotypes of CF alleles. It consists of 31 possible classes of mutations, including the original ones, as well as their 26 combinations, as shown in the Venn diagram in Figure 3. For example, according to the expanded scheme, *F508del* will be classified as class II–III– VI, reflecting the composite defects in mutant CFTR biology.

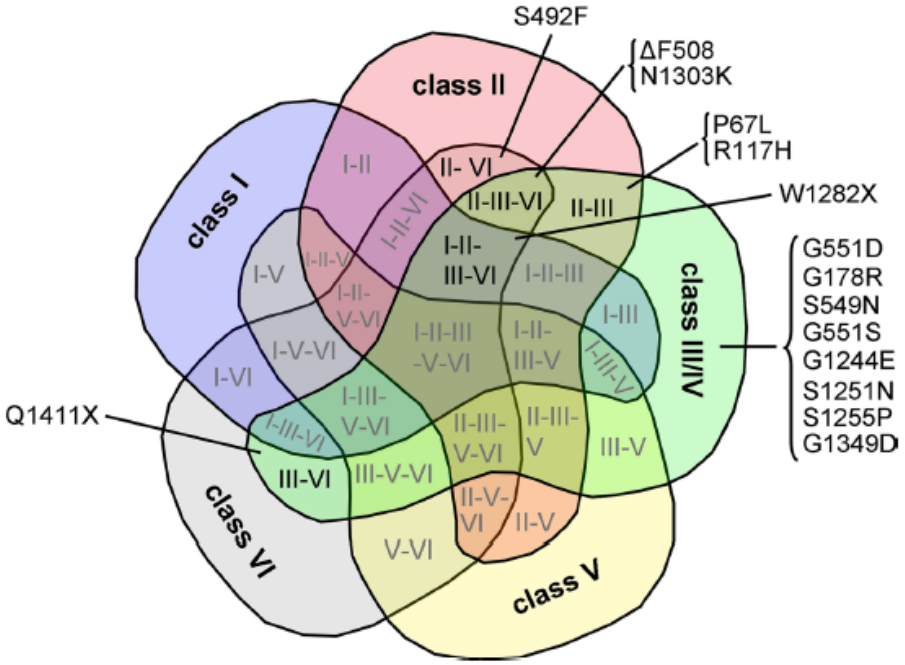


**Figure 3: Expanded classification of CF mutations accounting for complex phenotypes of major CFTR cellular defects (from Veit et al. 2016).** The Venn diagram indicates all combinations of mutation classes with selected examples. Possible combinations without identified mutation are indicated in gray.

CF-related symptoms occur throughout life, with strong overlap and variability of symptoms and timing. Figure 4 shows the indicative age of onset of some of the major clinical complications and secondary symptoms of the pathology.

The lungs of CF children seem normal at birth, but quickly become infected and inflamed, with polymorphonuclear cells found in bronchoalveolar lavage fluid obtained from even healthy-looking kids (Khan et al. 1995). Chronic airway infection, progressing to bronchiectasis, gas trapping, hypoxaemia, and hypercarbia are the signs of CF lung phenotype; pulmonary insufficiency is finally responsible for at least 85% of CF-related deaths (Flume et al. 2007). Typically, CF infants are quickly colonized by Haemophilus influenzae or Staphylococcus aureus, or even both. Rapidly, Pseudomonas aeruginosa becomes the predominant organism present in the airways (Rosenfeld et al. 2003; Burns et al. 2001). Prolonged infection causes the generation and secretion of chemotactic agents, which recruit large numbers of polymorphonuclear cells into the airways. Pseudomonas aeruginosa enhances the cycle of infection and inflammation with the release of toxins and elastases that

cleave crucial surface markers on polymorphonuclear cells. These cells then release their own proteases and elastases that damage any viable polymorphonuclear cells in the proximal area (Hartl et al. 2007). Thereafter, begins a vicious circle that leads to increased tissue damage. Furthermore, the release of DNA from senescent polymorphonuclear cells causes increased sputum viscosity (Chernick, Barbero 1959). There is an evident survival benefit for those patients who remain free of Pseudomonas infection (Konstan et al. 2007; Kosorok et al. 2001). Also mycobacteria and fungi are sometimes found in airway secretions from CF individuals.

Around 15% of CF infants are born with meconium ileus, an obstructive condition secondary to thicken material in the small and large bowels. Moreover, 85–90% of CF infants develop pancreatic insufficiency, which can be present already at birth or evolve after the first year of life. Pancreatic insufficiency provokes steatorrhoea, fat-soluble-vitamin deficiency and malnutrition. Pancreatic dysfunction is provoked by obstruction of intra-pancreatic ducts with thickened secretions. In time, the pancreas undergoes autolysis with the replacement of the normal body of the pancreas with fat. When a certain percentage of islet cells are impaired, the CF patient will develop insulin insufficiency and carbohydrate intolerance, possibly coexisting with insulin resistance (Marshall et al. 2005; Elder et al. 2007). CF-related diabetes mellitus (CFRD) is not the same as typical type I or type II diabetes mellitus; multiple factors typical of CF affect glucose metabolism, including increased energy expenditure, acute and chronic infection, glucagon deficiency, liver dysfunction, decreased intestinal transit time, and increased work of breathing (Marshall et al. 2005). Up to 30% of CF patients aged over 25 years are reported to have this secondary consequence; notably, female patients with diabetes have poorer survival chances than male patients (Milla et al. 2005).

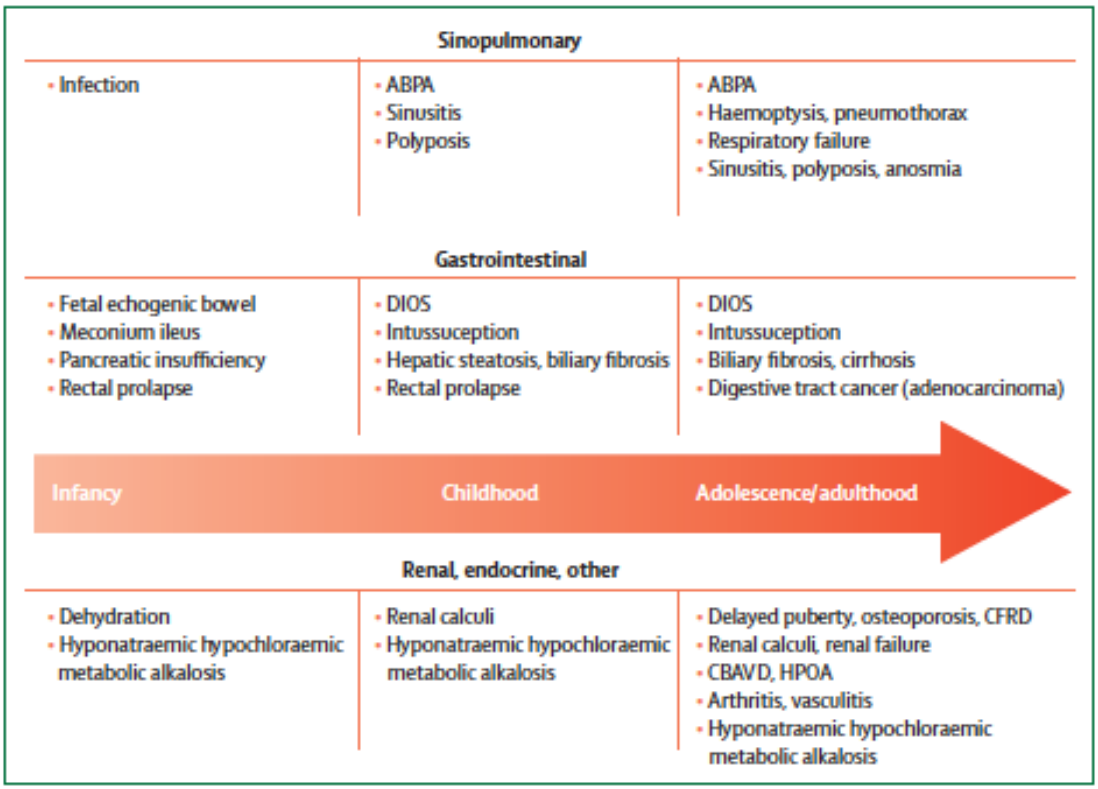


**Figure 4: Approximate age of onset of clinical manifestations of CF (from O'Sullivan & Freedman 2009).**

ABPA= allergic bronchopulmonary aspergillosis. CBAVD= congenital bilateral absence of the vas deferens. CFRD= CF-related diabetes mellitus. DIOS= distal intestinal obstruction syndrome. HPOA= hypertrophic pulmonary osteoarthritis.

When CF was first identified, the life expectancy of affected individuals was only months: death was indeed caused by malnutrition (Andersen 1938). By administrating pancreatic enzyme replacement therapy, malnutrition became manageable; however, adequate caloric assumption and correction of fat-soluble-vitamin deficiencies still remain crucial aspects of disease control (Borowitz et al. 2002). Thickened intestinal secretions, malabsorption, and decreased gut motility can cause distal intestinal obstruction or chronic constipation in older affected individuals (Wilschanski & Durie 2007). Impaired absorption of fat-soluble vitamins (A, D, E, and K) can induce acrodermatitis, anemia, neuropathy, night blindness, osteoporosis, and bleeding disorders. The obstruction of intrahepatic bile ducts could even cause focal biliary cirrhosis, which occurs in only about 5% of patients (Wilschanski & Durie 2007). Osteoporosis secondary to vitamin D deficiency, chronic inflammation, and intermittent corticosteroid use is increasingly being identified as a CF complication.

Osteopenia starts in childhood, but generally comes out in adulthood. Finally, the vas deferens is very susceptible to CFTR dysfunction. Virtually all CF male patients have azoospermia and are infertile because of congenital bilateral absence of the vas deferens (Boyle 2003; Yankaskas et al. 2004). On the contrary, CF female patients are fertile. Although pregnancy in CF is a debated issue, the consensus is that a woman who has adequate nutritional and pulmonary resources can successfully complete the term of pregnancy (McMullen et al. 2006).

### 2.2 Therapies for Cystic Fibrosis

From the first formal description of Cystic Fibrosis, advances in symptom-based treatments have led to consistent improvements in outcomes; these also include the development of CF care centers. Despite the multiple and serious consequences associated with CF, life expectancy has strongly increased over the past decades. In 1938, 70% of CF patients died before 1 year of age (Andersen 1938). With the systematic application of evidence-based therapies, the US median predicted survival rose from ~31 years in 2002 to ~41 years as of 2013 (Anon 2014). Treatments aiming to improve CF pulmonary disease are the most numerous and various and can be broadly classified as airway clearance treatments (both mechanical and pharmacologic), antibiotics, and anti-inflammatories.

Dornase-α helps to decrease excess DNA present in cellular debris and the mucus of chronically inflamed airways and has demonstrated benefit in CF patients with both mild and moderate-to-severe pathology (Goss et al. 2007; Mogayzel et al. 2013), improving lung function and reducing the incidence of pulmonary infections. Hypertonic saline improves airway hydration and thus increases mucociliary clearance (Donaldson et al. 2006). Although less studied, 7% hypertonic saline has been shown to ameliorate lung function and provide strong benefits on pulmonary exacerbations, reducing the incidence by nearly 50% compared with saline-treated controls (Elkins et al. 2006). Both dornase-α and hypertonic saline are strongly recommended for CF individuals beginning in childhood (Donaldson et al. 2006; Mogayzel et al. 2013). These treatments are effective but challenging, and Sawicki et al. (Sawicki et al. 2009) have estimated that CF patients spend about two hours daily on routine treatments. The Pseudomonas aeruginosa bacterium frequently infects CF individuals, with increased prevalence with age (Cystic Fibrosis Foundation 2012).

Colonization with Pseudomonas (particularly mucoid strains) is directly associated with a faster decline of pulmonary function (Emerson et al. 2002). For this reason, antibiotic therapy directed toward Pseudomonas has been widely studied for chronic infections. Inhaled tobramycin has been available for more than 15 years and is currently extensively used, with a strong recommendation to treat chronic Pseudomonas infection (Flume et al. 2007). Inhaled aztreonam lysinate used in a cycled treatment also ameliorates lung function and decreases the incidence of pulmonary Pseudomonas infections (Mogayzel et al. 2013). In addition to Pseudomonas, typically antibiotic-resistant pathogens such as Burkholderia cepacia, Achromobacter, Stenotrophomonas, and nontuberculous mycobacteria as well as fungal infections with Aspergillus can be dangerous in a minority of individuals, requiring specialized treatments that can be associated with drug toxicities. Anti-inflammatory therapy has also been investigated in CF application, including macrolide antibiotics and non-steroidal anti-inflammatory drugs. The medications that have been analyzed in large controlled trials in CF include azithromycin (a macrolide antibiotic, although its chronic application in CF is for its ability to reduce neutrophilic inflammation) and ibuprofen (Konstan et al. 1995; Lands et al. 2007; Saiman et al. 2012; Saiman et al. 2003). Azithromycin decreases pulmonary exacerbations and improves weight and lung function in patients chronically infected with Pseudomonas. Ibuprofen taken twice daily reduces the decline in lung function and is most effective in pediatric CF patients. Potential renal toxicity can be a concern with high-dose ibuprofen administration, combined with other nephrotoxic medications and this can be a problem in the setting of aminoglycoside antibiotics (Kovesi et al. 1998).

Lung transplantation still remains the final therapeutic option for patients with end-stage lung pathology. Transplantation has the potential to extend and substantially ameliorate quality of life in properly selected CF individuals. How best to identify patients, especially children, for this high-risk intervention is the subject of active debate (Egan 2008; Aurora et al. 2008; Liou et al. 2007). In Europe, it is unusual for CF children to be considered for transplantation, unless they have an expected life survival of less than 2 years, despite maximum medical treatment. 5-year survival post transplant for children is less than 50%, with poorly better results in adults (50% of recipients are alive 6 years post transplant) and many problems associated with the required lifelong immunosuppression (Goldberg & Deykin 2007; Trulock et al. 2007).

However, age, sex and lung infection influence the decision. The presence or absence of certain pathogens can affect outcome and should be taken into account when choosing lung transplant candidates (Murray et al. 2008).

Therapies throughout the last decade targeted also the downstream manifestations that develop as a consequence of CFTR dysfunction. Pancreatic insufficiency is treated with enzyme replacement therapy together with strict monitoring of growth and nutritional parameters, with caloric and nutrient supplementation if needed (Borowitz et al. 2002; Stallings et al. 2008). Importantly, with the introduction of universal newborn screening for CF in the United States, severe malnutrition is often avoided. The clinical path of children identified by newborn screening is better than that of patients diagnosed by clinical manifestations, and improved nutrition in childhood is directly associated with better growth and future adult lung function (Borowitz et al. 2009; Lai et al. 2005).

### 2.2.1 Animal models

Since the discovery of CF genetic cause, researchers have tried to identify a suitable animal model to study the disease progression and to test potential therapies. A frustrating issue of CF research has been the lack of a good animal model for recapitulating all the aspects of the disease. Unfortunately, the murine models created by targeted mutations in the *CFTR* gene typically show severe digestive/intestinal defect but do not exhibit the pathological abnormalities in the nasal airways and lungs observed in human CF patients, making them scarce surrogates to study pulmonary treatments (Grubb & Boucher 1999; Guilbault et al. 2007). Although important information has been obtained using CF mouse models, these mice do not allow a reliable prediction of potential therapeutic approaches in humans. The help of organ-specific conditional CFTR ablation could facilitate the generation of new, clinically relevant and research-friendly mouse models of CF (Murphy and Atala 2013). Larger animal models to study CF and its related potential therapies have been developed with pig and ferret. Rogers et al. (Rogers et al. 2008) by gene-targeting techniques, generated $CFTR^{-/-}$ pigs and confirmed a lack of functional CFTR by electrophysiological methods. These CF piglets show at birth severe meconium ileus, requiring surgical intervention; moreover their lungs and airways are histopathologically normal but develop lung disease within the first few months of life (Rogers et al. 2008). Furthermore, upon bacterial infection, $CFTR^{-/-}$ pigs fail to

effectively kill bacteria, suggesting a defective innate immune response, a characteristic aspect of the human CF phenotype, showing also airway wall thickening and mucus plugging (Stoltz et al. 2010). Ongoing studies are examining whether these porcine models will go on to develop spontaneous infections and CF-like lung pathology over time.

Human-like airway morphology and cell populations make the ferret a potential model to study CF lung disease. Engelhardt et al. (Engelhardt et al. 1995) have used recombinant adeno-associated virus-mediated gene targeting and nuclear transfer cloning to generate a $CFTR^{-/-}$ ferret. These animals are characterized by a phenotype similar to the porcine model, with intestinal defects causing severe perinatal mortality in newborns. Strikingly, $CFTR^{-/-}$ ferrets exhibit evidence of lung infections and defects in bacterial clearance early in life, (Sun et al. 2010). These newborn CF ferrets also show impaired endocrine pancreas function, characterized by abnormal glucose responsiveness of the islet to secrete insulin (Olivier et al. 2012). These observations suggest that the CF ferret model could also be useful to understand the development of CF-related diabetes (CFRD) in human patients. Because of the severity of the meconium ileus defect in CF ferrets, this group developed a **"**gut-corrected**"** ferret model expressing wild type CFTR only in intestinal epithelia, thus avoiding the severe meconium ileus, while maintaining the clinically important lung phenotype that is predominant in CF human individuals. Another advantage of the CF ferret is that ferrets are much easier to breed than piglets. These new animal models will help to complement studies in $CFTR^{-/-}$ mice and allow more detailed studies less reliable in mice.

### 2.2.2 Gene and DNA-editing therapies

During the last decades, major efforts employed by numerous groups tried to develop gene replacement approaches to provide CF patients with normal, functional CFTR. It should indeed be possible to treat an autosomal recessive disorder such as Cystic Fibrosis with the insertion of one copy of wild type functioning DNA into the affected cells. Such a treatment should be effective independent of patients' CFTR mutations. Although easy in concept, in practice gene therapy has demonstrated to be quite difficult. Armstrong et al. (Armstrong et al. 2014) have described historical approaches to CF gene therapy. Several challenges exist, most importantly the efficient delivery of transgenes and host inflammatory response (Knowles et al. 1995;

Konstan et al. 2004; Moss et al. 2007; Ruiz et al. 2001; Zabner et al. 1993; Welsh et al. 1994). The first gene therapy approaches with adenovirus vectors proved to be unsuitable because of immunogenicity and low efficiency of viral vectors to insert DNA into epithelial cells (Crystal et al. 1994; Joseph et al. 2001; Pickles 2004). Adeno-associated viruses (AAV) and liposomes have been proposed as potential vectors. Flotte and colleagues (Flotte et al. 2005) have demonstrated a physiological correction of chloride secretion in nasal epithelial cells from recombinant AAV-serotype-2 CFTR gene therapy recipients, even in those with low CFTR mRNA expression. Unfortunately, a phase IIb trial of repeated administrations of aerosolized AAV CFTR did not give significant amelioration in spirometric values (Moss et al. 2007). Moreover, concerns still remain about toxicity, and immunological responses to repeated doses of this vector (Tosi et al. 2004). The UK Cystic Fibrosis Gene Therapy Consortium has pointed the attention to develop non-viral vectors for gene transfer (Griesenbach et al. 2006). The phase II study dosed 62 placebo and 78 active drug patients (over 12 years of age) in a randomized, double-blind, placebo-controlled 12 months trial. The results showed stabilization of spirometric values over a one-year period in subjects receiving the lipid-based non-viral vector complexed with plasmid CFTR cDNA versus placebo (Alton et al. 2015). A considerable limitation of gene therapy is that gene delivery has historically been through the airway. For this reason the restoration of wild-type CFTR activity is currently limited to the CF lung. Finally, an ideal gene therapy would aim to intervene early enough to prevent the development of the pathology and to be systemically delivered for targeting CF-affected organs. Despite these challenges, the aim to develop genotype-independent gene therapy that addresses CF lung disease would be a major step to bring CFTR-directed therapy to all CF individuals. For now, however, the prospect of gene therapy remains a hope more than a reality.

Finally, another current idea includes DNA-editing (CRIPR/Cas9) and RNA-editing approaches which could be specifically designed for a patient's particular disease-causing mutation (Montiel-Gonzalez et al. 2013; Schwank et al. 2013).

### 2.2.3 Pharmacotherapy

A different idea took place in the early 2000s: the development of small molecules that target specific protein defects related with CFTR mutations. Obviously these compounds could be effective only for certain patients with specific mutations. This

strategy was possible because of the large knowledge that assigned different CFTR protein defects to single CFTR mutations (Riordan 2008). Agents under investigation are labeled correctors and potentiators. The first class of agents aims to correct one ore more of the defects found in class II mutations by rescuing proteins from ER degradation, improving CFTR trafficking to the cell surface and inhibiting proteins that are involved in CFTR recycling in the cell membrane. The second one has the purpose to potentiate impaired CFTR, which reaches the cell membrane in patients with specific mutations associated with abnormal gating (Van Goor et al. 2009).

VX-770 (ivacaftor) is the first potentiator to be U.S. Food and Drug Administration (FDA) approved for CF application. It directly acts on gating defect of the class III mutation G551D-CFTR (Van Goor et al. 2009). This compound was developed by Vertex Pharmaceuticals in conjunction with Cystic Fibrosis Foundation Therapeutics, Inc. (CFFT), and showed substantial clinical benefit in patients carrying the mutation in either one or two alleles (Van Goor et al. 2009; Accurso et al. 2010; Ramsey et al. 2011). The initial clinical trial of ivacaftor examined patients with at least one G551D mutation and demonstrated both clinically and statistically significant improvements in spirometric values and weight in patients as young as age 6 (Davies et al. 2013; Ramsey et al. 2011). Older patients (over age 12) also showed ameliorations in pulmonary exacerbation frequency (reduced by ≈ 60%) and respiratory symptoms. Biomarkers of CFTR function (sweat chloride levels and nasal potential difference) also improved (Davies et al. 2013; Accurso et al. 2010; Ramsey et al. 2011). Beneficial effects have been demonstrated to persist, with a long-term follow-up trial extending to 144 weeks showing continued benefits (McKone et al. 2014). The approval of VX-770 was also extended to eight additional class III mutations (G178R, S549N, S549R, G551S, G1244E, S1251N, S1255P, and G1349D) (Yu et al. 2012; Vertex Pharmaceuticals Press Release ID857163 2014) and recently to the class IV mutation R117H (Vertex Pharmaceuticals Press Release ID857163 2014).

Multiple correctors were developed using high-throughput screening methods in cells stably expressing *F508del-CFTR*, similar to the techniques used to identify ivacaftor. One such compound VX-809 (lumacaftor), produced by Vertex Pharmaceuticals, has been developed beside ivacaftor. *In vitro* studies showed that lumacaftor improved *F508del-CFTR* maturation and expression at the plasma membrane, increased half-life at the plasma membrane and ameliorated *F508del-CFTR*-mediated chloride

transport (Van Goor et al. 2011). Moreover, the addition of ivacaftor in these models improved activity to nearly 30% that of wild-type CFTR (Van Goor et al. 2011). For this reason, in moving lumacaftor development forward, efficacy studies combined the administration of lumacaftor and ivacaftor.

Class I nonsense mutations are single base substitutions that provoke premature termination codons (PTCs) and lead to a loss of production of full length CFTR. About 10% of CF patients carry in-frame nonsense mutations. However, it is possible to decrease the proofreading fidelity of the ribosomal unit and allow read-through of a PTC, thus resulting in a full-length protein, a phenomenon initially observed with aminoglycoside antibiotics. Studies have demonstrated that aminoglycoside antibiotics obtain this result both *in vitro* and *in vivo* in CF patients (Clancy et al. 2001; Dranchak et al. 2011; Malik, Louise R Rodino-Klapac, et al. 2010; Malik, Louise R. Rodino-Klapac, et al. 2010; Rowe & Clancy 2009; Sermet-Gaudelus et al. 2007; Mendell et al. 2010). Based on this finding, the molecule PTC124 (ataluren) was developed as a non-aminoglycoside compound proposed to induce PTC read-through. After multiple phase II studies (Kerem et al. 2008; Sermet-Gaudelus et al. 2010; Wilschanski et al. 2011; Rowe et al. 2007), Kerem and colleagues (Kerem et al. 2014) recently presented the results of a phase III study of ataluren. Unfortunately, they did not observed ameliorations in nasal potential difference or sweat chloride compared with placebo. A subgroup analysis displayed improvements in spirometric values compared with placebo among patients who were not using inhaled aminoglycoside antibiotics, which appear to interfere with ataluren activity *in vitro*. Investigation of ataluren is currently going on in a phase III trial that specifically excludes individuals using inhaled aminoglycosides (ClinicalTrials.gov ID NCT02107859). Preclinical results obtained in models of human airway epithelia as well as mice expressing the G542X class I mutation have demonstrated that synthetic aminoglycoside derivatives can suppress PTCs and that the resultant CFTR is sensible to augmentation with ivacaftor (Xue et al. 2014).

The efficacy of available therapies for some mutant CF alleles, which have been classified as class I, class II, or class III/IV mutations, is nowadays limited. For this reason, comprehensive mapping of the different molecular defects caused by a single or combination of mutations could offer sensible advantage for improving therapeutic approaches and for the future development of drug combinations. This new approach is called “theratyping” (Cutting 2015) and will lead the way to personalized medicine.

However, the assured prediction of the responsiveness of a mutant phenotype to drug therapy could be challenging and also depends on the used model (Pedemonte et al. 2010). The final goal of theratyping is to obtain an optimal correction of a specific mutant defect by identifying the most efficacious CFTR modulator(s), including correctors(s), potentiator(s), and/or read-through drugs, or, in particular, a combination of these drugs.

### 2.2.4 Cell Therapy

Regenerative medicine is an emerging and quickly evolving field of research and therapeutics. Advances in the understanding and application of stem cell-based therapies have generated hope that, by taking advance of this new powerful tool, researchers will be able to provide effective treatment for CF, where current therapies are still inadequate, at least for the totality of the patients. The idea to use stem cell-derived functional epithelial cells to replace dysfunctional ones in the lungs of CF patients would be a major advance for the cure of CF. Noteworthy, the evaluation of the level of normal CFTR message necessary to provide normal airway/lung function is estimated to be around 8% (Chu et al. 1992; Johnson et al. 1992; Dorin et al. 1996). Furthermore, it has also been reported that the over-expression of CFTR in a minority of cells may fully correct $Cl^-$ transport impairments, through the ability of polarized airway cells to passively equilibrate $Cl^-$ secretions thanks to the intracellular tight junctions (Driskell & Engelhardt 2003). In conclusion, since stem cells are characterized by both extensive self-renewal and differentiation into functional terminal cell types, a therapy that can provide functional lung cells into the CF lung has the potential for long-term restoration of CFTR function in all kind of affected patients. CF is also a potential candidate disease for stem cell therapy because of the persistent lung inflammation that leads to damage and remodeling, which could promote cell engraftment.

Stem cells can play a major role in development of new approaches, such as: the production of differentiated cell lines that could allow researchers to perform *in vitro* disease modeling and drug/toxicity testing; generation of terminally differentiated pulmonary cell types for cell-based therapies to correct CFTR defect and/or to modulate the inflammatory environment of the CF airways and consequently mitigate lung injury; finally, the use of stem cells in combination with lung scaffolds to produce replacement organs for end-stage transplantation (Murphy and Atala 2013).

While the majority of CF research has focused on therapies that target the lung, many of the techniques and strategies could also be suitable for the treatment of other CF-related diseases. CF stem cell lines can be used to improve our knowledge of CF-related diabetes, pancreatic and liver diseases; moreover, cellular therapies may also show efficacy in reducing the inflammation and fibrosis that occur in the pancreatic and hepatobiliary ducts.

In the past decade different groups have examined whether transplanted stem cells can engraft the airways and restore CFTR function in CF animal models. Multiple reports initially suggested that bone marrow-derived cells, including hematopoietic stem cells (HSCs), mesenchymal stem cells (MSCs), endothelial progenitor cells (EPCs), and other populations could structurally integrate as terminally differentiated airway and alveolar epithelial cells or as vascular or interstitial lung cells (Weiss et al. 2011; Kassmer & Krause 2010). Even if bone marrow or adipose-derived MSCs can be induced *in vitro* to express typical markers of alveolar or airway epithelial cells (Sueblinvong et al. 2008), a number of technical issues led to misinterpretation of results in these reports. With new sophisticated approaches, some recent works suggest that engraftment of the airways with several different types of bone marrow-derived cells can occur within a short temporal window (Sueblinvong et al. 2008; Loi et al. 2006; De Paepe et al. 2011; Kassmer et al. 2012). However, the engraftment of lung epithelium, vasculature, or interstitium by exogenously administered donor-stem or progenitor cells is still considered to be a rare phenomenon of poor physiologic or clinical significance (Weiss et al. 2011, Sueblinvong et al. 2008; Loi et al. 2006; De Paepe et al. 2011; Kotton et al. 2005). Whether engraftment can be obtained by intra-tracheal or systemic administration of endogenous lung progenitor cells has not yet been well explored. Loi et al. (Loi et al. 2006) transplanted bone marrow-derived MSCs expressing wild type CFTR into transgenic $CFTR^{-/-}$ mice. CFTR-positive cells were found in the lung epithelium of injected mice; however, the engraftment was a rare event (approximately 0.025%) and functional contribution was not even determined. Poor engraftment of stem cells in the airways has also been observed by Sueblinvong et al. (Sueblinvong et al. 2008) (0.5% at 3 months). The group studied umbilical cord blood (UCB) MSCs engraftment in the airway epithelia after systemic administration to immunotolerant mice with a low level of non-myeloablative radiation injury to the lung. Bruscia et al. (E M Bruscia et al. 2006) also observed engraftment of bone marrow-derived epithelial cells in the lung and gastrointestinal

tract after myeloablation (0.02% and 0.01%, respectively) but it was concluded that this level was too low to be considered of therapeutic value. However, when the transplantation was performed in newborn $CFTR^{-/-}$ mice, electrophysiology assays showed that cell transplantation rescued some level of chloride secretions across the epithelia. Carraro et al. (Carraro et al. 2008) studied the potential of amniotic fluid stem cells (AFSCs) to engraft murine lung and to differentiate into pulmonary cell types after either hypoxic or naphthalene-induced lung injury. Following systemic administration, AFSCs were identified within the distal and bronchial lungs and expressed typical alveolar and bronchiolar markers, depending on the type of injury received. Rosen et al. recently demonstrated that preconditioning the pulmonary niche with naphthalene injury and sub-lethal radiation, allows engraftment of mouse embryonic lung cells up to 16 weeks after transplantation (Rosen et al. 2015). Nevertheless, due to ethical limitations and to the high risk to form tumors, the use of ESCs for drug testing seems to be the most promising application of this cell type. Wong et al. studied the development of iPSCs from CF patients to use as cellular models of disease, drug discovery, and regenerative medicine. The gradual differentiation system with the addition of morphogens mimed lung development to generate human airway epithelium to test drugs for CF. The cells were then cultured in air liquid interface condition to obtain a heterogeneous, polarized and functional airway epithelium. The formed functional epithelium was similar to large airways with the expression of genes characterizing basal cells (p63), goblet cells (MUC5), and ciliated ones (FOXJ1). They next developed iPSC lines from patients with the *F508del CFTR* mutation (Wong et al. 2012). The differentiated airway epithelial cultures were then used to screen chemical compounds able to stabilize the mutant CFTR at the apical membrane and even identified one candidate compound. Ongoing studies will examine whether this stabilization and proper CFTR localization also results in a functional ion channel. Future analysis will take advance of these iPSC-derived epithelial layers to screen novel CFTR correctors and potentiators. Even if in the future iPSCs could probably also serve as a source for replacement therapies, a great amount of progress on the generation of specific lineages as well as deep studies on the efficacy and safety of this approach is required before this aim will be reached.

A recurrent principle in the cell therapy field is the capacity of the considered cellular populations to function through an immunomodulatory role, rather than regenerative medicine capacities *per se*. MSCs deriving from bone marrow, adipose, placental

tissue and other origins have been deeply investigated for their immunomodulatory effects in a wide range of inflammatory and immune diseases (Keating 2012; Prockop & Oh 2012). The mechanisms of MSC behaviors are only in part understood and in addition to paracrine effects of soluble peptide and other mediators, a growing body of evidence suggests that the release of episomal or microsomal particles by MSCs can condition both surrounding resident cells and also inflammatory ones. MSCs can also behave as antigen presenting cells and have recently been demonstrated to move mitochondria and probably other cytosolic components through connexin bridges (Islam et al. 2013). The intra-tracheal or intravenous administration of mouse or human bone marrow–derived MSCs in mice reduced mortality if compared with fibroblast and phosphate buffered saline controls (Gupta et al. 2012; Gupta et al. 2007; A. Krasnodembskaya et al. 2012). Administration of MSCs decreased pro-inflammatory cytokines and pulmonary edema. Also, human MSCs showed an antimicrobial effect in the pneumonia and peritonitis models, in part from increased release of the antimicrobial factor LL-37 and enhanced monocyte phagocytosis (A. Krasnodembskaya et al. 2012;  a. Krasnodembskaya et al. 2012). Good results have been also obtained with MSCs for experimental lung injury, including a decrease in lung endothelial and alveolar epithelial injury, a decreased acute inflammation, increased resolution of alveolar edema and even antimicrobial effects. Nevertheless, MSCs may not always resolve lung injury and some pre-clinical data suggest that MSCs could even contribute to established lung fibrosis (Epperly et al. 2003; Yan et al. 2007). Moreover, although intravenously injected MSCs are initially “trapped” in the lung, imaging studies have failed to demonstrate significant long-term pulmonary engraftment (Schrepfer et al. 2007). An overview of the different sources and techniques used to produce cell populations with therapeutic potential for CF is summarized in Figure 5.

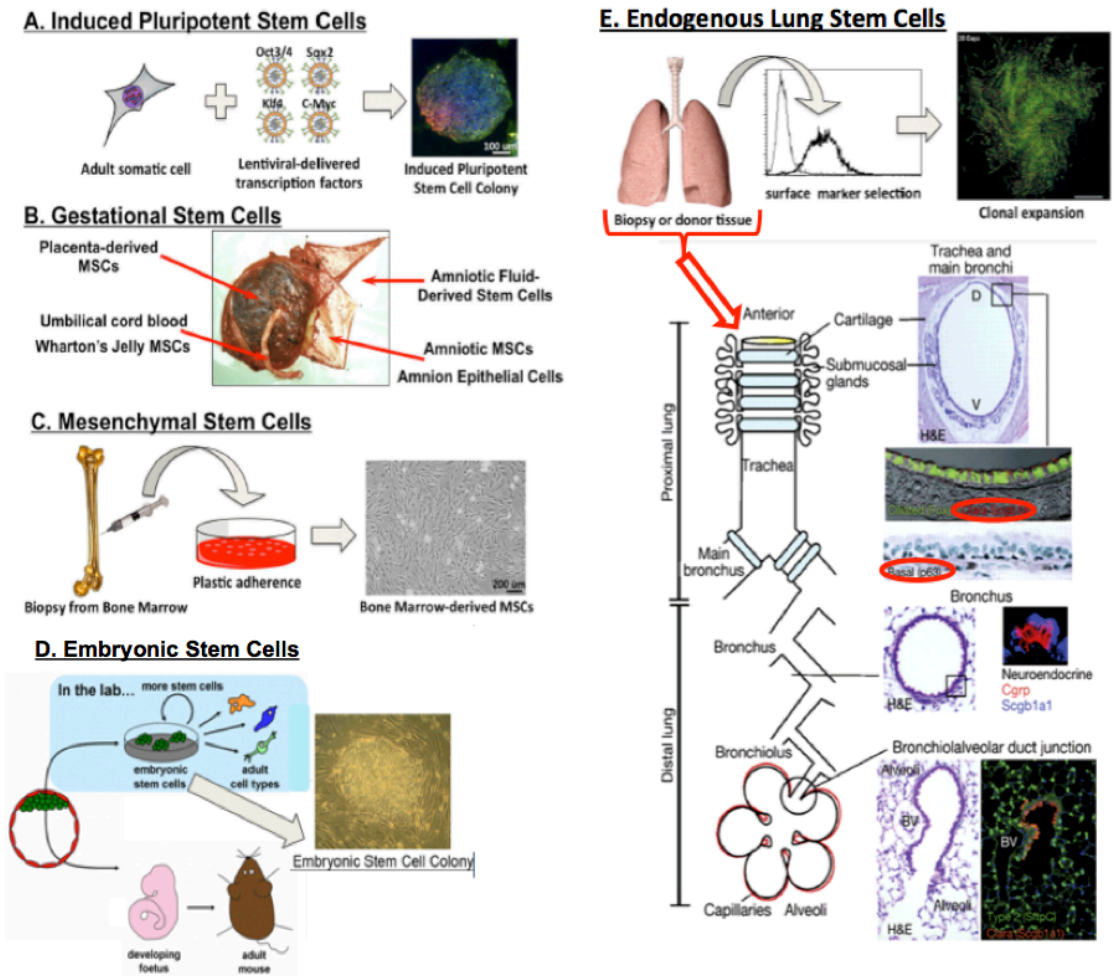


**Figure 5: An overview of the sources and techniques used to produce cell populations with therapeutic potential for CF (adapted from Murphy and Atala 2013).** (**A**) Induced pluripotent stem cells (iPSCs) can be generated by inducing the expression of four genes (Oct3/4, Sox2, Klf4 and c-Myc) in adult somatic cells. (**B**) Cell populations have been isolated from human placenta, placental membrane, umbilical cord and amniotic fluid that have been shown to be multipotent and to display anti-inflammatory features. (**C**) Mesenchymal stem cells (MSCs) are usually isolated from bone marrow but are also present in adipose tissue, synovial membrane, muscle, dermis, blood and other tissues. While considered to have a more restricted differentiation potential, MSCs have been tested as a cell-based anti-inflammatory therapy for the treatment of acute lung injury. (**D**) Embryonic stem cells (ESCs) have largely been demonstrated to display the ability to differentiate into different airways epithelial cell types. Due to ethical limitations and to the high risk to form tumors, the use of ESCs for drug testing seems to be the most promising application of this cell

type. (**E**) Airways-specific progenitors are thought to function as the primary repair sources. Several groups have identified and isolated lung stem cell populations that showed potential for future therapeutic applications.

The comparison of the efficacy of cell replacement approaches is challenging, due to the different range of cell types and injury models used for these experiments. Cell engraftment in the airways is widely influenced by the type and severity of injury, with a certain necessary level to enhance the recall of stem cells in the required site (Herzog et al. 2006). While the described approaches used various types of acute lung insult, it is possible that a chronic injury model would be more suitable to study long-term engraftment of stem cells in CF airway. It should also be underlined that the CF mouse models used in these studies do not spontaneously develop substantial lung inflammation and for this reason they are often combined with methods of lung injury. There are still several challenges that need to be addressed to make stem cell therapy an effective strategy for CF. First, it needs to be demonstrated that cells can be delivered to the airways and survive to the characteristic inflammatory status of CF lungs. Second, the level of engraftment needs to be sufficient to restore normal chloride transport to improve airway function (Kotton et al. 2005). Multiple researchers have demonstrated that cell engraftment is higher in injured lungs than in uninjured ones (Herzog et al. 2006; Ortiz et al. 2003), but it is not still clear whether the inflammation and remodeling taking place in CF lungs would facilitate cell recall and integration. Finally, to avoid immune rejection of allogeneic administered cells and the requirement of immune suppression, autologous cells should need to be isolated from the patient, expanded *in vitro*, "corrected" for the CFTR mutation and then transplanted back to the individual. Currently, it has still to be demonstrated that the combination of all these approaches together is feasible, even if progress has been made for each of these steps. The use of disease specific human ESC and iPS cells from CF patients provides further opportunities to study lung diseases and to further understand injury and repair processes in the lung (Pickering et al. 2005; Somers et al. 2010). Nevertheless, the current knowledge does not yet allow the clinical use of either ESCs or iPS cells for the treatment of lung diseases. Surely, a deeper understanding and a reached consensus regarding lung stem cells and their role in lung regeneration could help researchers in achieving effective cell-based therapies for not only CF, but also for other incurable lung diseases (Murphy and Atala 2013).

It is now accepted that both epithelial and mesenchymal compartments contain several cell types that can be classified as "endogenous progenitor cells," and lung injury models are often required to interrogate the growth and differentiation potential of individual progenitors (Leeman et al. 2014; Wansleeben et al. 2013; Barkauskas CE, Cronce MJ, Rackley CR, Bowie EJ, Keene DR, Stripp BR, Randell SH, Noble PW 2013; Morrisey et al. 2013; Vaughan & Chapman 2013; Rackley & Stripp 2012; Reynolds et al. 2012; Kotton & Morrisey 2014). Emerging themes also include the growing recognition that epithelial–mesenchymal interactions are not only important during lung development but remain necessary to maintain adult lung homeostasis, repair and regeneration, functionally distinct processes that likely involve different cell types and signaling pathways.

The lung is a complex organ composed by several distinct epithelial cell types distributed in many different regional microenvironments along the pulmonary tract, represented in a schematic form in Figure 6. For this reason, while the identification of cells in the airways that can proliferate under steady state or after injury has been relatively easy, the characterization and classification of presumed endogenous lung stem and progenitor cells has been hard to realize. A growing body of literature, predominantly in mouse models, describes endogenous adult stem or progenitor cells that activate to replace or repair damaged lung epithelia or vasculature (Rock & Hogan 2011; Mcqualter & Bertoncello 2012; Rackley & Stripp 2012; Reynolds et al. 2012; Rock & Königshoff 2012; Rawlins & Hogan 2006; Borthwick et al. 2001). Importantly, there seems to be regional specificity in mouse lungs with different epithelial stem or progenitor types identified for proximal airways, distal airways, and alveoli. Nevertheless, some of the published works have generated controversy and there is still not uniform agreement about the identity and/or function of endogenous stem or progenitor cells in either mouse or human lungs (Rock & Hogan 2011; Mcqualter & Bertoncello 2012; Rackley & Stripp 2012; Anversa et al. 2011; Dobbs et al. 2010). For this reason lung injury approaches, specific to particular regions, such as sulfur dioxide, ozone or nitrogen dioxide inhalation (against trachea, large airways), naphthalene administration (against non-ciliated club cells, also known as Clara cells, in the bronchiolar epithelium), or bleomycin (against alveolar epithelium) have been largely used in mice and other adult animal models to characterize stem/progenitor cells by inducing cellular repopulation (Rock & Hogan 2011; Mcqualter & Bertoncello 2012; Rackley & Stripp 2012; Reynolds et al. 2012; Rock &

Königshoff 2012; Rawlins & Hogan 2006; Borthwick et al. 2001; Anversa et al. 2011; Dobbs et al. 2010). Based on lineage tracing and injury models, three different cell populations have been classically accepted as endogenous progenitors of the adult respiratory system: basal and club cells in airways and type II alveolar epithelial cells in the alveoli. There is evidence that these cell types actually include distinct subpopulations with different characteristics and functions. A large body of evidence in mouse models has suggested that basal cells can activate and differentiate into club cells and ciliated cells in the proximal airways during both homeostasis and after sulfur dioxide injury (Rock et al. 2010; Ghosh et al. 2011). Club cells are a widely heterogeneous population of facultative progenitors in the bronchiolar epithelium in rodents and humans, able, although displaying a low steady-state proliferative rate, to self-renew and give rise to ciliated cells. This heterogeneity is displayed in multiple ways, such as their ability to undergo mucous metaplasia (Evans et al. 1978) or survive to naphthalene injury (Reynolds et al. 2000). These properties seem to be associated with the regional localization of these cells and depend on interactions with the surrounding microenvironment, through mechanisms still unknown. A subpopulation of naphthalene-resistant club cells, named variant club cells (vCE), can function as bronchiolar stem cells located in two separate niches: the neuroepithelial body (NEB) and the bronchoalveolar duct junction (BADJ) (Hong et al. 2001; Giangreco et al. 2002). Other presumed distal airway progenitor cells described in adult mice include bronchoalveolar stem cells (BASCs), CD45-/ CD31-/ EpCAMhigh/ CD104+/ CD24low, integrinα6β4+/SPC- cells, and CK5+/p63+ cells (Bender Kim et al. 2005; Teisanu et al. 2011; Chapman et al. 2011; Kumar et al. 2011; Chen et al. 2012). These cells can both have different localizations in the airways and could differently function in repair from experimentally induced lung damage (Giangreco et al. 2002; Chen et al. 2012). Alveolar epithelial repair and regeneration remain fixed on the concept that type II alveolar epithelial cell (ATII) are precursors for type I alveolar epithelial cells (ATI) (Dobbs et al. 2010). Nevertheless, recent evidences suggest that many populations of distal airways in adult mice, including BASCs and CK5+/p63+ cells can differentiate into ATI and ATII cells *in vitro* and conceivably could take part to repair of damaged alveoli *in vivo* (Bender Kim et al. 2005; Kumar et al. 2011). Further research to deeply explore heterogeneity of basal, club, and type II cells is needed and will be of great value to future studies for lung cell therapy.

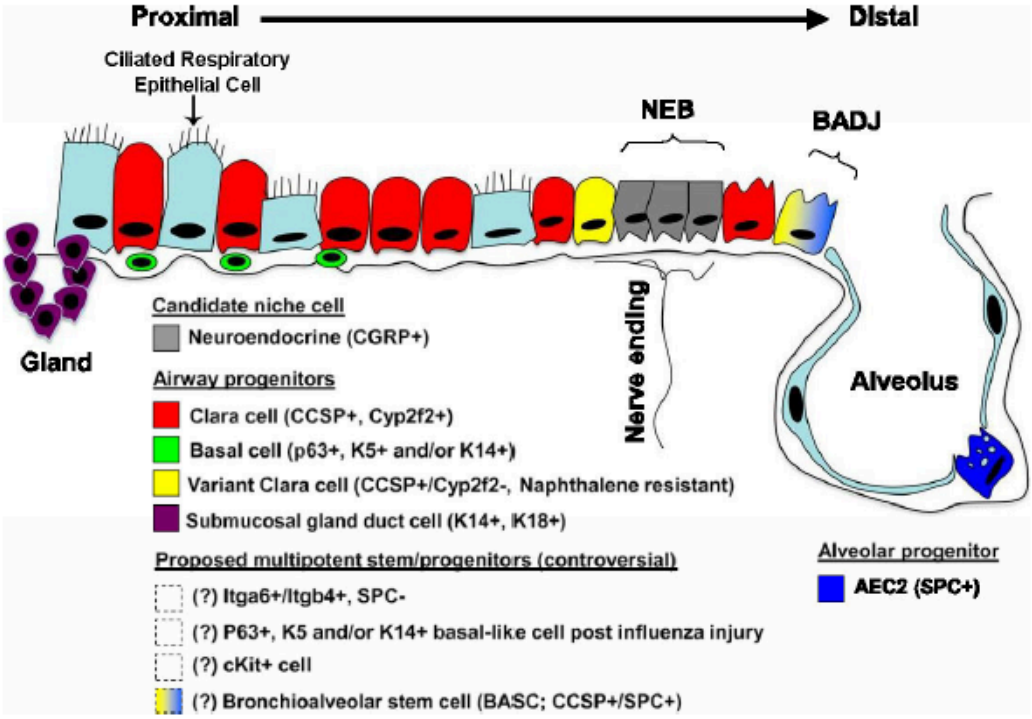


**Figure 6: Schematic representation of proposed lung epithelial candidate stem or progenitor cells and their niches in the proximal conducting airways and distal alveoli (from Weiss 2014)**. Cells whose localization or existence is still not clear or confirmed are indicated with dashed boxes and/or question marks. AEC2 = type II alveolar epithelial cell; BADJ = bronchoalveolar duct junction; Gland = submucosal gland duct; NEB = neuroepithelial body. Marker abbreviations used for each cell subtype include the following: CCSP = club (Clara) cell secretory protein; CGFP = calcitonin gene– related peptide; Itg = integrin; K = cytokeratin; SPC = surfactant protein C.

### 2.3 Mesoangioblasts

Stem cells are non-specialized cells, which maintain the capacity of indefinitely proliferate and, if properly stimulated, the one to differentiate into mature cells with specific functions and features. To be defined as stem, a cell needs to satisfy two main properties: the self-renewal and the pluripotency. Within the last concept is also included the trans-differentiation, that is the skill of a differentiating stem cell to modify its current development program (Kimble & White 1981; Clevers 2005; Doe & Bowerman 2001). In the last decades the notion of plasticity associated to stem

cells has undergone a change of interpretation due to the discovery of progenitor cells, in many adult tissues, able to differentiate if subjected to particular stimuli. For example bone-marrow cells can functionally integrate in muscular tissue (Ferrari et al. 1998), liver (Lagasse et al. 2000; Petersen et al. 1999) and in the central nervous system (SNC) (Brazelton et al. 2000). On the other hand, cells deriving from SNC have been demonstrated able to differentiate in cells of hematopoietic tissue (Bjornson et al. 1999) or skeletal muscle (Galli et al. 2000). Nevertheless, this multipotency seems to counter with the concept of irreversible and programmed fate associated to stem cells during embryogenesis. About that, some decades ago studies have been conducted to investigate the origin of myogenic cells during development. Thus, it has been identified a subpopulation of cells with myogenic potentiality, characterized by the expression of early endothelial markers, localized in the dorsal aorta rather then in the somites, which is the classical source of myogenic precursors (De Angelis et al. 1999). Moreover, a parallel study found progenitor cells in the skeletal muscle able to repopulate the hematopoietic system in mice (Jackson et al. 1999). In the light of this evidence, it has been proposed the idea that during histogenesis, when blood vessels enter in the developing tissues a population of vessel-associated progenitors cells, likely deriving from a common ancestor, leaves the vessels to adopt the fate of the contacted tissue (Bianco & Cossu 1999). The choice of the destiny likely depends on signals released by the local cells, resident in the target tissue and is functionally different from the embryonic driven one, although it seems that the same molecules are involved. To validate this hypothesis embryonic dorsal aorta deriving cells from mice and quail have been transplanted into host chick embryos (Minasi et al. 2002). Donor cells, firstly incorporated into the host vessels contributing to their development, were later integrated into mesodermal tissues, including blood, cartilage, bone, smooth, skeletal and cardiac muscle (Minasi et al. 2002).

This last evidence allowed the identification of a new class of pluripotent progenitors, associated to the dorsal aorta, able to generate several types of specialized mesodermal cells during post-embryonic and fetal development. These cells have the ability to give rise to clones, which can be maintained in culture *in vitro* during time, without entering the senescence program, thus they could be considered immortalized. These clones display the same morphology; express "hemo-angioblastic" markers such as CD34, Flk1 and Kit and preserve the mesodermal

differentiation potential both *in vitro* and *in vivo*. In the light of these evidences, these embryonic aorta-associated progenitors have been described as a new type of stem cells named mesoangioblasts (MABs), distinct from both ESCs and satellite cells (Minasi et al. 2002). The name 'mesoangioblasts' was chosen to indicate a common progenitor for vascular and extravascular mesodermal derivatives, appropriate for marking the conceptual similarity of this novel entity with the hemoangioblast, a common progenitor for vascular and hematopoietic (intravascular) mesodermal derivatives. At variance with hemoangioblasts, the ultimate progenitors of all definitive, quickly turning over hematopoietic cells, mesoangioblasts would be an additional source of post-natal differentiated mesoderm-derived tissues (the majority of which derives from canonical embryonic sources during development and turns over slowly) but likely a main source of post-natal progenitors of them. According to some studies, there is a common ancestor for hemoangioblasts and mesoangioblasts, expressing Flk1 (the receptor for the vascular growth factor VEGF) that, depending from the received stimuli, is driven towards a specific differentiation fate.

During the last fifteen years mesoangioblasts have been isolated and characterized from mice (Minasi et al. 2002), dogs (Sampaolesi et al. 2006) and humans (Dellavalle 2007). MABs differentiate in many mesodermal-derived tissues including smooth, skeletal and cardiac muscle, adipose tissue, bone and cartilage, in presence of specific signal-molecules or co-cultured with cells deriving from specific mesodermal-derived tissues. However, to date, their biology and the mechanisms that regulate their differentiation, both in embryonic and adult tissues, are still not totally understood. It is not currently known, for example, whether the inability to contribute to ectoderm- or endoderm-derived tissues is intrinsic to MABs or simply reflects inadequate experimental conditions *in vitro* or physical barriers *in vivo* (a few quail cells in the chick epidermis were indeed found) (Minasi et al. 2002).

The most interesting aspect of these cells is that, when systemic delivered in different dystrophic animal models, they are able to cross blood vessel wall, join the damaged muscle and rescue the dystrophic phenotype (Sampaolesi et al. 2003; Sampaolesi et al. 2006). Since the first identification of MABs in mouse embryos, all MABs so far isolated from different species (mouse, dog and human) and developmental stages have been demonstrated to contribute to muscle regeneration *in vivo*. Although alkaline phosphatase expression can be used to identify adult human MABs in skeletal muscle, no single unequivocal marker has been found that denotes MAB

identity across species (Minasi et al. 2002; Díaz-Manera et al. 2010; Sampaolesi et al. 2006; Dellavalle 2007). Consequently, MABs are defined predominantly by their isolation methods and functional properties. Only recently, it has been identified a marker that is expressed by all embryonic and adult populations of MABs, named PW1 (Bonfanti et al. 2015). A cross-analysis of independent microarrays performed on different human and murine MAB populations underlined that the transcription factors PW1 and Pax3 are highly interesting and expressed (Tagliafico 2004). In detail, it has been observed how the absence of Pax3 inhibits skeletal muscle differentiation in murine embryonic MABs (Messina et al. 2009) but not in adult ones (Bonfanti et al. 2015). Moreover, gene expression profiling studies performed on all the MAB classes isolated so far, revealed that PW1 is the only maker expressed at high levels, independently from the species and developmental stages. It has been indeed demonstrated that PW1 expression is related to the migratory capacity and to the myogenic potential of mesoangioblasts (Bonfanti et al. 2015).

### 2.3.1 Murine mesoangioblasts

Embryonic murine mesoangioblasts (mMABs), isolated from the dorsal aorta (E10.5), are characterized by the expression of different early endothelial markers such as Flk1, Sca1 (stem cell antigen 1), VE-cadherin (vascular-endothelial cadherin), c-kit, CD34, but do not express late endothelial markers such as vWF (Von Willebrand factor) for the interaction with platelets (Tonlorenzi et al. 2007). All polyclonal populations are also characterized by high levels of α–SMA (α smooth muscle actin) (Minasi et al. 2002), a myogenic marker expressed by myoblasts and pericytes (Springer et al. 2002; Schlingemann et al. 1991; Hirschi & D'Amore 1996). Consistent with their differentiation potential, embryonic mMABs express typical mesodermal genes, some of which are receptors and signal molecules, such as *BMP* (bone morphogenic protein), *Wnt* and *Notch* (Sampaolesi et al. 2003). Furthermore, if maintained in culture under specific conditions, embryonic mMABs display multiple differentiation features: the co-culture with cardiomyocytes induces a cardiomyogenic differentiation (Condorelli et al. 2001); following BMP-2 (bone morphogenic protein 2) administration embryonic mMABs express alkaline phosphatase and typical osteogenic markers; conversely, if fed with an adipogenic factors-enriched culture medium, they are capable to differentiate in fat cells (Minasi et al. 2002); finally, if

treated with TGF-β (transforming growth factor beta), embryonic mMABs easily differentiate in smooth muscle (Tagliafico 2004), recalling the behavior of post-natal pericytes (Verbeek et al. 1994). Moreover, when co-cultured with myoblasts embryonic mMABs express genes specific of skeletal muscle differentiation such as *MyoD* and *Myf5* (Minasi et al. 2002; Tonlorenzi et al. 2007). These genes are not normally expressed since embryonic mMABs do not spontaneously differentiate towards muscle, but only under the specific conditions above cited.

Subsequently isolated adult mMABs display a substantial experimental advantage compared to their embryonic counterpart, since they are able to spontaneously differentiate towards skeletal muscle without needing the co-culture with myoblasts (Díaz-Manera et al. 2010).

Recently it has been reported that the inhibition of Rho kinase (ROCK) pathway drives mesoangioblasts to differentiate in oligodendrocytes and Schwann cells, both deriving from the ectoderm (Berry et al. 2007; Wang et al. 2012). Furthermore, the same group demonstrated that postnatal aorta-derived mesoangioblasts recombined with uterine mesenchyme (UtM) differentiate in uterine epithelium (UtE), with the typical CK8+ simple columnar epithelial phenotype, responsive to estrogen stimulation. Nevertheless, they fail to demonstrate MAB capacity to differentiate into prostatic epithelium or epidermis (Simon et al. 2013). All these data support the hypothesis that MABs are capable to differentiate, if properly stimulated, in many different tissues deriving from both mesoderm and ectoderm.

A comparative analysis performed on four clonal mMAB populations compared to embryonic fibroblasts 10T/2 demonstrated that mMABs have a gene expression profile similar to that of embryonic hematopoietic and neural stem cells (Tagliafico 2004), characterized by the expression of different genes involved in inflammatory processes such as cytokines and their receptors (Ramalho-Santos et al. 2003; Ivanova et al. 2010).

If maintained in culture in proper conditions or in the presence of specific factors, mMABs can be expanded for several passages (more than fifty) and, once at confluence, their growth capacity results impaired. Furthermore, tumorigenesis assays performed on nude mice demonstrated that mMABs are not tumorigenic (Sampaolesi et al. 2003; Sampaolesi et al. 2006; Díaz-Manera et al. 2010; Tedesco et al. 2011; Tedesco et al. 2012; Domi et al. 2015). Maintaining mMABs in culture for long periods decreases the expression of some endothelial markers such as c-kit and

VE-cadherin but they still keep the same differentiation features (Cossu & Bianco 2003).

mMAB myogenic potentialities observed *in vitro* have been subsequently demonstrated also *in vivo,* in the *α-sarcoglycan* (*α-SG*) *null* mouse which models the limb-girdle muscular dystrophy. Following intra-arterial transplantation of different mMAB clones, it has been observed a partial but significant functional and structural rescue of the impaired muscles (Sampaolesi et al., 2003) (Figure 7). This result was even enhanced by injecting mMABs pre-treated with cytokines and adhesion molecules such as TNF-α (tumor necrosis factor α) and α4-integrin, thus giving prove of MAB potential clinical application (Galvez et al. 2006; Palumbo et al. 2004).

MAB myogenic potential has been confirmed, both *in vitro* and *in vivo*, also in dog. *In vitro*, following co-culture with murine myoblasts C2C12 they form myotubes; *in vivo*, the study has been realized with the golden retriever dog model of muscular dystrophy (GRMD). Intra-arterial injections of MABs led to a morphological and functional rescue of damaged muscles (Sampaolesi et al. 2006).

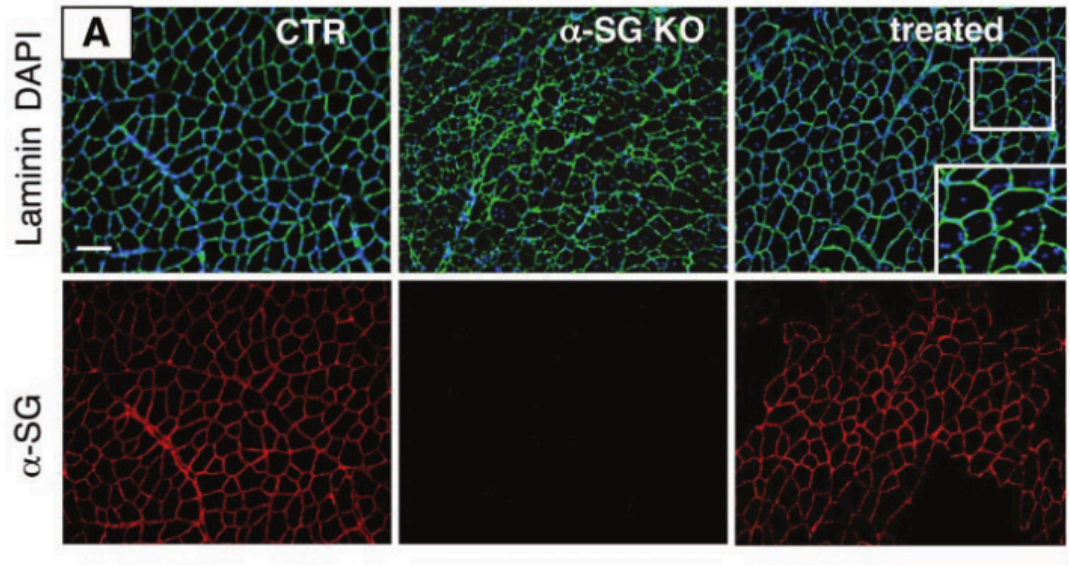


**Figure 7: Expression of α-SG and other dystrophin-associated proteins in *α-SG null* mice after intra-arterial delivery of wild-type mesoangioblasts (from Sampaolesi et al., 2003).** Low magnification of quadriceps from control (CTR) mice (left), *α-SG null* (α-SG KO) mice (center), and treated *α-SG null mice* (injected with wild-type mesoangioblasts 2 months before the analysis) (right). Large areas of the treated muscle expressed ***α***-SG after staining with a specific antibody (red). Sections

were also stained with antibodies to laminin (green) and DAPI to indicate nuclei (blue). Laminin distribution in ***α-SG null*** treated muscle results similar to the wild type one. Inset: Higher magnification of treated muscle with centrally located nuclei. Scale bar 100 μm.

### 2.3.2 Human mesoangioblasts

The identification of myogenic progenitors isolated from the dorsal aorta of murine embryos (Minasi et al. 2002) and from adult muscles from mice and dogs (Sampaolesi et al. 2003; Sampaolesi et al. 2006), together with the significant phenotype rescue following their intra-arterial injection in pre-clinical dystrophic models (Sampaolesi et al. 2003; Sampaolesi et al. 2006), have suggested the possibility to isolate similar cells also from humans. In fact some years after the characterization of murine and dog MABs, cells with analogue features have also been found in the postnatal human microvasculature (hMABs). The analysis of muscular biopsies deriving from healthy and dystrophic human patients indeed allowed the identification of a cell population capable to regenerate skeletal muscle in a similar way compared to embryonic murine MABs (Dellavalle et al. 2007). These cells have been obtained from the dissection of skeletal muscle fragments; following the initial expansion of fibroblasts, it has been observed the presence of small, round, low adherent cells (Dellavalle et al. 2007) (Figure 8).

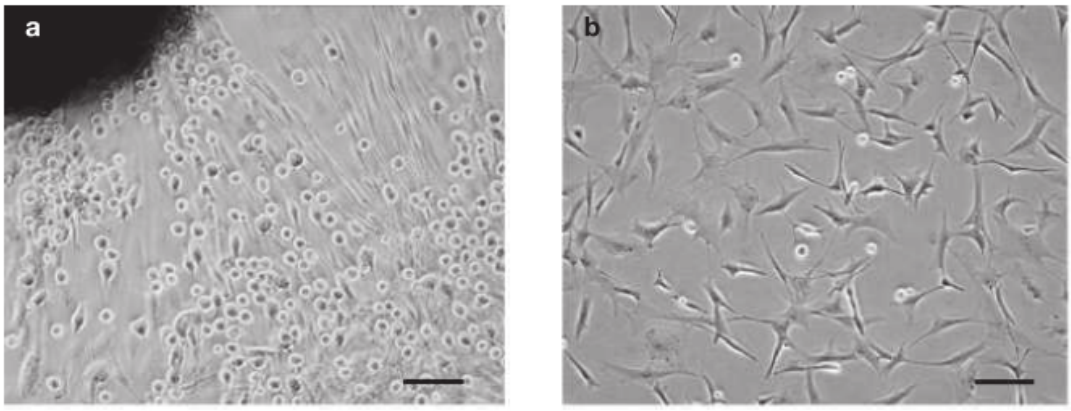


**Figure 8: *In vitro* characterization of human adult interstitial cells (from Dellavalle et al. 2007).** (**A**) Phase-contrast morphology of the cellular outgrowth of a fragment of interstitial tissue containing a small vessel cultured from a biopsy of normal adult human muscle. Round and refractile cells are visible on top of a layer of

fibroblast-like cells. (**B**) Phase-contrast morphology of a polyclonal population isolated from an explant culture after 5 passages in vitro. Scale bar 10 μm.

Gene expression profile of the isolated cells revealed that they express high levels of typical pericytes genes (*annexin V*, *alkaline phosphatase*, *desmin*, *smooth muscle actin*, *vimentin*), but they do not express *M-cadherin*, cytokeratines or endothelial markers, likewise their murine counterpart. Moreover, from the analysis of the superficial antigen they resulted CD31, CD34, CD45 negative and CD13, CD44 positive (Dellavalle et al. 2007).

The ability of these cells to spontaneously express high levels of alkaline phosphatase allowed their easy isolation from the population of satellite cells. Furthermore, since in the adult skeletal muscle only pericytes express alkaline phosphatase (Safadi et al. 1991), it has been hypothesized that human MABs derive from pericytes.

hMABs, if maintained in culture with a proper medium, could be expanded *in vitro* until around the twelfth passage, limit beyond which they become senescent. Moreover, if properly stimulated, they can differentiate towards smooth muscle and fat cells; on the contrary, if cultured with a specific differentiation medium (DMEM, 2% Horse Serum), they spontaneously differentiate towards skeletal muscle (Dellavalle et al. 2007).

Human MAB myogenic potential has been tested also *in vivo* in dystrophic immunodeficient mice *mdx-SCID* (Dellavalle et al. 2007) observing that the area surrounding the injection site resulted regenerated with human dystrophin-expressing fibers (Dellavalle 2007; Meng et al. 2011). This body of evidence further confirmed the therapeutic potential of MABs for the cure of Muscular Dystrophies.

Furthermore, since a significant trouble in all allogeneic cell therapies is the immune rejection and some tested stem cells displayed immunomodulatory features, it has also been investigated MAB immunogenicity. English et al. indeed demonstrated that hMABs suppress T Cell proliferation through IDO- (indoleamine 2,3-dioxygenase) and PGE- (prostaglandin E-2) dependent pathways (English et al. 2013), thus modulating the immune response. One year later the same skill has been also confirmed for human iPSC-derived MABs (Li et al. 2013).

For all these reasons hMABs have been used in a clinical trial in human patients affected by Duchenne Muscular Dystrophy (DMD) that definitely demonstrated that

intra-arterial transplantation of donor MABs in human is feasible and safe (Cossu et al. 2015).

### 2.3.3 MAB transplantation as a potential cell-based approach to cure Cystic Fibrosis

During studies performed to further characterize the biology of MABs, it has been observed that mMABs, when systemically delivered, do not engraft muscles of healthy wild type mice. It has been indeed noticed that, nLacZ-mMAB (previously transduced with nuclear LacZ lentivirus to easily detect mMABs in mouse tissues), when systemically transplanted in the caudal vein of healthy wild type (wt) mice (C57BL/6) distribute throughout filter organs, such as lung, kidney and spleen. Interestingly, we noticed that mMABs engraft lung, tracheal and intestinal epithelium up to one month from their transplantation (Figure 9) (Vezzali et al. in preparation). The unexpected substantial mMAB engraftment in the epithelia of the airways and intestine represented the starting point to consider these cells as a potential tool for a cell-based therapy for Cystic Fibrosis, which, as described before, mainly affects the airway and intestinal tracts. The ability of MABs to cross the vessel wall and their systemic delivery confer them an advantage as therapeutic donor cells compared with other stem populations that need to be delivered directly into the airways, facing significant physical/immunological obstacles.

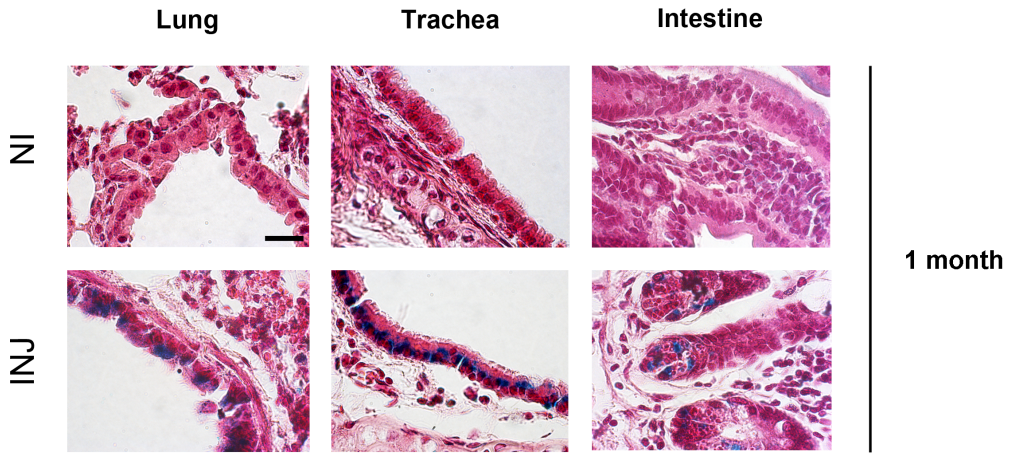


**Figure 9: nLacZ-mMABs, after systemic transplantation, engraft lung, tracheal and intestinal epithelium in C57BL/6 wt mice (from Vezzali et al. in preparation).** Carmallume/Eosin and X-Gal staining on serial transverse sections of lung lobes, trachea and intestine of transplanted (INJ) and not-transplanted (NI) C57BL/6 wt mice at 1 month from nLacZ-mMAB systemic transplantation. X-gal was used to identify transplanted nLacZ-mMABs (blue). Scale bar 20 μm.

# AIM OF THE PROJECT

Since the *CFTR* gene was cloned in 1989 (Riordan et al. 1989), several strategies aiming to correct CF lung disease have been explored. However, over 20 years later, effective treatments have not been proved for the majority of CF patients. Among the tested approaches, cell-based therapy is under investigation, since it would be effective for any kind of CF patients. Several sources of stem cells demonstrated their ability to develop epithelial features and have been used to complement CFTR defects (Sean V. Murphy and Anthony Atala 2013; Weiss 2014). In all cases, stem cell-based approaches have not achieved the efficiencies of delivery and engraftment needed for CF therapy. The reasons rely in the low engraftment in the lungs after systemic or intra-tracheal administration of donor cells, in the small percentage of cells differentiated in airway epithelia and in the even less percentage of CFTR expression (Murphy and Atala 2013; Sueblinvong & Weiss 2010; Weiss 2014). Moreover, it has been proved that any benefit that might arise from these cells would probably be due to paracrine effects, including stimulation of angiogenesis and modulation of local inflammatory and immune responses in mouse lung disease models (Lama et al. 2007; Keating 2012). During recent works on MABs isolated from adult mouse skeletal muscle (mMABs) (Diaz-Manera et al. 2010), we observed that nLacZ-mMABs when systemically transplanted in healthy, wild type mouse (C57BL/6) do not engraft skeletal muscle but distribute throughout filter organs. Interestingly, we noticed that mMABs engraft lung, tracheal and intestinal epithelium up to one month from their single transplantation. These observations led us to investigate on a possible use of MABs for a cell-based therapy for CF. The ability of MABs to cross the vessel wall and their systemic delivery confer them an advantage as therapeutic donor cells compared with other stem populations that need to be delivered directly into the airways, facing significant physical/immunological obstacles.

For these reasons, the main aim of this project was to provide evidence on a possible use of MABs as a potential new tool for the cure of CF. In detail, this work has been developed by studying different aspects:

- The characterization of mMAB engraftment overtime in the airway and intestinal epithelium of C57BL/6 wild type mice and the investigation of their tumorigenic potential in CD1 nude mice, as a necessary starting point to consider these cells as potential candidates for a cell-based therapy approach.

- The study of CFTR expression in mMABs in terms of proper channel localization and activity *in vitro*. These analyses aimed to verify whether mMABs have the proper cellular mechanisms necessary to express a functional CFTR channel, whose dysfunction causes the pathology under investigation. mMABs have been assessed for their ability to express functional CFTR by biochemical assays and *in vitro* measurements of CFTR-dependent $Cl^-$ current.
- The evaluation of mMAB transplantation in rescuing CF phenotype. We therefore wondered if mMABs would be able to engraft the respiratory and the intestinal epithelium in the CF mouse models *F508del CFTR* (van Doorninck et al. 1995) and *KOCftr*$^{tm1UNC}$ (*CFTR ko*) (Snouwaert et al. 1992) and if this engraftment would lead to a general amelioration of the pathology, following CFTR functional rescue. mMAB engraftment has been characterized overtime in CF mice and donor-derived cells have been assessed for their capability of expressing functional CFTR by *ex-vivo* and *in-vivo* trans-epithelial potential difference measurements.
- The study of mMAB potential to differentiate in epithelial cells and/or to participate to the epithelial stem cell niches. Since it has never been explored so far the ability of MABs to make epithelium, it would be necessary and interesting to investigate on MAB plasticity that would make them eligible cells for two completely different pathologies such as the Muscular Dystrophies (MD) and the Cystic Fibrosis. Therefore, we faced this aim by different *in/ex vivo* and *in vitro* approaches to characterize the epithelial markers expressed by mMABs and to understand the mechanisms through which the epithelial context could drive mMABs to acquire an epithelial fate.

The results of this study will potentially lead to the identification of MABs as a new tool to cure CF disease.

# MAIN RESULTS

## 4.1 mMABs engraft lung, tracheal and intestinal epithelium in C57BL/6 wild type mice

To investigate and characterize the potential mMAB engraftment as a possible tool for a targeted cell therapy, we injected 30x10^4 mMABs, previously tranduced with a lentiviral vector expressing nuclear LacZ (nLacZ-mMABs), in the caudal vein of wild type mice. After mMAB injection in healthy C57BL/6 wild type (wt) mice (n=3 for each time point), we examined if their engraftment in multiple organs would persist even after 2 months. Strikingly, we noticed that mMABs engraft lung, tracheal and intestinal epithelium up to two months from their single transplantation. In fact, lung, tracheal and intestinal epithelium derived from nLacZ-mMAB-injected mice clearly reveals the presence of donor β-gal-positive nuclei in the stratified epithelium, whose architecture still remains preserved. As control, we performed the same analysis on C57BL/6 not transplanted mice (n=3 for each time point) and we never found LacZ-positive staining. Moreover, to investigate the possible tumorigenic potential of mMABs we performed a subcutaneous tumor assay in CD1 nude mice, by injecting 2x10^6 nLacZ-mMABs (n=6) and we compared their possible tumor forming ability with that of nLacZ-S180 sarcoma cell line (n=6). Eight months after transplantation we observed that none of the mice injected with nLacZ-mMABs displayed micro and or macroscopic tumor masses, while all CD1 nude mice injected with S180 cells showed tumor masses, already detectable one week after transplantation. This result clearly demonstrates the safety of mMABs and further confirmed data already published by others (Sampaolesi et al. 2003, 2006; Diaz-Manera et al. 2010; Tedesco et al. 2011, 2012; Domi et al. 2015).

These evidences unequivocally demonstrate the ability of mMABs to properly engraft and integrate in the lung, tracheal and intestinal epithelia of C57BL/6 wt mice.

## 4.2 mMABs can express functional CFTR channel

After demonstrating mMAB engraftment in the proximal and distal airway epithelia, we decided to investigate CFTR expression in mMABs.

To this aim, we evaluated CFTR expression in mMABs in terms of gene expression and activity *in vitro*. Regarding CFTR expression, we first measured CFTR transcript levels by qRT-PCR, which demonstrates the presence of CFTR mRNA in mMABs *in*

*vitro,* compared to *CFTR ko* nasal epithelial cells. Once demonstrated the gene expression of *CFTR* in mMABs we also started to investigate its functional activity, *in vitro*. The study on the protein expression and localization is still ongoing. This issue is controversial in the field and it relies on the fact that the few antibodies that are supposed to recognize the murine CFTR by WB are not good and reliable. Nevertheless, to verify whether mMABs have the proper cellular mechanisms necessary to express a correctly localized and functional CFTR channel, we compared CFTR-dependent halide expression in ctl versus mMABS transiently transfected with two plasmids, the first carrying the *wt CFTR* and the second the *F508del* mutated form (*F508del*), together with a halide-sensitive YFP (HS-YFP) variant. In the YFP based microfluorimetric assay, a quantitative procedure that exploits halide-sensitivity of YFP variants, we analyzed CFTR-mediated halide transport (Pedemonte et al. 2005). Cells transfected with *F508del* mutant were tested under control condition or following 24 h-treatment with a well established corrector of *F508del* CFTR misfolding, the VX-809 compound (1 M) (Van Goor et al. 2011). At the time of the assay, cells were acutely stimulated with forskolin (20 M) alone (mMABs transfected with the empty vector and *wt CFTR*) or forskolin plus genistein (50 M; for cells expressing *F508del* CFTR). CFTR activity for each condition was determined by measuring the rate of cell fluorescence quenching after addition of the iodide-rich solution. We then observed that mMABs display no endogenous CFTR activity, while cells transfected with *wt CFTR* have significantly higher quenching rate values, suggesting that mMABs can express a functional channel. As expected, cells transfected with the *F508del* mutant do not have functional activity, showing that mMABs are a very stringent cell model with very low levels of expression of the *F508del CFTR*. However, when treated for 24 h with the corrector VX-809, *F508del* mMABs show a significantly increased anion transport.

### 4.3 mMABs efficiently engraft overtime the epithelium of airways and intestine of the *F508del CFTR* mouse model

We then proceeded to verify the potential of mMAB transplantation in the mouse model of CF *F508del CFTR* and whether this engraftment would persist overtime. This model was used because it carries the same mutation (belonging to class II) that affects almost the 70% of human patients (van Doorninck et al. 1995). Moreover,

since these mice display basal inflammation and a prolonged and exuberant inflammatory response to bacteria and bacterial products (Luciani et al. 2012), this CF mouse model represents a valuable tool for studying certain aspects of CF lung disease, albeit not reproducing all aspects of the pathology (e.g. chronic bacterial lung colonization, viscous mucus) (van Doorninck et al. 1995; Clarke et al. 1992; Wilke et al. 2011).

To this aim mMABs have been transduced with a lentiviral vector carrying the GFP marker and 30x10^4 GFP-mMABs were systemically transplanted, through the caudal vein, in *F508del CFTR* mice (n=3 for each condition, transplanted and not-transplanted). Mice were sacrificed at 2 weeks, 1, 2, 4 and 6 months after transplantation. We then observed that GFP-mMABs properly engraft the E-cadherin-positive epithelium in the lung, trachea and intestine up to 6 months from their single transplantation. At the same time points we also evaluated engrafted mMAB proliferation by analyzing the expression of the proliferative marker Ki67, revealing that very few mMABs proliferate once localized in the host epithelia.

To further confirm our previous results we replicated the same experiments by injecting different polyclonal classes of mesoangioblasts, named mMABs #2 and #3. To this aim, we repeated the *in vivo* experiments, by injecting 30x10^4 GFP- #2 / #3 mMABs in the caudal vein of *F508del CFTR* mice and we analyzed the engraftment of the donor GFP-cells after 1 month from the transplantation in the lung, tracheal and intestinal epithelium. Both #2 and #3 MABs engraft the E-cadherin positive epithelia of the considered organs, demonstrating that mMAB epithelial engraftment is an intrinsic and specific property of mMABs regardless of a particular mMAB cell preparation.

### 4.4 Transplanted mMABs in *F508del CFTR* mice significantly decrease the inflammatory marker TNF-α

To preliminarily test if mMAB engraftment would correspond to a decrease of local inflammation, we delivered GFP-mMABs in *F508del CFTR* mice as previously described. Transplanted mice were sacrificed after 2 months following mMAB injection and lungs collected to check, by qRT-PCR, TNF-α expression, a well-known inflammatory marker. This analysis demonstrated that TNF-α is 2.5 less expressed in mMAB transplanted lungs at 2 months from cell administration. This

result, although preliminary, is significant in particular considering that the reduction of this inflammatory parameter has been observed after only 2 months from a single MAB injection in *F508del CFTR* mice. This preliminary result indicates that the engraftment of mMABs in the lungs correlates with a general amelioration of the inflammatory status of cystic fibrotic lungs.

**4.5 mMABs rescue CFTR activity in *CFTR ko* mouse model**

To test whether mMABs could even restore CFTR-dependent chloride secretion *in vivo* once engrafted in the epithelia, they were transplanted in homozygous CFTR knockout mice (*KOCftr*$^{tm1UNC}$ mice, *CFTR ko;* Snouwaert et al. 1992). *CFTR ko* mice do not express any CFTR protein and they recapitulate the electrophysiological abnormalities observed in individuals affected by CF, such as $Na^+$ hyperabsorption and lack of cAMP-dependent $Cl^-$ secretions in their intestine and respiratory epithelia (Clarke et al. 1992; Grubb et al., 2002; Fischer et al., 2002). For all these reasons these mice represent the most valuable model for assessing a potential rescue of functional CFTR after mMAB transplantation. In this study, wt and *KOCftr*$^{tm1UNC}$ mice were transplanted *via* caudal vein with 30x10^4 GFP-mMABs. First we evaluated mMABs engraftment in *CFTR ko* mice, analyzing the presence of the donor-engrafted GFP-cells in the lung epithelium. We indeed found GFP-mMABs engrafted in the E-cadherin-positive epithelium of transplanted lungs at 2 weeks and 4 months from cell transplantation.

In view of measuring the nasal potential difference across the nasal epithelium in *CFTR ko* mMAB-injected mice, we firstly proceeded by evaluating mMAB engraftment in that tissue. We then isolated epithelial cells from the nasal cavity of *CFTR ko* mice, untreated and injected with GFP-mMABs after 4 months from transplantation and we found GFP-positive cells in the nasal epithelium of transplanted mice. Strikingly, we also observed that engrafted GFP-mMABs express the epithelial marker E-cadherin. To further confirm the colonization of GFP-positive mMABs, we measured, by qRT-PCR, the transcript levels of GFP and CFTR from the nasal epithelial cells of wt and *CFTR ko* mice, untreated and injected with GFP-mMABs after 2 weeks and 4 months from transplantation. We then reported that the transcript levels of GFP are statistically significant higher in transplanted mice, both

wt and *CFTR ko*, respect to the untreated ones. Moreover, the level of CFTR mRNA was increased, definitively confirming the occurred engraftment.

To evaluate the rescue of CFTR activity we then measured, at the same time points, the potential difference across the nasal epithelia (nasal potential difference, NPD). In this assay, the removal of luminal $Cl^-$ and the subsequent exposure to CFTR stimulators such forskolin (FSK) and 3-isobutyl-1methylxantine (IBMX) induced a hyperpolarization (more negative potential difference) in wt animals, which is not substantially altered in wt animals injected with mMABs (n = 6) compared to wt untreated mice (n = 9) (-2.67 ± 0.7 mV vs. -3.82± 1.1 mV, *P* = 0.19). On the contrary, the change in NPD in response to $Cl^-$-free bicarbonate Kreb's solution/amiloride/FSK/IBMX (ΔNPD) is statistically significant different between *CFTR ko* untreated mice (n = 15) and transplanted ones, after 2 weeks (n = 9) and also after 4 months (n = 10) (KO NI, ΔNPD = 2.78 ± 0.6 mV; KO INJ 2w, ΔNPD = -0.77 ± 0.7 mV, *P* = 0.0008; KO INJ 4m, ΔNPD = -0.11 ± 0.9 mV, *P* = 0.0067). *CFTR ko* transplanted mice have a more negative PD indeed, in response to $Cl^-$-free bicarbonate Kreb's solution/amiloride/FSK/IBMX compared to *CFTR ko* untreated mice, suggesting some CFTR-dependent chloride secretion. Furthermore, in order to definitively remove any variability given by the *in vivo* assay, we measured the ΔNPD in the same mice before and after the transplantation of mMABs. We observed that the average value of the ΔNPD measured after mMAB injection is statistically significant more negative if compared to the measurements performed on the same *CFTR ko* mice before the transplantation.

Finally, CFTR function was also measured *ex vivo* after 4 months from mMAB transplantation by the Ussing chamber assay, the gold standard method to test CFTR activity. We therefore examined the change in $I_{sc}$ ($\Delta I_{sc}/cm^2$) by Ussing chamber analysis on the distal colon of all mice studied, first in response to apical $0Cl^-$ and then to FSK. After FSK stimulation, the wt group (n = 6) has a $\Delta I_{sc}$ of 40.7± 3.7 $\mu A/cm^2$ which is not essentially different from transplanted wt mice (n = 3) with a $\Delta I_{sc}$ of 37.6 ± 0.3 $\mu A/cm^2$ (*P* = 0.22) as expected. The FSK-derived $\Delta I_{sc}/cm^2$ in the distal colon of *CFTR ko* not injected mice (n = 5) and that of mMAB-transplanted ones (n = 11) is -3.2 ± 1.7 and 2.2 ± 1.6 $\mu A/cm^2$ respectively. Strikingly, we observed a statistical significant difference in terms of the change in $I_{sc}$ in mMAB-transplanted *CFTR ko* mice, if compared to untreated ones (*P* = 0,02). Overall, these

results unequivocally confirm mMAB ability to functionally rescue the CFTR-dependent chloride secretion in the most severe mouse model of CF.

**4.6 mMABs differentiate in epithelial cells once engrafted in the lung**

Since the results shown so far clearly demonstrate that mMABs engraft lung and intestinal epithelia overtime, we investigated their ability to differentiate in epithelial cells and, alternately, their contribution to the stem cell niches, issue never investigated so far. We hypothesized that the epithelial environment could drive mMABs towards an epithelial fate, since they showed a good tropism to epithelial tissues. We faced this aim by different *in/ex vivo* and *in vitro* approaches. Firstly, we re-isolated GFP-mMABs from 5 months injected *F508del CFTR* lungs (n = 5) by FACS. We obtained a 97% of mMABs purity after re-isolation, data also confirmed by both immunofluorescence and qRT-PCR for GFP. Interestingly, re-isolated GFP-mMABs (around 0.8% of the total cells) express statistically significant higher levels of mRNA of the epithelial marker E-cadherin and of SCGB1a1, if compared to not-transplanted mMABs. In particular, *SCGB1a1* encodes for a well known and studied secretoglobin firstly called Clara cell secretory protein (CCSP/CC10), expressed by noncilated bronchiolar club (Clara) cells lining the distal bronchiolar epithelium (BRANDT et al. 1985; LUND et al. 1985; Singh et al. 1985; Singh & Katyal 1997) that in the adult murine lung constitute the majority of the bronchiolar epithelium (around 64% of the volume) and have a role of progenitors/stem cells (Plopper 1983; Karnati & Baumgart-Vogt 2008; Karnati et al. 2016). Moreover, we confirmed by immunofluorescence that mMABs are not only engrafted in the CC10-positive terminal bronchiolar epithelium of transplanted *F508del CFTR* mice after 6 months of engraftment, but that they simultaneously express this marker. We further demonstrated by immunofluorescence that donor engrafted mMABs, after 6 months, also express the epithelial markers Cytokeratin 6 and Cytokeratin 5, but it seems they do not differentiate in SPC+ alveolar epithelial type II cells or Acetylated a-Tubulin+ ciliated cells. Injected mMABs, once reached the colonization site, also express E-cadherin. The analysis of transplanted epithelia, performed by confocal microscopy, showed in the orthogonal projection that engrafted GFP-mMABs at 2 months already express E-cadherin, once localized in the lung and in the trachea of injected *F508del*

*CFTR* mice, suggesting their plasticity to differentiate in epithelial-like cells once engrafted in the airways.

**4.7 mMABs contribute to lung homeostasis after acute lung injury**

Since we have demonstrated engrafted-mMAB competence to express CC10, the marker of club cells, we wondered if mMABs could contribute to lung homeostasis and stem cell niches also following acute injury. To this aim, we used an established and widely accepted injury method employed for assessing upper airway epithelial regeneration, which is based on naphthalene-induced damage as described (Stripp et al. 1995; Hong et al. 2004). Naphthalene ablates noncilated bronchiolar club (Clara) cells and leads to a dramatic impairment of the epithelial structure in the bifurcations of terminal bronchioles. To test mMAB contribution to epithelial repair in the respiratory tract, for each time point 3 C57BL/6 wt mice were exposed to naphthalene. Club cell depletion is described between 24 and 120 hours after naphthalene treatment, with a maximum damage at 72 hours, when lung endogenous cells start to re-populate the injured epithelium. By 480 hours the damage is completely resolved (Stripp et al. 1995). Naphthalene-treated mice were then transplanted with 30.10^4 GFP-mMABs through the caudal vein at 24, 48 and 72 hours from the injury. As control we used 3 animals treated with vehicle alone (corn oil). Mice were then sacrificed at 72, 120, 168 and 480 hours from injury. At each time point we weighted the mice and we observed, starting from the 48 hours time point, that mMAB-injected injured mice displayed an increased body weight, compared to not injected ones, with a striking difference at 168 and 480 hours. We then evaluated the colonization of GFP-mMABs measuring, by qRT-PCR, the transcript levels of GFP of injured mice untreated and injected with GFP-mMABs at each time point. Therefore, we reported that the transcript levels of GFP are statistically significant higher in transplanted mice respect to the untreated ones, with no more GFP reported expression at 480 hours. We further confirmed mMAB engraftment by immunofluorescence at 72 hours, in correspondence with the GFP peak of expression observed in the gene expression analysis. Of note, at this time point, the majority of mMABs are proliferating, as revealed by the co-localization of GFP and Ki67 signals. Moreover, in order to evaluate a potential rescue after naphthalene damage, in terms of increased number of club cells and E-cadherin expressing cells, we analyzed the transcript levels of SCGB1a1 and E-cadherin.

Interestingly, we observed that at 168 hours, the time point at which we noticed the increased weight of mMAB-injected mice, the mRNA levels of SCGB1a1 and E-cadherin are statistically significant higher in transplanted mice, compared to untreated ones. Taken together these results, although still preliminary, demonstrate that mMABs can engraft the lung epithelium also in acute injury condition, thus contributing to its repair and homeostasis, followed by a general amelioration of the phenotype.

**4.8 mMABs, under specific stimuli, express different epithelial markers *in vitro***

To induce mMAB differentiation in epithelial cells we tested different conditions *in vitro* trying to mimic, as much as possible, the physiological, complex environment present *in vivo*. First we cultured mMABs with Human Bronchial/Tracheal Epithelial Cells (HBTEC) differentiation medium, optimized for the mucociliar differentiation of tracheal and bronchial epithelial cells, until reaching cell confluence and then we evaluated the expression of E-cadherin. From the gene expression analysis we noticed that the mRNA levels of E-cadherin increase in mMABs cultured with HBTEC medium in time, compared to mMABs cultured with the standard medium. This result was then confirmed at protein level by immunofluorescence staining. In detail, we observed how some mMABs, after 15 days in culture with HBTEC medium, start to express E-cadherin, although not completely correctly localized. In the second approach, we cultured mMABs with Small Airway Grow Medium (SAGM) until the confluence was reached. SAGM medium is a specific cell medium used for culturing alveolar cells (Ali et al. 2002). In this culture condition, mMABs express high levels of E-cadherin, properly localized in correspondence of the adherens junctions. We also analyzed by qRT-PCR the transcript levels of some epithelial and mesenchymal markers. We then found a statistical significant increase of the epithelial marker E-cadherin and that of the metalloproteinase Adam10, involved in E-cadherin's physiological turnover. In parallel, we evaluated whether the increase of the expression of epithelial markers is accompanied by the decrease of specific mesenchymal markers such as Fibronectin and Vimentin. qRT-PCR revealed a statistical significant decrease of mesenchymal markers in mMABs cultured in SAGM medium respect to the control mMABs cultured with the conventional medium. Moreover, to investigate whether the use of a specific medium for the

culture of epithelial cells was sufficient to drive mMABs towards a Mesenchymal to Epithelial Transition (MET), we also examined the mRNA levels of the Epithelial to Mesenchymal Transition (EMT) transcription factors, together with other well-known markers involved in this process. Interestingly, the transcript levels of Snail and N-cadherin are statistically significant decreased, compared to mMABs cultured in standard conditions. Finally, to confirm the loss of intrinsic muscular differentiation features of mMABs, we analyzed the expression of myogenic markers such as MyoD and Myogenin, responsible with the other Myogenic Regulatory Factors, of the differentiation of myogenic progenitors (Black & Olson 1998). Strikingly, mMABs cultured in SAGM medium display statistically significant lower mRNA levels of MyoD and Myogenin compared to mMABs cultured with conventional medium. As last *in vitro* approach, we cultured mMABs in air liquid interface (ALI) condition, which is considered the best way to mimic in culture the physiological *in vivo* respiratory environment (Jong et al. 1993; Grubb et al. 2006). To do that we co-cultured in ALI condition mMABs together with primary nasal epithelial cells extracted from *CFTR ko* mice and we analyzed E-cadherin expression by confocal microscope with a further orthogonal projection analysis. We then observed that GFP-mMABs express properly localized E-cadherin in the cell surface membrane. Taken together, all the *in vitro* data obtained confirm that mMAB have a sufficient plasticity to change their intrinsic differentiation fate towards an epithelial differentiation.

### 4.9 Clones of mMABs display different potential of epithelial commitment

As described in the State of the Art, mMABs are a polyclonal population of vessel-associated progenitor cells, able to spontaneously differentiate in skeletal muscle. Nevertheless, it has been demonstrated that different clones of mMABs are characterized by different levels of PW1 expression, thus affecting mMAB competence to differentiate in skeletal muscle and to migrate towards blood vessels wall (Bonfanti et al. 2015). We therefore cultured two different clones of mMABs named mMABs U and mMABs S, which respectively have high and low PW1 expression levels, with HBTEC medium until the confluence was reached. The aim of this experiment was to evaluate if the epithelial differentiation potential would be influenced by the intrinsic myogenic commitment of the different clones. It has been firstly observed a striking morphological change of mMABs S, which acquire an

epithelial-like phenotype compared to the same cells, cultured with the normal medium. Interestingly, this change was not observed in mMABs U, which indeed formed myotubes, as also confirmed by the immunofluorescence analysis of the sarcomeric Myosin. We then proceeded by analyzing the gene expression of some markers of interest by qRT-PCR. For what concerns the epithelial markers, we found that the mRNA levels of E-cadherin and TPJ-1 (this last encoding for the tight-junction protein ZO-1) are statistically significant higher in mMABs S cultured in HBTEC medium if compared to the same cells cultured in normal condition. This increase was not obtained with mMABs U cultured in the same way. We also evaluated the gene expression of mesenchymal markers such as *Vimentin* and *Fibronectin* and, as expected, we observed a statistical significant increase of their expression in mMABs U, while we noticed a significant decrease of *Fibronectin* in mMABs U, both cultured in HBTEC medium. Furthermore, we examined the mRNA levels of the EMT and MET transcription factors. Interestingly, the transcript levels of Snail are statistically significant increased in mMABs U; contrary to what we observed in mMABs S, compared to the same cells cultured in standard conditions. Consistent to what observed so far, the myogenic genes *MyoD* and *Myogenin* increase in mMABs U and decrease in mMABs S, after culture in HBTEC medium, suggesting that the intrinsic myogenic commitment of mMAB clones influences the epithelial differentiation potential.

# CONCLUSIONS AND FUTURE PERSPECTIVES

In the last decades the identification of progenitor cells able to differentiate into cell types which are different from their embryonic origin has determined a change of interpretation about the notion of plasticity associated to stem cells.

Studies aiming to investigate the origin of myogenic cells led to the discovery of a subpopulation of multipotent vessel-associated progenitors distinct from both embryonic and adult stem cells: the mesoangioblasts (MABs) (De Angelis et al. 1999; Minasi et al. 2002). MABs are able to self-renew and to differentiate in many mesodermal-derived tissues (Cossu & Bianco 2003) and have been isolated and characterized from embryonic and adult tissues of mouse (Minasi et al. 2002), dog (Sampaolesi et al. 2006) and human origin (Dellavalle 2007). Furthermore, the expression of endothelial receptors confers to MABs the extraordinary ability to cross blood vessel wall. *In vivo* experiments have subsequently demonstrated how systemic-delivered MABs can rescue the dystrophic phenotype in multiple pre-clinical models of DMD (Sampaolesi et al. 2003; Sampaolesi et al. 2006; Diaz-Manera et al. 2010; Tedesco et al. 2011). Thanks to these exceptional features, MABs have been considered promising candidates for a cell therapy applied to DMD. hMABs have been indeed used in a trial in DMD human patients that definitely demonstrated that intra-arterial transplantation of donor MABs in humans is feasible and safe (Cossu et al. 2015).

During studies performed to characterize MABs as a new tool for DMD, it has been observed that nLacZ-mMAB (previously transduced with nuclear LacZ lentivirus to easily detect mMABs in mouse tissues), when systemically transplanted in healthy wild type mice (C57BL/6), engraft lung, tracheal and intestinal epithelium up to one month from their transplantation. The unexpected substantial mMAB engraftment in the respiratory and intestinal epithelia represented the starting point to consider these cells as a potential tool for a cell-based therapy for Cystic Fibrosis, which indeed mainly affects the airway and intestinal tracts. The ability of MABs to cross the vessel wall and their systemic delivery confer them an advantage as therapeutic donor cells, compared with other stem populations that need to be delivered directly into the airways, facing significant physical/immunological obstacles. Between the different tested approaches to cure CF, cell therapy indeed still did not give good results. The reasons rely in the low engraftment in the lungs after systemic or intra-tracheal

administration of donor cells, in the small percentage of cells differentiated in airway epithelia and in the even less percentage of CFTR expression (Murphy and Atala 2013; Sueblinvong and Weiss 2010; Weiss 2014).

The results presented here demonstrate mMAB exceptional homing towards the epithelia of the most compromised organs in CF, such as the lungs and intestine. The substantial engraftment does not affect the structure, morphology or functionality of the target organs, while on the contrary corroborates mMAB tropism towards the epithelia, even in absence of an inflammatory or damaged status, as in this case in healthy wild type mice. Furthermore, the consolidated demonstration that MABs are not tumorigenic is of fundamental importance for a therapeutic use of these cells.

In the light of this evidence and of the previous literature, which reports numerous examples of not epithelial cells expressing CFTR channel, such as skeletal muscle cells (Divangahi et al. 2009; Vandebrouck et al. 2006), endothelial cells (Robert et al. 2007), macrophages (Di et al. 2006), chondrocytes and osteoblasts (Liang et al. 2010; Bronckers et al. 2010), we also investigated on mMAB capability to express this channel, whose dysfunction causes CF disease, demonstrating the presence of CFTR mRNA. The over-expression of the *wt CFTR* form shows high CFTR activity in electrophysiological *in vitro* studies, thus demonstrating that mMABs have the proper cellular mechanisms necessary to express a correctly localized and functional CFTR channel. This evidence was of fundamental relevance in order to go on with mMAB transplantation in CF mouse models and to understand if the potential rescue would have been due to paracrine effects or to mMAB ability, once engrafted, to express a functional CFTR channel. Actually, the prove that mMABs can express a functional CFTR channel was obtained *in vivo*, by transplanting them in the *CFTR ko* mouse model (*KOCftr*$^{tm1UNC}$ mice*;* Snouwaert et al. 1992), which does not express any CFTR protein and recapitulates the electrophysiological abnormalities observed in individuals affected by CF (Clarke et al. 1992; Grubb et al., 2002; Fischer et al., 2002). We indeed observed that, once engrafted in the nasal and intestinal epithelia of *CFTR ko* mice, mMABs lead to a significant rescue of CFTR-dependent chloride secretions, as measured in electrophysiological assays. This evidence is striking, since it has been evaluated that the level of normal CFTR message necessary to provide normal airway/lung function is estimated to be around 8% (Chu et al. 1992; Johnson et al. 1992; Dorin et al. 1996). Moreover, since *CFTR ko* mice display high mortality at the weaving time when kept in normal diet (90% of mortality), their

survival upon mMAB transplantation is currently under investigation. This potential result is of extreme importance in view of a future cell therapy for CF.

We were also able to demonstrate that mMABs, upon a single systemic transplantation, efficiently engraft the airway epithelium in *CFTR ko* mice up to four months and in the CF mouse model *F508del CFTR* up to six months. This second model was used because it carries the same mutation that affects almost the 70% of human patients (van Doorninck et al. 1995) and represents a valuable tool for studying certain aspects of CF lung disease, albeit not reproducing all the aspects of the pathology (van Doorninck et al. 1995; Clarke et al. 1992; Wilke et al. 2011). This data is extremely interesting, since the stem cells tested so far did not show comparable results in terms of time lasting and extent of engraftment (Murphy and Atala 2013; Weiss 2014). Moreover, the demonstration that other populations of mMABs share the same features prove that mMAB epithelial engraftment is an intrinsic and specific property of mMABs, regardless of a particular mMAB cell preparation. Furthermore, the significant reduction of the TNF-α transcript in the lungs of *F508del CFTR* transplanted mice, only after two months from mMAB administration, although preliminary is cheering. Certainly we will deeply analyze this issue at later time points and in view of increasing the engraftment and the subsequent potential amelioration of the inflammatory status, we are now performing multiple mMAB injection in CF mice during time.

Reports of MABs derived from bone marrow, atria and ventricles, aorta and skeletal muscle have focused primarily on their myogenic potential. As Minasi previously suggested in his work, MAB plasticity towards ectoderm or endoderm has never been properly documented, even if he indeed reported some MAB engraftment in the epidermis (Minasi et al. 2002). Interestingly, Berry's group recently reported that MABs, under specific stimuli, are also able to differentiate in oligodendrocytes, Schwann cells, and uterine epithelium, all deriving from the ectoderm (Berry et al. 2007; Wang et al. 2012; Simon et al. 2013). All these data support the hypothesis that MABs are also capable to differentiate, if properly stimulated, in many different tissues deriving not only from mesoderm but also from ectoderm. The obtained data made us speculate about the possibility, never investigated so far, that MABs could participate to the engrafted epithelium and/or to its stem cell niches. This hypothesis is indeed supported by the observation that mMABs localize in the intestine also at

the level of the crypts of Lieberkühn, known source of highly proliferating stem cells. The characterization of the markers expressed by mMABs once engrafted in the intestine is still on going, but will for sure shed light on the possibility to apply MAB transplantation even to other degenerative intestinal pathologies. Furthermore, for what concerns the respiratory epithelium, even if the resident stem cells are distributed through the entire tract, we observed that mMABs preferentially engraft the ciliated columnar epithelium of the trachea and bronchioles, where are respectively located p63+ basal cells and SCGB1a1+ club cells (Weiss et al. 2011). We hypothesized that the epithelial environment could drive mMABs towards an epithelial fate, since they showed a good tropism to epithelial tissues. This could explain MAB plasticity that would make them an eligible tool for two completely different pathologies such as the Muscular Dystrophies and CF. Moreover, the ability of MABs to differentiate in epithelial cells would represent an incredible advantage in a cell therapy approach, since these cells would not only reconstitute CFTR activity, but also contribute to the epithelial homeostasis.

Our present results indicate that donor-derived mMABs express the epithelial marker E-cadherin and, surprisingly, the univocal marker of club cells CC10. Despite these last cells were firstly identified in 1881 by Kolliker, to date their physiological functions still remain not completely clarified. It is known from the literature that club cells have a role of progenitor/stem cell (Kotton & Morrisey 2014). Moreover, it also seems that CC10 limits lung inflammation *in vivo* (Singh & Katyal 1997). This evidence is particularly interesting, together with the observation that donor-derived mMABs do not express markers of highly specialized and differentiated respiratory epithelial cells, such as alveolar epithelial type II cells or ciliated cells and that their proliferation once engrafted is quite rare (adult lung cells are indeed almost quiescent). We indeed speculated that mMABs, once reached the lung, could contribute to its homeostasis and stem cell niches, trans-differentiating in epithelial progenitors. This hypothesis was also preliminary confirmed in a condition of acute lung injury, injecting naphthalene in wild type mice to ablate club cells. Using this method, first of all we demonstrated that naphthalene-treated, mMAB-injected mice display an increased body weight from the 48 hours time point, with a striking difference at 168 and 480 hours respect to controls, indicating a general phenotypic amelioration. Furthermore, our present results also indicate that naphthalene-treated, mMAB-injected mice have higher levels of SCGB1a1 and E-cadherin mRNA, which

respectively correlate with a rescue in club cells number and re-epithelialization, thus demonstrating that mMABs can engraft the lung epithelium also in acute injury condition, contributing to its repair and homeostasis. The reason of the lack of detected GFP signal at 480 hours is still under investigation; we speculated that probably the inflammation is anyway so high to provoke the elimination of exogenous transplanted cells.

Finally, we also started to investigate the possible mechanisms through which mMABs could be driven towards an epithelial differentiation *in vitro*. Culturing mMABs with Small Airway Grow Medium (SAGM), specific for alveolar cells (Ali et al. 2002), provokes an increase of the expression of epithelial markers (E-cadherin and its metalloproteinase Adam10) together with a decrease of mesenchymal (Fibronectin and Vimentin) and myogenic ones (MyoD and Myogenin). We therefore hypothesized that the differentiation of mMABs into epithelial cells could be driven by the reverse of the Epithelial to Mesenchymal Transition, the Mesenchymal to Epithelial Transition process. The well-described EMT implies the conversion of an epithelial into a mesenchymal cell with the ability to migrate and invade adjacent tissues (Acloque et al. 2009; Alipio et al. 2011; RIPPON et al. 2006). This process during embryo development, fibrosis and cancer cell dissemination, is triggered in response to extracellular signals (Thiery et al. 2009; Nieto 2011), which in turns activate one or several pleiotropic transcription factors (TFs), belonging to different families, including Snail, Twist, Zeb, and others (Peinado et al. 2007). These EMT-TFs, induce the EMT program by directly repressing epithelial molecules (such as E-Cadherin, ZO-1, cytokeratins) and by enhancing the expression of mesenchymal markers (e.g. N-Cadherin, Vimentin, α-SMA, Fibronectin), leading to a complete phenotypic switch from epithelial to mesenchymal (Peinado 2007). Although many signaling pathways for EMT have been identified, the signals involved in the activation of MET have not been well characterized so far (Craene & Berx 2012); nevertheless it has been demonstrated that MET is strictly associated to the loss of migratory capacity and acquisition of adhesive properties (Li et al. 2011). All these evidences correlate with our present results, together with the decrease of the expression of the TF Snail and the marker N-cadherin in mMABs cultured in SAGM. Our data let suppose that mMABs, if properly conditioned, could undergo a MET, process that we will deeply study by re-isolating donor-derived mMABs and

analyzing their gene expression profile by using customized qRT-PCR cards, to evaluate the expression of epithelial/mesencymal/MET/stemness markers prior and after mMAB engraftment.

Finally, we are now approaching to hMABs as first step towards a clinical use of MABs in CF. We will evaluate hMAB ability to express CFTR, to be driven towards an epithelial differentiation and also to engraft the epithelia of immunodeficient-CF mice to avoid hMABs rejection (i.e. *SCID-F508del CFTR* and *SCID-KOCftr*$^{tm1UNC}$ mouse models).

In conclusion, this body of evidence represents a major advance over any other cell-based therapeutic strategy for CF. We believe we can now answer a range of basic questions regarding the mechanisms of cell engraftment in lung epithelium that can have the potential to direct future research into therapeutic concrete goals. MAB homing towards the epithelium of the main compromised organs in CF, their persistence over time and their capability to rescue CFTR function make these cells eligible for a cell based therapy of CF. Therefore, this project is of major relevance to public health and to CF patients. This experimental strategy will lead to future clinical translation; the results obtained from this project will indeed represent the first step towards a pre-clinical study in more severe models such as the CF pigs (Rogers et al. 2008). Notably, this study may also generate a conceptual insight highly relevant in the cell-based therapy field, not only limited to CF.

# REFERENCES


Accurso, F.J. et al., 2010. Effect of VX-770 in Persons with Cystic Fibrosis and the G551D- CFTR Mutation. *N Engl J Med*, 363(21), pp.1991–2003.

Acloque, H. et al., 2009. Epithelial-mesenchymal transitions: The importance of changing cell state in development and disease. *Journal of Clinical Investigation*, 119(6), pp.1438–1449.

Ali, N.N. et al., 2002. Derivation of type II alveolar epithelial cells from murine embryonic stem cells. *Tissue Eng*, 8(4), pp.541–550.

Alipio, Z.A. et al., 2011. Epithelial to mesenchymal transition (EMT) induced by bleomycin or TFG.

Alton, E. et al., 2015. Repeated nebulisation of non-viral *CFTR* gene therapy in patients with cystic fibrosis: a randomised, double-blind, placebo-controlled, phase 2b trial. *Lancet Respir Med.,* 3(9), pp.684–691.

Andersen, D., 1938. Cystic fibrosis of the pancreas and its relation to celiac disease. *Am. J. Dis. Child.*, 56, pp.344-399.

De Angelis, L. et al., 1999. Skeletal myogenic progenitors originating from embryonic dorsal aorta coexpress endothelial and myogenic markers and contribute to postnatal muscle growth and regeneration. *Journal of Cell Biology*, 147(4), pp.869–877.

Anon, 2014. Cystic Fibrosis Foundation Patient Registry 2013 Annual Data Report to the Center Directors. *Cystic Fibrosis Foundation*, pp.1–92.

Anversa, P. et al., 2011. Tissue-specific adult stem cells in the human lung. *Nature medicine*, 17(9), pp.1038–1039.

Armstrong, D.K. et al., 2014. Gene therapy in cystic fibrosis. *Translational Research*, 161(4), pp.255–264.

Aurora, P., Spencer, H. & Moreno-Gald??, A., 2008. Lung transplantation in children with cystic fibrosis: A view from Europe. *American Journal of Respiratory and Critical Care Medicine*, 177(9), pp.935–936.

Barkauskas CE, Cronce MJ, Rackley CR, Bowie EJ, Keene DR, Stripp BR, Randell SH, Noble PW, H.B., 2013. Type 2 alveolar cells are stem cells in adult lung. *J Clin Invest*, 123(7), pp.3025–3036.

Barr, H.L. et al., 2011. Association between socioeconomic status, sex, and age at death from cystic fibrosis in England and Wales (1959 to 2008): cross sectional study. *BMJ (Clinical research ed.)*, 343, p.d4662.

Bender Kim, C.F. et al., 2005. Identification of bronchioalveolar stem cells in normal lung and lung cancer. *Cell*, 121(6), pp.823–835.

Berry, S.E. et al., 2007. Multipotential mesoangioblast stem cell therapy in the mdx / utrn -/- mouse model for Duchenne muscular dystrophy. , 2, pp.275–288.

Bianco, P. & Cossu, G., 1999. Uno, nessuno e centomila: searching for the identity of mesodermal progenitors. *Experimental cell research*, 251(2), pp.257–263.

Bjornson, C.R. et al., 1999. Turning brain into blood: a hematopoietic fate adopted by adult neural stem cells in vivo. *Science*, 283(5401), pp.534–537.

Black, B.L. & Olson, E.N., 1998. Transcriptional Control of Muscle Development By Myocyte Enhancer Factor-2 (Mef2) Proteins. *Annu. Rev. Cell Dev. Biol*, 14, pp.167–96.

Bobadilla, J.L. et al., 2002. Cystic fibrosis: A worldwide analysis of CFTR mutations - Correlation with incidence data and application to screening. *Human Mutation*, 19(6), pp.575–606.

Bonfanti, C. et al., 2015. PW1/Peg3 expression regulates key properties that determine mesoangioblast stem cell competence. *Nature communications*, 6(May 2014), p.6364.

Borowitz, D. et al., 2002. Consensus report on nutrition for pediatric patients with cystic fibrosis. *Journal of pediatric gastroenterology and nutrition*, 35(September), pp.246–259.

Borowitz, D. et al., 2009. Cystic fibrosis Foundation evidence-based guidelines for management of infants with cystic fibrosis. *Journal of Pediatrics*, 155(6 SUPPL.), pp.S73–S93.

Borthwick, D.W. et al., 2001. Evidence for stem-cell niches in the tracheal epithelium. *American Journal of Respiratory Cell and Molecular Biology*, 24(6), pp.662–670.

Boucher, R.C., 2007. Airway surface dehydration in cystic fibrosis: pathogenesis and therapy. *Annual review of medicine*, 58, pp.157–170.

Bove, P.F. et al., 2010. Human alveolar type II cells secrete and absorb liquid in response to local nucleotide signaling. *J. Biol. Chem.*, 285(45), pp.34939–49.

Boyle, M.P., 2003. Nonclassic cystic fibrosis and CFTR-related diseases. *Current opinion in pulmonary medicine*, 9(6), pp.498–503.

BRANDT, I. et al., 1985. TARGET CELLS FOR THE POLYCHLORINATED BIS(METHYLSULFONYL)-2,2',5,5'-TETRACHLOROBIPHENYL IN LUNG AND KIDNEY.

, pp.490–496.
Brazelton, T.R. et al., 2000. From marrow to brain: expression of neuronal phenotypes in adult mice. *Science (New York, N.Y.)*, 290(5497), pp.1775–9.
Bronckers, A. et al., 2010. Regulator ( Cftr ) Is Expressed in Maturation Stage. , 46(4), pp.1188–1196.
Bruscia, E.M. et al., 2006. Assessment of cystic fibrosis transmembrane conductance regulator (CFTR) activity in CFTR-null mice after bone marrow transplantation. *Proc.Natl.Acad.Sci.U.S.A.*, 103(8), pp.2965–2970.
Bruscia, E.M. et al., 2006. Engraftment of donor-derived epithelial cells in multiple organs following bone marrow transplantation into newborn mice. *Stem cells (Dayton, Ohio)*, 24(10), pp.2299–308.
Bruscia, E.M. et al., 2009. Macrophages directly contribute to the exaggerated inflammatory response in cystic fibrosis transmembrane conductance regulator-/-mice. *American Journal of Respiratory Cell and Molecular Biology*, 40(3), pp.295–304.
Burns, J.L. et al., 2001. Longitudinal assessment of Pseudomonas aeruginosa in young children with cystic fibrosis. *The Journal of infectious diseases*, 183(3), pp.444–452.
Carraro, G. et al., 2008. Human Amniotic Fluid Stem Cells Can Integrate and Differentiate into Epithelial Lung Lineages. *Stem Cells*, 26(11), pp.2902–2911.
Chapman, H.A. et al., 2011. Integrin α6β4 identifies an adult distal lung epithelial population with regenerative potential in mice. *Journal of Clinical Investigation*, 121(7), pp.2855–2862.
Chen, H. et al., 2012. Airway epithelial progenitors are region specific and show differential responses to bleomycin-induced lung injury. *Stem Cells*, 30(9), pp.1948–1960.
Cheng, S.H. et al., 1990. Defective intracellular transport and processing of CFTR is the molecular basis of most cystic fibrosis. *Cell*, 63(4), pp.827–834.
Chernick, Barbero, G., 1959. COMPOSITION OF TRACHEOBRONCHIAL SECRETIONS IN CYSTIC FIBROSIS OF THE PANCREAS AND BRONCHIECTASIS. *Pediatrics*, 24, pp.739–745.
Chu, C.S. et al., 1992. Extensive posttranscriptional deletion of the coding sequences for part of nucleotide-binding fold 1 in respiratory epithelial mRNA transcripts of the cystic fibrosis transmembrane conductance regulator gene is not associated with the clinical manifestati. *The Journal of clinical investigation*, 90(3), pp.785–90.
Clancy, J.P. et al., 2001. Evidence that systemic gentamicin suppresses premature stop mutations in patients with cystic fibrosis. *American Journal of Respiratory and Critical Care Medicine*, 163(7), pp.1683–1692.
Clarke, L.L. et al., 1992. Defective Epithelial Chloride Transport in a Gene-Targeted Mouse Model of Cystic Fibrosis. *Science*, 257(5073), pp.1125–1128.
Clevers, H., 2005. Stem cells, asymmetric division and cancer. *Nature genetics*, 37(4), pp.1027–1028.
Condorelli, G. et al., 2001. Cardiomyocytes induce endothelial cells to trans-differentiate into cardiac muscle: implications for myocardium regeneration. *Proceedings of the National Academy of Sciences of the United States of America*, 98(19), pp.10733–10738.
Cossu, G. et al., 2015. Intra-arterial transplantation of HLA-matched donor mesoangioblasts in Duchenne muscular dystrophy. *EMBO molecular medicine*, 7(12), pp.1513–28.
Cossu, G. & Bianco, P., 2003. Mesoangioblasts - Vascular progenitors for extravascular mesodermal tissues. *Current Opinion in Genetics and Development*, 13(5), pp.537–542.
Craene, B. & Berx, G., 2012. Regulatory networks defining EMT during cancer initiation and progression. *Nature reviews. Cancer*, 13(2), pp.97–110.
Crystal, R.G. et al., 1994. Administration of an adenovirus containing the human CFTR cDNA to the respiratory tract of individuals with cystic fibrosis. *Nature genetics*, 8(1), pp.42–51.
Cutting, G.R., 2015. Cystic fibrosis genetics: from molecular understanding to clinical application. *HHS Public Access*, 16(1), pp.45–56.
Cutting, G.R., 2010. Modifier genes in Mendelian disorders: the example of cystic fibrosis. , pp.57–69.
Cyr, D.M., 2005. Arrest of CFTRΔF508 folding. *Nature Structural & Molecular Biology*, 12(1), pp.2–3.
Cystic Fibrosis Foundation, 2012. Patient Registry. Annual Data Report 2012. , p.28.
Dalemans, W. et al., 1991. Altered chloride ion channel kinetics associated with the DF508 cystic fibrosis mutation. *Nature*, 354, pp.526–528.
Davies, J.C. et al., 2013. Efficacy and safety of ivacaftor in patients aged 6 to 11 years with cystic fibrosis with a G551D mutation. *American Journal of Respiratory and Critical Care Medicine*, 187(11), pp.1219–1225.
Davis, P.B., 2006. Cystic fibrosis since 1938. *American Journal of Respiratory and Critical Care Medicine*, 173(5), pp.475–482.

Dellavalle, A., 2007. Pericytes of human skeletal muscle are myogenic precursors distinct from satellite cells. , 9(3), pp.1–20.

Derichs, N. et al., 2011. Hyperviscous airway periciliary and mucous liquid layers in cystic fibrosis measured by confocal fluorescence photobleaching. *The FASEB journal : official publication of the Federation of American Societies for Experimental Biology*, 25, pp.2325–2332.

Di, A. et al., 2006. CFTR regulates phagosome acidification in macrophages and alters bactericidal activity. *Nature cell biology*, 8(9), pp.933–44.

Díaz-Manera, J. et al., 2010. Partial dysferlin reconstitution by adult murine mesoangioblasts is sufficient for full functional recovery in a murine model of dysferlinopathy. *Cell death & disease*, 1, p.e61.

Divangahi, M. et al., 2009. Lack of CFTR in skeletal muscle predisposes to muscle wasting and diaphragm muscle pump failure in cystic fibrosis mice. *PLoS Genetics*, 5(7).

Dobbs, L. et al., 2010. The great big alveolar TI cell: Evolving concepts and paradigms. *Cellular Physiology and Biochemistry*, 25(1), pp.55–62.

Doe, C.Q. & Bowerman, B., 2001. Asymmetric cell division: Fly neuroblast meets worm zygote. *Current Opinion in Cell Biology*, 13(1), pp.68–75.

Domi, T. et al., 2015. Mesoangioblast delivery of miniagrin ameliorates murine model of merosin-deficient congenital muscular dystrophy type 1A. *Skeletal muscle*, 5, p.30.

Donaldson, S.H. et al., 2006. Mucus clearance and lung function in cystic fibrosis with hypertonic saline. *The New England journal of medicine*, 354(3), pp.241–250.

van Doorninck, J.H. et al., 1995. A mouse model for the cystic fibrosis delta F508 mutation. *The EMBO journal*, 14(18), pp.4403–4411.

Dorin, J.R. et al., 1996. A demonstration using mouse models that successful gene therapy for cystic fibrosis requires only partial gene correction. *Gene Ther*, 3(9), pp. 797-801.

Dranchak, P.K. et al., 2011. NIH Public Access. , 112(5), pp.1250–1258.

Driskell, R.A. & Engelhardt, J.F., 2003. Current status of gene therapy for inherited lung diseases. *Annual review of physiology*, 65(1), pp.585–612.

Egan, T.M., 2008. Solid benefit of lung transplantation for some children with cystic fibrosis. *Pediatric Transplantation*, 12(2), pp.125–128.

Elder, D. a et al., 2007. Glucose tolerance, insulin secretion, and insulin sensitivity in children and adolescents with cystic fibrosis and no prior history of diabetes. *The Journal of pediatrics*, 151, pp.653–658.

Elkins, M.R. et al., 2006. A Controlled Trial of Long-Term Inhaled Hypertonic Saline in Patients with Cystic Fibrosis. , 354(3), pp.229–240.

Emerson, J. et al., 2002. Pseudomonas aeruginosa and other predictors of mortality and morbidity in young children with cystic fibrosis. *Pediatric Pulmonology*, 34(2), pp.91–100.

Engelhardt, J.F. et al., 1995. Progenitor cells of the adult human airway involved in submucosal gland development. *Development*, 121(7), pp.2031–2046.

English, K. et al., 2013. Mesoangioblasts suppress T cell proliferation through IDO and PGE-2-dependent pathways. *Stem cells and development*, 22(3), pp.512–23.

Epperly, M.W. et al., 2003. Bone marrow origin of myofibroblasts in irradiation pulmonary fibrosis. *American Journal of Respiratory Cell and Molecular Biology*, 29(2), pp.213–224.

Evans, M.J. et al., 1978. Role of Clara cell in renewal of the bronchiolar epithelium. *Lab Invest,* 38, pp.648-653.

Farrell, P.M., 2008. The prevalence of cystic fibrosis in the European Union. *Journal of Cystic Fibrosis*, 7(5), pp.450–453.

Ferrari, G. et al., 1998. Muscle regeneration by bone marrow-derived myogenic progenitors. *Science (New York, N.Y.)*, 279(March), pp.1528–1530.

Fischer H., 2002. Electrophysiological approach to studying CFTR. *Methods Mol Med*., 70, pp. 49-65.

Flotte, T.R. et al., 2005. Correlation between DNA transfer and cystic fibrosis airway epithelial cell correction after recombinant adeno-associated virus serotype 2 gene therapy. *Hum.Gene Ther.*, 16(8), pp.921–928.

Flume, P. a et al., 2007. Cystic Fibrosis Pulmonary Guidelines. *American Journal of Respiratory and Critical Care Medicine*, 176, pp.957–969.

Galli, R. et al., 2000. Skeletal myogenic potential of human and mouse neural stem cells. *Nat Neurosci*, 3(10), pp.986–991.

Galvez, B.G. et al., 2006. Complete repair of dystrophic skeletal muscle by mesoangioblasts with enhanced migration ability. *Journal of Cell Biology*, 174(2), pp.231–243.

Ghosh, M. et al., 2011. Context-dependent differentiation of multipotential keratin 14-expressing tracheal basal cells. *American Journal of Respiratory Cell and Molecular Biology*, 45(2),

pp.403–410.
Giangreco, A., Reynolds, S.D. & Stripp, B.R., 2016. Terminal Bronchioles Harbor a Unique Airway Stem Cell Population That Localizes to the Bronchoalveolar Duct Junction. *The American Journal of Pathology*, 161(1), pp.173–182.
Goldberg, H.J. & Deykin, A., 2007. Advances in Lung Transplantation for Patients Who Have Cystic Fibrosis. *Clinics in Chest Medicine*, 28(2), pp.445–457.
Van Goor, F. et al., 2011. Correction of the F508del-CFTR protein processing defect in vitro by the investigational drug VX-809. *Proceedings of the National Academy of Sciences of the United States of America*, 108(46), pp.18843–8.
Van Goor, F. et al., 2009. Rescue of CF airway epithelial cell function in vitro by a CFTR potentiator, VX-770. *Proceedings of the National Academy of Sciences of the United States of America*, 106(44), pp.18825–30.
Goss, C.H. et al., 2007. Cystic Fibrosis Pulmonary Guidelines. *American Journal of Respiratory and Critical Care Medicine*, 176, pp.957–969.
Griesenbach, U., Geddes, D. & Alton, E., 2006. Gene therapy progress and prospects: cystic fibrosis. *Gene therapy*, 13, pp.1061–1067.
Grubb, B.R. et al., 2006. Culture of murine nasal epithelia: model for cystic fibrosis. *American journal of physiology. Lung cellular and molecular physiology*, 290(2), pp.L270–L277.
Grubb, B.R. & Boucher, R.C., 1999. Pathophysiology of gene-targeted mouse models for cystic fibrosis. *Physiological reviews*, 79(1), pp.S193–S214.
Grubb, B.R., 2002. Bioelectric measurement of CFTR function in mice. *Methods Mol Med*., 70, pp. 525-535.
Guilbault, C. et al., 2007. Cystic fibrosis mouse models. *American Journal of Respiratory Cell and Molecular Biology*, 36(1), pp.1–7.
Gupta, N. et al., 2007. Intrapulmonary delivery of bone marrow-derived mesenchymal stem cells improves survival and attenuates endotoxin-induced acute lung injury in mice. *J Immunol*, 179(3), pp.1855–1863.
Gupta, N. et al., 2012. Mesenchymal stem cells enhance survival and bacterial clearance in murine Escherichia coli pneumonia. *Thorax*, 67(6), pp.533–9.
Haardt, M. et al., 1999. C-terminal truncations destabilize the cystic fibrosis transmembrane conductance regulator without impairing its biogenesis. A novel class of mutation. *Journal of Biological Chemistry*, 274(31), pp.21873–21877.
Hammerle, M.M., Aleksandrov, A.A. & Riordan, J.R., 2001. Disease-associated Mutations in the Extracytoplasmic Loops of Cystic Fibrosis Transmembrane Conductance Regulator Do Not Impede Biosynthetic Processing but Impair Chloride Channel Stability. *Journal of Biological Chemistry*, 276(18), pp.14848–14854.
Hartl, D. et al., 2007. Cleavage of CXCR1 on neutrophils disables bacterial killing in cystic fibrosis lung disease. *Nature medicine*, 13(12), pp.1423–30.
Herzog, E.L. et al., 2006. Threshold of lung injury required for the appearance of marrow-derived lung epithelia. *Stem cells (Dayton, Ohio)*, 24(8), pp.1986–92.
Highsmith, W.E. et al., 1997. Identification of a splice site mutation (2789 + 5 G>A) associated with small amounts of normal CFTR mRNA and mild cystic fibrosis. *Human Mutation*, 9(4), pp.332–338.
Hirschi, K.K. & D'Amore, P. a, 1996. Pericytes in the mircovasculature. *Cardiovascular Research*, 32, pp.687–698.
Hong, K.U. et al., Clara Cell Secretory Protein – Expressing Cells of the Airway Neuroepithelial Body Microenvironment Include a Label-Retaining Subset and Are Critical for Epithelial Renewal after Progenitor Cell Depletion. , (8).
Hong, K.U. et al., 2004. In vivo differentiation potential of tracheal basal cells: evidence for multipotent and unipotent subpopulations. *Am J Physiol Lung Cell Mol Physiol*, 286(4), pp.L643–9.
Islam, M.N. et al., 2013. Mitochondrial transfer from bone marrow-derived stromal cells to pulmonary alveoli protets against acute lung injury. *Nature Medicine*, 18(5), pp.759–765.
Ivanova, N.B. et al., 2010. R EPORTS A Stem Cell Molecular Signature. , 601(2002).
Jackson, K. a, Mi, T. & Goodell, M. a, 1999. Hematopoietic potential of stem cells isolated from murine skeletal muscle. *Proceedings of the National Academy of Sciences of the United States of America*, 96(25), pp.14482–14486.
Johnson, L.G. et al., 1992. Efficiency of gene transfer for restoration of normal airway epithelial function in cystic fibrosis. *Nature genetics*, 2(1), pp.21–25.
Jong, P.M. De et al., 1993. Ciliogenesis in Human Bronchial Epithelial Cells Cultured at the Air-

Liquid Interface.
Joseph M. Collaco & Cutting, G.R., 2008. Update on gene modifiers in cystic fibrosis. *Curr Opin Pulm Med*, 14(6), pp.559–566.
Joseph, P.M. et al., 2001. Aerosol and lobar administration of a recombinant adenovirus to individuals with cystic fibrosis. I. Methods, safety, and clinical implications. *Hum Gene Ther*, 12(11), pp.1369–1382.
Karnati, S. et al., 2016. Postnatal development of the bronchiolar club cells of distal airways in the mouse lung: stereological and molecular biological studies. *Cell and Tissue Research*.
Karnati, S. & Baumgart-Vogt, E., 2008. Peroxisomes in mouse and human lung: Their involvement in pulmonary lipid metabolism. *Histochemistry and Cell Biology*, 130(4), pp.719–740.
Kassmer, S.H. et al., 2012. Nonhematopoietic Cells are the Primary Source of Bone Marrow- Derived Lung Epithelial Cells. *Stem Cells*, 30(3), pp.491–499.
Kassmer, S.H. & Krause, D.S., 2010. Detection of Bone Marrow Derived Lung Epithelial Cells Susannah. , 38(7), pp.564–573.
Keating, A., 2012. Mesenchymal stromal cells: New directions. *Cell Stem Cell*, 10(6), pp.709–716.
Kerem, B. et al., 1989. Identification of the Cystic Fibrosis Gene: Genetic Analysis. *Science*, 245(4922), pp.1073–1080.
Kerem, E. et al., 2014. Ataluren for the treatment of nonsense-mutation cystic fibrosis: A randomised, double-blind, placebo-controlled phase 3 trial. *The Lancet Respiratory Medicine*, 2(7), pp.539–547.
Kerem, E. et al., 2008. Effectiveness of PTC124 treatment of cystic fibrosis caused by nonsense mutations: a prospective phase II trial. *The Lancet*, 372(9640), pp.719–727.
Kerr, I.D., 2002. Structure and association of ATP-binding cassette transporter nucleotide-binding domains. *Biochimica et Biophysica Acta - Biomembranes*, 1561(1), pp.47–64.
Khan, T. et al., 1995. Early pulmonary inflammation in Infants with Cystic Fibrosis. *Am J Respir Crit Care Med*, 151, pp.1075–1082.
Kim, S.J. & Skach, W.R., 2012. Mechanisms of CFTR folding at the endoplasmic reticulum. *Frontiers in Pharmacology of Ion Channels and Channelopathies*, 3(December), p.201.
Kimble, J.E. & White, J.G., 1981. On the control of germ cell development in Caenorhabditis elegans. *Developmental Biology*, 81(2), pp.208–219.
Knowles, M.R. et al., 1995. A Controlled Study of Adenoviral-Vector-Mediated Gene Transfer in the Nasal Epithelium of Patients with Cystic Fibrosis. *N Engl J Med*, 333(13), pp.823–831.
Konstan, M.W. et al., 2004. Compacted DNA nanoparticles administered to the nasal mucosa of cystic fibrosis subjects are safe and demonstrate partial to complete cystic fibrosis transmembrane regulator reconstitution. *Human gene therapy*, 15(12), pp.1255–1269.
Konstan, M.W. et al., 1995. Effect of high-dose ibuprofen in patients with cystic fibrosis. *The New England journal of medicine*, 332(13), pp.848–854.
Konstan, M.W. et al., 2007. Risk Factors For Rate of Decline in Forced Expiratory Volume in One Second in Children and Adolescents with Cystic Fibrosis. *Journal of Pediatrics*, 151(2).
Kopp, B.T. et al., 2015. Detrimental effects of secondhand smoke exposure on infants with cystic fibrosis. *Pediatric Pulmonology*, 50(1), pp.25–34.
Kosorok, M.R. et al., 2001. Acceleration of lung disease in children with cystic fibrosis after Pseudomonas aeruginosa acquisition. *Pediatric pulmonology*, 32(June), pp.277–287.
Kotton, D.N., Fabian, A.J. & Mulligan, R.C., 2005. Rapid Communication. *Cellular & Molecular Biology (Oxford)*.
Kotton, D.N. & Morrisey, E.E., 2014. Lung regeneration: mechanisms, applications and emerging stem cell populations. *Nat Med*, 20(8), pp.822–832.
Kovesi, T. et al., 1998. Meta-analyses and large randomized, controlled trials. The New England journal of medicine, 338 (1), pp.61-62.
Krasnodembskaya, a. et al., 2012. Human mesenchymal stem cells reduce mortality and bacteremia in gram-negative sepsis in mice in part by enhancing the phagocytic activity of blood monocytes. *AJP: Lung Cellular and Molecular Physiology*, 302(March), pp.L1003–L1013.
Krasnodembskaya, A. et al., 2012. Antibacterial Effect of Human Mesenchymal Stem Cells Is Mediated in Part from Secretion of the Antimicrobial Peptide LL-37. *Stem Cells*, 28(12), pp.2229–2238.
Kumar, P.A. et al., 2014. Distal Airway Stem Cells Render Alveoli in Vitro and During Lung Regeneration Following H1N1 Influenza Infection. 147(3), pp.525–538.
Lagasse, E. et al., 2000. Purified hematopoietic stem cells can differentiate into hepatocytes in vivo. *Nature Medicine*, 6(11), pp.1229–1234.
Lai, H.J., Cheng, Y. & Farrell, P.M., 2005. The survival advantage of patients with cystic fibrosis

diagnosed through neonatal screening: Evidence from the United States cystic fibrosis Foundation Registry data. *Journal of Pediatrics*, 147(3 SUPPL.), pp.57–63.

Lama, V.N. et al., 2007. Evidence for tissue-resident mesenchymal stem cells in human adult lung from studies of transplanted allografts. *Journal of Clinical Investigation*, 117(4), pp.989–996.

Lands, L.C. et al., 2007. High-Dose Ibuprofen in Cystic Fibrosis: Canadian Safety and Effectiveness Trial. *Journal of Pediatrics*, 151(3), pp.249–254.

Leeman, K.T., Fillmore, C.M. & Kim, C.F., 2014. Lung Stem and Progenitor Cells in Tissue Homeostasis and Disease. *Current Topics in Developmental Biology*, 107, pp.207–233.

Li, B. et al., 2011. Evidence for mesenchymal-epithelial transition associated with mouse hepatic stem cell differentiation. *PLoS ONE*, 6(2).

Li, O. et al., 2013. Human iPSC-derived mesoangioblasts, like their tissue-derived counterparts, suppress T cell proliferation through IDO- and PGE-2-dependent pathways. *F1000Research*, 2(0), p.24.

Liang, H. et al., 2010. Functional expression of cystic fibrosis transmembrane conductance regulator in mouse chondrocytes. *Clinical and Experimental Pharmacology and Physiology*, 37, pp.506–508.

Liou, T.G. et al., 2007. Lung Transplantation and Survival in Children with Cystic Fibrosis. *N Engl J Med.*, 357(21), pp.2143–2152.

Loi, R. et al., 2006. Limited restoration of cystic fibrosis lung epithelium in vivo with adult bone marrow-derived cells. *American Journal of Respiratory and Critical Care Medicine*, 173(2), pp.171–179.

Luciani, A. et al., 2012. Targeting autophagy as a novel strategy for facilitating the therapeutic action of potentiators on Delta F508 cystic fibrosis transmembrane conductance regulator. *Autophagy*, 8(11), pp.1657–1672.

Lukacs, G.L. et al., 1994. Conformational maturation of CFTR but not its mutant counterpart (delta F508) occurs in the endoplasmic reticulum and requires ATP. *The EMBO journal*, 13(24), pp.6076–86.

Lukacs, G.L. et al., 1993. The DF508 mutation decreases the stability of cystic fibrosis transmembrane conductance regulator in the plasma membrane: Determination of functional half-lives on transfected cells. *Journal of Biological Chemistry*, 268(29), pp.21592–21598.

LUND, J. et al., 1985. Target Cells for the Polychlorinated Biphenyl Metabolite Bis ( methylsulfonyl ) -2 Characterization of High Affinity Binding Rat and Mouse Lung Cytosol. *MOLECULAR PHARMACOLOGY*, pp.314–323.

Malik, V., Rodino-Klapac, L.R., et al., 2010. Aminoglycoside-induced mutation suppression (stop codon readthrough) as a therapeutic strategy for Duchenne muscular dystrophy. *Therapeutic advances in neurological disorders*, 3(6), pp.379–89.

Malik, V., Rodino-Klapac, L.R., et al., 2010. Gentamicin-induced readthrough of stop codons in Duchenne muscular dystrophy. *Annals of Neurology*, 67(6), pp.771–780.

Marshall, B.C. et al., 2005. Epidemiology of cystic fibrosis-related diabetes. *Journal of Pediatrics*, 146(5), pp.681–687.

McKone, E.F. et al., 2014. Long-term safety and efficacy of ivacaftor in patients with cystic fibrosis who have the Gly551Asp-CFTR mutation: A phase 3, open-label extension study (PERSIST). *The Lancet Respiratory Medicine*, 2(11), pp.902–910.

McMullen, A.H. et al., 2006. Impact of pregnancy on women with cystic fibrosis. *Chest*, 129(3), pp.706–711.

Mcqualter, J.L. & Bertoncello, I., 2012. Concise review: Deconstructing the lung to reveal its regenerative potential. *Stem Cells*, 30(5), pp.811–816.

Mehta, A., 2005. CFTR: More than just a chloride channel. *Pediatric Pulmonology*, 39(4), pp.292–298.

Mendell, J.R., Rodino-Klapac, L.R. & Malik, V., 2010. Molecular Therapeutic Strategies Targeting Duchenne Muscular Dystrophy. , 25(9), pp.1145–1148.

Meng, J. et al., 2011. Contribution of human muscle-derived cells to skeletal muscle regeneration in dystrophic host mice. *PLoS ONE*, 6(3).

Messina, G. et al., 2009. Skeletal muscle differentiation of embryonic mesoangioblasts requires pax3 activity. *Stem Cells*, 27(1), pp.157–164.

Milla, C.E., Billings, J. & Moran, A., 2005. Diabetes is associated with dramatically decreased survival in female but not male subjects with cystic fibrosis. *Diabetes Care.*, 28(9), pp.2141–2144.

Minasi, M.G. et al., 2002. The meso-angioblast: a multipotent, self-renewing cell that originates from the dorsal aorta and differentiates into most mesodermal tissues. *Development (Cambridge, England)*, 129(11), pp.2773–2783.

Mogayzel, P.J. et al., 2013. Cystic fibrosis pulmonary guidelines: Chronic medications for maintenance of lung health. *American Journal of Respiratory and Critical Care Medicine*, 187(7), pp.680–

689.
Montiel-Gonzalez, M.F. et al., 2013. Correction of mutations within the cystic fibrosis transmembrane conductance regulator by site-directed RNA editing. *Proceedings of the National Academy of Sciences of the United States of America*, 110(45), pp.18285–90.
Morrisey, E.E. et al., 2013. Molecular determinants of lung development. *Annals of the American Thoracic Society*, 10(2).
Moss, R.B. et al., 2007. Repeated aerosolized AAV-CFTR for treatment of cystic fibrosis: a randomized placebo-controlled phase 2B trial. *Human gene therapy*, 18(August), pp.726–732.
Murray, S. et al., 2008. Impact of Burkholderia infection on lung transplantation in cystic fibrosis. *American Journal of Respiratory and Critical Care Medicine*, 178(4), pp.363–371.
Nieto, M.A., 2011. The ins and outs of the epithelial to mesenchymal transition in health and disease. *Annu Rev Cell Dev Biol*, 27, pp.347–376.
Niu, N. et al., 2009. Cystic fibrosis transmembrane conductance regulator expression in human spinal and sympathetic ganglia. *Laboratory investigation; a journal of technical methods and pathology*, 89(6), pp.636–44.
O'Sullivan, B.P. & Freedman, S.D., 2009. Cystic fibrosis. *The Lancet*, 373(9678), pp.1891–1904.
Olivier, A.K. et al., 2012. Abnormal endocrine pancreas function at birth in cystic fibrosis ferrets. *Journal of Clinical Investigation*, 122(10), pp.3755–3768.
Ortiz, L.A. et al., 2003. Mesenchymal stem cell engraftment in lung is enhanced in response to bleomycin exposure and ameliorates its fibrotic effects. *Proceedings of the National Academy of Sciences of the United States of America*, 100(14), pp.8407–11.
De Paepe, M.E. et al., 2011. Alveolar epithelial cell therapy with human cord blood-derived hematopoietic progenitor cells. *The American journal of pathology*, 178(3), pp.1329–39.
Palumbo, R. et al., 2004. Extracellular HMGB1, a signal of tissue damage, induces mesoangioblast migration and proliferation. *Journal of Cell Biology*, 164(3), pp.441–449.
Pedemonte, N. et al., 2010. Influence of cell background on pharmacological rescue of mutant CFTR. *American journal of physiology. Cell physiology*, 298(4), pp.C866–C874.
Pedemonte, N. et al., 2005. Small Molecule. *Journal Of clinical investigation*, 115(9).
Peinado, H., Olmeda, D. & Cano, A., 2007. Snail, Zeb and bHLH factors in tumour progression: an alliance against the epithelial phenotype? *Nature Reviews Cancer*, 7(6), pp.415–428.
Petersen, B.E. et al., 1999. Bone marrow as a potential source of hepatic oval cells. *Science (New York, N.Y.)*, 284(5417), pp.1168–1170.
Pickering, S.J. et al., 2005. Generation of a human embryonic stem cell line encoding the cystic fibrosis mutation deltaF508, using preimplantation genetic diagnosis. *Reprod.Biomed.Online.*, 10(3), pp.390–397.
Pickles, R.J., 2004. Physical and biological barriers to viral vector-mediated delivery of genes to the airway epithelium. *Proceedings of the American Thoracic Society*, 1(4), pp.302–8.
Plopper, G.C., 1983. Comparative morphologic features of bronchiolar epithelial cells. The Clara cell. *Am. Rev. Respir. Dis.*, 128(August), pp.S37–S41.
Prockop, D.J. & Oh, J.Y., 2012. Medical Therapies with Adult Stem/Progenitor Cells (MSCs): A Backward Journey from Dramatic Results in Vivo to the Cellular and Molecular Explanations. *J. Cell Biochem.*, 113(5), pp.1460–1469.
Quinton, P.M., 2008. Cystic fibrosis: impaired bicarbonate secretion and mucoviscidosis. *The Lancet*, 372(9636), pp.415–417.
R.S. Pettit; C. Fellner, 2014. CFTR Modulators for the Treatment of Cystic Fibrosis. *Annual Reports in Medicinal Chemistry*, 39(7), pp.500–511.
Rackley, C.R. & Stripp, B.R., 2012. Building and maintaining the epithelium of the lung. *Journal of Clinical Investigation*, 122(8), pp.2724–2730.
Ramalho-Santos, M. et al., 2003. Transcriptional Profiling of Embryonic and Adult Stem Cells. *October*, 302, pp.37102–37102. Available at: http://www.ncbi.nlm.nih.gov/pubmed/14563991.
Ramsey, B.W. et al., 2011. A CFTR Potentiator in Patients with Cystic Fibrosis and the G551D Mutation. , 365(18), pp.1663–1672.
Rawlins, E.L. & Hogan, B.L.M., 2006. Epithelial stem cells of the lung: privileged few or opportunities for many? *Development (Cambridge, England)*, 133(13), pp.2455–65.
Reisin, I.L. et al., 1994. The cystic fibrosis transmembrane conductance regulator is a dual ATP and chloride channel. *The Journal of biological chemistry*, 269(32), pp.20584–91.
Reynolds, S.D. et al., 2012. Lung epithelial healing: a modified seed and soil concept. *Proceedings of the American Thoracic Society*, 9(2), pp.27–37.
Reynolds, S.D. et al., 2000. Neuroepithelial bodies of pulmonary airways serve as a reservoir of progenitor cells capable of epithelial regeneration. *Am J Pathol*, 156(1), pp.269–278.

Riordan, J. et al., 1989. Identification of the cystic fibrosis gene: cloning and characterization of complementary DNA. *Science (New York, N.Y.)*, 245(4922), pp.1066–1073.

Riordan, J.R., 2008. CFTR function and prospects for therapy. *Annual review of biochemistry*, 77(1), pp.701–726.

Riordan, J.R., 1993. The Cystic Fibrosis Transmembrane Conductance Regulator. *Annu. Rev. Physiol.* 55, pp.609-30

RIPPON, H.J. et al., 2006. Derivation of Distal Lung Epithelial Progenitors from Murine Embryonic Stem Cells Using a Novel Three-Step. *Stem Cells*, 24, pp.1389–1398.

Robert, R. et al., 2007. Expression and function of cystic fibrosis transmembrane conductance regulator in rat intrapulmonary arteries. *The European respiratory journal*, 30(5), pp.857–64.

Rock, J. & Königshoff, M., 2012. Endogenous lung regeneration: Potential and limitations. *American Journal of Respiratory and Critical Care Medicine*, 186(12), pp.1213–1219.

Rock, J.R. & Hogan, B.L.M., 2011. Epithelial progenitor cells in lung development, maintenance, repair, and disease. *Annual review of cell and developmental biology*, 27, pp.493–512.

Rock, J.R., Randell, S.H. & Hogan, B.L.M., 2010. Airway basal stem cells: a perspective on their roles in epithelial homeostasis and remodeling. *Disease models & mechanisms*, 3(9-10), pp.545–556.

Rogers, C.S. et al., 2008. Disruption of the CFTR gene produces a model of cystic fibrosis in newborn pigs. *Science*, 321(5897), pp.1837–41.

Rommens, J. et al., 1989. Identification of the cystic fibrosis gene: chromosome walking and jumping. *Science*, 245(4922), pp.1059 –1065.

Rommens, J.M. et al., 1988. Identification and regional localization of DNA markers on chromosome 7 for the cloning of the cystic fibrosis gene. *American journal of human genetics*, 43(5), pp.645–663.

Rosen, C. et al., 2015. Preconditioning allows engraftment of mouse and human embryonic lung cells, enabling lung repair in mice. *Nature medicine*, 21(8), pp.869–79.

Rosenfeld, M., Ramsey, B.W. & Gibson, R.L., 2003. Pseudomonas acquisition in young patients with cystic fibrosis: pathophysiology, diagnosis, and management. *Current opinion in pulmonary medicine*, 9, pp.492–497.

Rossi, G. et al., 2016. Nfix Regulates Temporal Progression of Muscle Regeneration through Modulation of Myostatin Article Nfix Regulates Temporal Progression of Muscle Regeneration through Modulation of Myostatin Expression. *CellReports*, 14(9), pp.1–12.

Rowe, S.M. et al., 2005. Cystic Fibrosis. *Murray and Nadel's Textbook of Respiratory Medicine*, pp.822–852.e17.

Rowe, S.M., Accurso, F. & Clancy, J.P., 2007. Detection of cystic fibrosis transmembrane conductance regulator activity in early-phase clinical trials. *Proceedings of the American Thoracic Society*, 4(4), pp.387–398.

Rowe, S.M. & Clancy, J.P., 2009. Pharmaceuticals Targeting Nonsense Mutations in Genetic Diseases. *DRUG DEVELOPMENT*, 23(2), pp.1–10.

Ruiz, F.E. et al., 2001. A Clinical Inflammatory Syndrome Attributable to Aerosolized Lipid–DNA Administration in Cystic Fibrosis. *Human Gene Therapy*, 12(7), pp.751–761.

Safadi, A. et al., 1991. Activity of alkaline phosphatase in rat skeletal muscle localized along the sarcolemma and endothelial cell membranes. *J Histochem Cytochem*, 39(2), pp.199–203.

Saiman, L. et al., 2003. Azithromycin in Patients With. *The Journal of The American Medical Association*, 290(13), pp.1749–1756.

Saiman, L. et al., 2012. Effect of Azithromycin on Pulmonary Function in Patients With Cystic Fibrosis Uninfected With Pseudomonas aeruginosa. , 303(17), pp.1707–1715.

Sampaolesi, M. et al., 2003. Cell therapy of alpha-sarcoglycan null dystrophic mice through intra-arterial delivery of mesoangioblasts. *Science*, 301(5632), pp.487–492.

Sampaolesi, M. et al., 2006. Mesoangioblast stem cells ameliorate muscle function in dystrophic dogs. *Nature*, 444(7119), pp.574–579.

Sawicki, G.S., Sellers, D.E. & Robinson, W.M., 2009. High treatment burden in adults with cystic fibrosis: Challenges to disease self-management. *Journal of Cystic Fibrosis*, 8(2), pp.91–96.

Schechter, M.S. et al., 2001. The association of socioeconomic status with outcomes in cystic fibrosis patients in the United States. *Am J Respir Crit Care Med*, 163, pp.1331–1337.

Schlingemann, R.O. et al., 1991. Differential expression of markers for endothelial cells, pericytes, and basal lamina in the microvasculature of tumors and granulation tissue. *The American journal of pathology*, 138(6), pp.1335–1347.

Schrepfer, S. et al., 2007. Stem Cell Transplantation: The Lung Barrier. *Transplantation Proceedings*, 39(2), pp.573–576.

Schwank, G. et al., 2013. Functional repair of CFTR by CRISPR/Cas9 in intestinal stem cell organoids

of cystic fibrosis patients. *Cell Stem Cell*, 13(6), pp.653–658.
Schwiebert, E.M. et al., 1995. CFTR regulates outwardly rectifying chloride channels through an autocrine mechanism involving ATP. *Cell*, 81(7), pp.1063–1073.
Sean V. Murphy and Anthony Atala, 2013. Cell therapy for cystic fibrosis Sean. *Journal of tissue engineering and regenerative medicine*.
Sermet-Gaudelus, I. et al., 2010. Ataluren (PTC124) induces cystic fibrosis transmembrane conductance regulator protein expression and activity in children with nonsense mutation cystic fibrosis. *American Journal of Respiratory and Critical Care Medicine*, 182(10), pp.1262–1272.
Sermet-Gaudelus, I. et al., 2007. In vitro prediction of stop-codon suppression by intravenous gentamicin in patients with cystic fibrosis: a pilot study. *BMC medicine*, 5, p.5.
Sheppard, D. et al., 1993. Mutations in CFTR associated with mild-disease-form Cl- channels with altered pore properties. *Nature*, 362, pp.160–164.
Silvis, M.R. et al., 2003. A mutation in the cystic fibrosis transmembrane conductance regulator generates a novel internalization sequence and enhances endocytic rates. *Journal of Biological Chemistry*, 278(13), pp.11554–11560.
Simon, L., Cooke, P.S. & Berry, S.E., 2013. Aorta-derived mesoangioblasts can be differentiated into functional uterine epithelium, but not prostatic epithelium or epidermis, by instructive mesenchymes. *Cells Tissues Organs*, 198(3), pp.169–178.
Singh, G. et al., 1985. Secretory Proteins of the Lung in Rodents. *The Journal of Histochemistry and Cytochemistry*, pp.564–568.
Singh, G. & Katyal, S.L., 1997. Clara Cells and Clara Cell 10 kD Protein (CC10). *American Journal of Respiratory Cell and Molecular Biology*.
Snouwaert, J.N. et al., 1992. An animal model for cystic fibrosis made by gene targeting. , 257(5073), pp.1083–1088.
Somers, A. et al., 2010. Generation of transgene-free lung disease-specific human induced pluripotent stem cells using a single excisable lentiviral stem cell cassette. *Stem Cells*, 28(10), pp.1728–1740.
Sorio, C. et al., 2011. Defective CFTR expression and function are detectable in blood monocytes: Development of a new blood test for cystic fibrosis. *PLoS ONE*, 6(7).
Sosnay, P.R. et al., 2014. Defining the disease liability of variants in the cystic fibrosis transmembrane conductance regulator gene. , 45(10), pp.1–23.
Springer, M.L., Ozawa, C.R. & Blau, H.M., 2002. Transient production of α-smooth muscle actin by skeletal myoblasts during differentiation in culture and following intramuscular implantation. *Cell Motility and the Cytoskeleton*, 51(4), pp.177–186.
Stallings, V.A. et al., 2008. Evidence-Based Practice Recommendations for Nutrition-Related Management of Children and Adults with Cystic Fibrosis and Pancreatic Insufficiency: Results of a Systematic Review. *Journal of the American Dietetic Association*, 108(5), pp.832–839.
Stoltz, D.A. et al., 2010. Bacterial Eradication at Birth. *Sci Transl Med*, 2(29), pp.1–18.
Stripp, B.R. et al., 1995. Plasticity of airway cell proliferation and gene expression after acute naphthalene injury. *The American journal of physiology*, 269(6 Pt 1), pp.L791–9.
Stutts, M.J. et al., 1995. CFTR as a cAMP-dependent regulator of sodium channels. *Science (New York, N.Y.)*, 269(5225), pp.847–850.
Sueblinvong, V. et al., 2008. Derivation of lung epithelium from human cord blood-derived mesenchymal stem cells. *American Journal of Respiratory and Critical Care Medicine*, 177(7), pp.701–711.
Sueblinvong, V. & Weiss, D.J., 2010. Stem cells and cell therapy approaches in lung biology and diseases. *Translational research : the journal of laboratory and clinical medicine*, 156(3), pp.188–205.
Sun, X. et al., 2010. Technical advance Disease phenotype of a ferret CFTR -knockout model of cystic fibrosis. , 120(9), pp.3149–3160.
Tagliafico, E., 2004. TGF /BMP activate the smooth muscle/bone differentiation programs in mesoangioblasts. *Journal of Cell Science*, 117(19), pp.4377–4388.
Tarran, R. et al., 2001. The CF salt controversy: In vivo observations and therapeutic approaches. *Molecular Cell*, 8(1), pp.149–158.
Tedesco, F.S. et al., 2011. Stem cell-mediated transfer of a human artificial chromosome ameliorates muscular dystrophy. *Science translational medicine*, 3(96), p.96ra78.
Tedesco, F.S. et al., 2012. Transplantation of genetically corrected human iPSC-derived progenitors in mice with limb-girdle muscular dystrophy. *Science translational medicine*, 4(140), pp.14089–14099.
Teisanu, R.M. et al., 2011. Functional analysis of two distinct bronchiolar progenitors during lung

injury and repair. *American Journal of Respiratory Cell and Molecular Biology*, 44(6), pp.794–803.

Thiery, J.P. et al., 2009. Epithelial-Mesenchymal Transitions in Development and Disease. *Cell*, 139(5), pp.871–890.

Tonlorenzi, R. et al., 2007. Isolation and characterization of mesoangioblasts from mouse, dog, and human tissues. *Current protocols in stem cell biology*, Chapter 2(December), p.Unit 2B.1.

Tosi, M.F. et al., 2004. Effect of Pseudomonas-induced chronic lung inflammation on specific cytotoxic T-cell responses to adenoviral vectors in mice. *Gene therapy*, 11(19), pp.1427–33.

Trulock, E.P. et al., 2007. Registry of the International Society for Heart and Lung Transplantation: Twenty-fourth Official Adult Lung and Heart-Lung Transplantation Report-2007. *Journal of Heart and Lung Transplantation*, 26(8), pp.782–795.

Vandebrouck, C. et al., 2006. Evidence that CFTR is expressed in rat tracheal smooth muscle cells and contributes to bronchodilation. *Respiratory research*, 7, p.113.

Vankeerberghen, A., Cuppens, H. & Cassiman, J.J., 2002. The cystic fibrosis transmembrane conductance regulator: An intriguing protein with pleiotropic functions. *Journal of Cystic Fibrosis*, 1(1), pp.13–29.

Vaughan, A.E. & Chapman, H.A., 2013. Regenerative activity of the lung after epithelial injury. *Biochimica et Biophysica Acta - Molecular Basis of Disease*, 1832(7), pp.922–930.

Veit, G. et al., 2016. From CFTR biology toward combinatorial pharmacotherapy : expanded classification of cystic fibrosis mutations. , 27.

Verbeek, M.M. et al., 1994. Induction of alpha-smooth muscle actin expression in cultured human brain pericytes by transforming growth factor-beta 1. *The American journal of pathology*, 144(2), pp.372–382.

Vertex Pharmaceuticals Press Release ID857163, 2014. U.S. Food and Drug Administration Approves KALYDECO® (ivacaftor) for Use in People with Cystic Fibrosis Ages 6 and Older Who Have the R117H Mutation. , pp.2–4.

Wang, L. et al., 2012. Aorta-derived mesoangioblasts differentiate into the oligodendrocytes by inhibition of the rho kinase signaling pathway. *Stem cells and development*, 21(7), pp.1069–1089.

Wansleeben, C. et al., 2013. Stem cells of the adult lung: Their development and role in homeostasis, regeneration, and disease. *Wiley Interdisciplinary Reviews: Developmental Biology*, 2(1), pp.131–148.

Welsh, M.J. et al., 2001. Cystic Fibrosis. In the metabolic and Molecular Bases of Inherited Disease. pp. 5121-88

Weiss, D.J., 2014. Current Status of Stem Cells and Regenerative Medicine in Lung Biology and Diseases. *Journal of tissue engineering and regenerative medicine*, pp.16–25.

Weiss, D.J. et al., 2011. Stem cells and cell therapies in lung biology and lung diseases. *Proceedings of the American Thoracic Society*, 8(3), pp.223–272.

Welsh, M.J. et al., 1994. Cystic Fibrosis Gene Therapy Using an Adenovirus Vector : In Vivo Safety and Efficacy in Nasal Epithelium. *HUMA N GEN E THERAPY*, 5, pp.209–219.

Welsh, M.J. & Smith, A.E., 1993. Molecular mechanisms of CFTR chloride channel dysfunction in cystic fibrosis. *Cell*, 73(7), pp.1251–1254.

WHO/ECFTN, 2004. The molecular genetic epidemiology of cystic fibrosis. *World Health*.

Wilke, M. et al., 2011. Mouse models of cystic fibrosis: Phenotypic analysis and research applications. *Journal of Cystic Fibrosis*, 10(SUPPL. 2), pp.S152–S171.

Wilschanski, M. et al., 2011. Chronic ataluren (PTC124) treatment of nonsense mutation cystic fibrosis. *European Respiratory Journal*, 38(1), pp.59–69.

Wilschanski, M. & Durie, P.R., 2007. Patterns of GI disease in adulthood associated with mutations in the CFTR gene. *Gut*, 56(8), pp.1153–63.

Wong, A.P. et al., 2012. Directed differentiation of human pluripotent stem cells into mature airway epithelia expressing functional CFTR protein. *Nature Biotechnology*, 30(9), pp.876–882.

www.cftr2.org

www.genet.sickkids.on.ca

Xue, X. et al., 2014. Synthetic aminoglycosides efficiently suppress cystic fibrosis transmembrane conductance regulator nonsense mutations and are enhanced by ivacaftor. *American Journal of Respiratory Cell and Molecular Biology*, 50(4), pp.805–816.

Yan, X. et al., 2007. Injured microenvironment directly guides the differentiation of engrafted Flk-1+ mesenchymal stem cell in lung. *Experimental Hematology*, 35(9), pp.1466–1475.

Yankaskas, J.R. et al., 2004. Cystic Fibrosis Adult Care: Consensus Conference Report. *Chest*, 125(1 SUPPL.), p.1S–39S.

Yu, H. et al., 2012. Ivacaftor potentiation of multiple CFTR channels with gating mutations. *Journal of Cystic Fibrosis*, 11(3), pp.237–245.

Zabner, J. et al., 1993. Adenovirus-mediated gene transfer transiently corrects the chloride transport defect in nasal epithelia of patients with cystic fibrosis. *Cell*, 75(2), pp.207–216.

Zielenski, J. & Tsui, L.C., 1995. Cystic fibrosis: genotypic and phenotypic variations. *Annual Review of Genetics*, 29(1), pp.777–807.

Zolin, A., McKone, E. & van Rens, J., 2014. ECFSPR Annual Report 2010. , p.102.

# PART II

## LIST OF PUBLISHED PAPERS

Rossi G, Antonini S, Bonfanti C, Monteverde S, **Vezzali C**, Tajbakhsh S, Cossu G and Messina G (2016) Nfix regulates temporal progression of muscle regeneration through modulation of myostatin expression. *Cell Reports* **14**, 2238-2249

Article

Cell Reports

# Nfix Regulates Temporal Progression of Muscle Regeneration through Modulation of Myostatin Expression

## Graphical Abstract

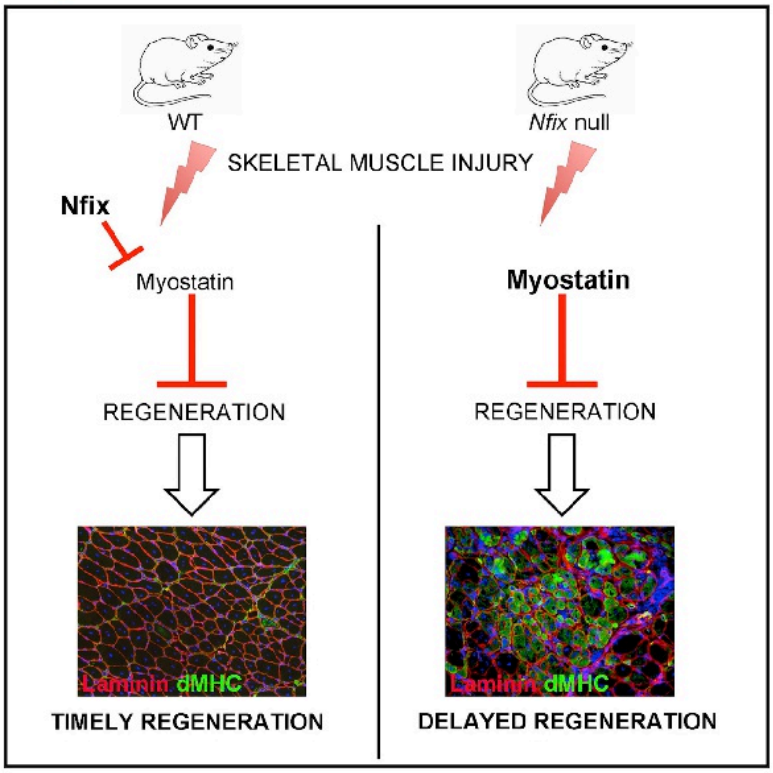


## Authors

Giuliana Rossi, Stefania Antonini, Chiara Bonfanti, ..., Shahragim Tajbakhsh, Giulio Cossu, Graziella Messina

## Correspondence

graziella.messina@unimi.it

## In Brief

Rossi et al. highlight a function for Nfix during postnatal skeletal muscle regeneration and a link with Myostatin. During regeneration, Nfix regulates Myostatin expression, thus controlling the temporal progression of the regeneration process. When Nfix is deficient, regeneration is markedly delayed.

## Highlights

- Muscle differentiation is delayed in *Nfix*-null satellite cells in vitro
- Mice lacking Nfix in satellite cells show delayed regeneration upon injury
- Nfix directly regulates Myostatin expression during regeneration
- In vivo silencing of Myostatin rescues the regeneration deficit in *Nfix*-null mice

Rossi et al., 2016, Cell Reports *14*, 2238–2249
March 8, 2016 
http://dx.doi.org/10.1016/j.celrep.2016.02.014

CellPress

OPEN ACCESS
CellPress

Cell Reports
Article

# Nfix Regulates Temporal Progression of Muscle Regeneration through Modulation of Myostatin Expression

Giuliana Rossi,[1] Stefania Antonini,[1] Chiara Bonfanti,[1] Stefania Monteverde,[1] Chiara Vezzali,[1] Shahragim Tajbakhsh,[2] Giulio Cossu,[1,3] and Graziella Messina[1,*]

[1]Department of Biosciences, University of Milan, Via Celoria 26, 20133 Milan, Italy

[2]Stem Cells and Development, Department of Developmental & Stem Cell Biology, CNRS UMR 3738, Institut Pasteur, 25 Rue du Dr. Roux, 75015 Paris, France

[3]Institute of Inflammation and Repair, University of Manchester, Oxford Road, M13 9PL Manchester, UK

*Correspondence: graziella.messina@unimi.it

http://dx.doi.org/10.1016/j.celrep.2016.02.014



## SUMMARY

**Nfix belongs to a family of four highly conserved proteins that act as transcriptional activators and/or repressors of cellular and viral genes. We previously showed a pivotal role for Nfix in regulating the transcriptional switch from embryonic to fetal myogenesis. Here, we show that Nfix directly represses the Myostatin promoter, thus controlling the proper timing of satellite cell differentiation and muscle regeneration. *Nfix*-null mice display delayed regeneration after injury, and this deficit is reversed upon in vivo Myostatin silencing. Conditional deletion of *Nfix* in satellite cells results in a similar delay in regeneration, confirming the functional requirement for Nfix in satellite cells. Moreover, mice lacking Nfix show reduced myofiber cross sectional area and a predominant slow twitching phenotype. These data define a role for Nfix in postnatal skeletal muscle and unveil a mechanism for Myostatin regulation, thus providing insights into the modulation of its complex signaling pathway.**

## INTRODUCTION

Skeletal muscles play a critical role in voluntary movement, and proper regeneration of this tissue after injury can be severely compromised in a variety of contexts including neuromuscular disorders. In vertebrates, muscle progenitors originating from presomitic and cranial mesoderm give rise to "embryonic" or primary myogenesis, necessary to establish the basic muscle pattern, and "fetal" secondary myogenesis, characterized by growth and maturation of the muscle masses and by onset of innervation (Biressi et al., 2007a). These two waves of myogenesis are mediated by distinct embryonic and fetal myoblasts, respectively, each characterized by differentially expressed genes and properties of the myoblasts as well as the differentiated cells that they produce (Biressi et al., 2007b; Hutcheson et al., 2009). A key regulator of the embryonic and fetal classes is Nuclear Factor I X (*Nfix*), which is abundant in the fetus and almost absent in the embryo (Biressi et al., 2007b; Messina et al., 2010). Nfix drives the transcriptional changes from embryonic to fetal myogenesis by specifically repressing embryonic and activating fetal specific genes (Messina et al., 2010), and its role is partially conserved during evolution (Pistocchi et al., 2013).

Nfix is part of a family of highly conserved DNA-binding proteins that function as transcriptional activators and/or repressors: *Nfia*, *Nfib*, *Nfic*, and *Nfix*. NFI-binding sites are present in the promoter, enhancer and silencer regions of many cellular and viral genes (Kruse and Sippel, 1994), and NFI binding motifs were detected in promoters of genes expressed in different organs, such as brain (Bedford et al., 1998), lung (Bachurski et al., 1997), liver (Jackson et al., 1993), intestine (Xu et al., 2005), muscle (Spitz et al., 1997), connective tissue and skeletal elements (Szabó et al., 1995). *Nfix*-null mice are characterized by a reduced body size and inability to fully extend their limbs as well as CNS and skeletal deficits (Campbell et al., 2008; Driller et al., 2007). NFI binding sites are present in the promoters of the differentiation gene *Myogenin* and muscle-specific phospho-fructo-kinase (Darville et al., 1992; Edmondson et al., 1992), and they can form a complex with Myogenin, thus increasing their affinity for muscle-specific genes (Funk and Wright, 1992; Johanson et al., 1999).

Another critical regulator of prenatal and postnatal myogenesis is Myostatin, a secreted factor of the TGFβ superfamily that was shown to be a negative regulator of muscle size, where loss-of-function mutations result in a dramatic increase in muscle mass in different species including human (McPherron et al., 1997; McPherron and Lee, 1997; Schuelke et al., 2004). Although interference of this pathway was reported to lead to functional improvement of dystrophic muscles in mice (Bogdanovich et al., 2002), the precise mode of action of this powerful signaling pathway as a potential therapeutic agent for myopathies remains unclear. Notably, the contextual role of Myostatin was highlighted, where in the embryo it regulates the balance between proliferation and differentiation of muscle progenitors (Manceau et al., 2008), whereas in the adult, opposing roles in

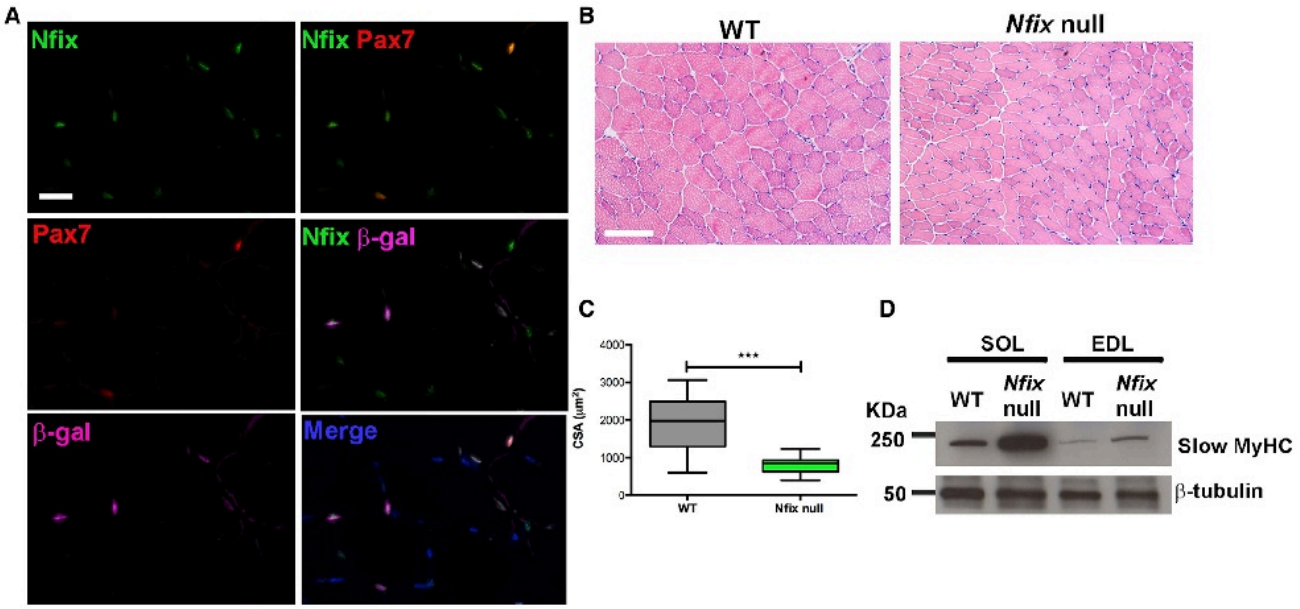


**Figure 1. Nfix Is Expressed by SCs and Its Absence Leads to a Reduced Myofiber Cross Sectional Area and to an Increased Slow MyHC Expression**

(A) Immunofluorescence analysis of Nfix expression (green) in Pax7$^+$ SCs (red) on a *Tibialis anterior* muscle section of a *Mlc3f-lacz* mouse, where myonuclei are in purple (β-gal). Hoechst was used to stain nuclei (n = 4 mice). The scale bar represents 25 μm.

(B) H&E staining on *Tibialis anterior* muscles from WT and *Nfix*-null mice (n = 5 mice). The scale bar represents 100 μm.

(C) Graphical representation of the myofiber cross sectional area (CSA) in WT and *Nfix*-null muscles. The plotted values represent the distribution of n = 65 measurements on five random microscope fields (***$p < 0.001$ and two-tailed unpaired t test). The data are presented as mean ± whiskers from min to max.

(D) Western blot analysis of slow MyHC expression in WT and *Nfix*-null *Soleus* (SOL) and EDL muscles. The β-tubulin was used to normalize.

See also Figure S1.

regulating myogenic differentiation have been reported (Langley et al., 2002; Thomas et al., 2000; McCroskery et al., 2003; Taylor et al., 2001).

Postnatal myogenesis is assured by satellite cells (SCs) that are located between the basal lamina and the myofiber plasma membrane (Mauro, 1961). Although they account for less than 5% of total muscle nuclei in adult muscles, they play an indispensible role in the regeneration of adult skeletal muscle (Lepper et al., 2011; McCarthy et al., 2011; Murphy et al., 2011; Relaix and Zammit, 2012; Sambasivan et al., 2011).

Here, we report that absence of Nfix provokes an imbalance in skeletal muscle homeostasis and regeneration. Moreover, we identify Nfix as a regulator of Myostatin, where in vivo silencing of Myostatin in regenerating *Nfix*-null muscles rescues the regeneration defect. These findings have broad implications for the understanding of pathways regulating postnatal myogenesis and regeneration as well as providing insights into the role of Myostatin as a critical regulator of skeletal muscle differentiation.

## RESULTS

### Altered Skeletal Muscle Phenotype in *Nfix*-Null Mice

We demonstrated previously that Nfix plays a critical role in the switch from embryonic to fetal myogenesis (Messina et al., 2010). Interestingly, *Nfix*-null mice are characterized by reduced body size and inability to fully extend their limbs, suggesting a possible muscular phenotype (Driller et al., 2007). To explore the role of *Nfix* in adult myogenesis, we examined its expression and observed that both myonuclei and Pax7$^+$ SCs express *Nfix* (Figure 1A). Histological analysis of *Nfix*-null muscles showed a marked reduction in the cross sectional area of myofibers, although general muscle architecture remained normal compared to wild-type littermates (Figures 1B and 1C). In addition, *Nfix*-null SC-derived myoblasts were able to differentiate in vitro (Figure S1A), with no significant difference in proliferation and apoptosis rates with respect to the wild-type (Figures S1B and S1C). We reported previously that the embryonic marker slow MyHC is negatively regulated by Nfix, through repression of its activator Nfatc4 (Messina et al., 2010). Interestingly, adult muscles lacking Nfix were characterized by an increased expression of slow MyHC, which is evident in both typically slow-twitching muscles (such as the *Soleus*) and fast-twitching muscles (such as the EDL, *Extensor Digitorum Longus*) (Figure 1D). Notably, *Nfix*-null differentiated SC-derived myotubes in vitro also expressed higher levels of slow MyHC compared to wild-type (Figure S1D).

### SC Differentiation and Muscle Regeneration Are Delayed in the Absence of Nfix

To assess the role of *Nfix* during regeneration, we first examined single muscle fibers isolated from wild-type and *Nfix*-null mice. Freshly isolated wild-type and *Nfix*-null single fibers had

comparable numbers of associated Pax7$^+$ SCs (Figure S2A) and after 24 hr in culture the number of MyoD expressing cells was similar (Figure S2B). Analysis of SC proliferation and percentage of MyoD expression during the first 12 hr in culture revealed no difference between the two groups (Figures S2C and S2D). Although no significant alterations in numbers of Pax7$^+$ and MyoD$^+$ SCs were noted on *Nfix*-null myofibers, immunostaining for MyoD and Myogenin on wild-type and *Nfix*-null myofibers showed a marked reduction in the number of double Myod$^+$/Myogenin$^+$ cells in absence of Nfix (Figures 2A and 2B). Notably, this loss of differentiated cells in *Nfix*-null myofibers was more pronounced after 72 hr in culture, suggesting a possible involvement of Nfix during SC differentiation. Interestingly, the reduction in Myogenin$^+$ cells was less evident at later stages (Figure 2B), thus suggesting a delay in muscle differentiation rather than a general block of the differentiation process.

We reasoned that a delay in myogenic differentiation in absence of Nfix could result in an altered regeneration in vivo. We therefore injected the *Tibialis anterior* muscle of wild-type and *Nfix*-null mice with the snake venom cardiotoxin (CTX) to induce muscle regeneration. Following tissue damage, we observed a striking delay in muscle regeneration after injury of *Nfix*-null mice, as observed by persistent expression of developmental MyHC (Collins et al., 2005; Sartore et al., 1982; Schiaffino et al., 1986) (dMHC) expression (Figures 3A and 3D). In addition, the *Nfix*-null exhibited smaller regenerating myofibers compared to wild-type (Figure S2E). Accordingly, Myogenin expression was delayed and protracted in *Nfix*-null muscles (Figure 3B), in keeping with our in vitro observations (Figures 2A and 2B). Nevertheless, in spite of this altered timing, muscle regeneration appeared complete at later time points in the *Nfix*-null (28 days after injury, see Figure 3A). Interestingly, in *Nfix*-null mice, we observed a marked upregulation of Myostatin, a potent inhibitor of myogenesis, suggesting that this signaling pathway might be involved in the delayed muscle regeneration phenotype (Figure 3B). This was most evident from day 5 after CTX injection at a time when differentiation has already initiated, and it was accompanied by the upregulation of the Myostatin downstream effector phosphorylated Smad3 (pSmad3), particularly after 7 days (Figure 3C), suggesting a functional role for Myostatin signaling. These results clearly indicate a role for Nfix in regulating the proper timing of Myostatin expression and, in turn, of muscle regeneration upon injury. Analysis of Myostatin expression in uninjured muscles revealed no difference between wild-type and *Nfix*-null animals (data not shown), suggesting that the upregulation of Myostatin expression specifically occurs as a consequence of muscle injury.

## Specific Deletion of Nfix in SCs Recapitulates the Regeneration Defects

Since Nfix expression is not restricted to SCs, we investigated muscle regeneration after CTX injury in tamoxifen treated *Tg:Pax7-Cre$^{ERT2}$:Nfix$^{fl/-}$* mice (see Figure S3A) to examine the specific role of Nfix in Pax7$^+$ SCs. Tamoxifen treated *Tg:Pax7-Cre$^{ERT2}$:Nfix$^{fl/-}$* mice were compared with both tamoxifen untreated mice and mice expressing only the *Tg:Pax7-Cre$^{ERT2}$* allele and treated with tamoxifen, as controls. To verify the efficacy of tamoxifen treatment, sections of regenerating mouse muscles from each group were stained for Nfix. In both *Tg:Pax7-Cre$^{ERT2}$:Nfix$^{+/+}$* and tamoxifen untreated *Tg:Pax7-Cre$^{ERT2}$:Nfix$^{fl/-}$* mice, all the centrally nucleated myofibers were Nfix$^+$, as expected (Figure S3C). In tamoxifen treated *Tg:Pax7-Cre$^{ERT2}$:Nfix$^{fl/-}$* mice, Nfix expression was completely abolished in regenerating myonuclei, while it was still present in non-muscle nuclei, thereby confirming the specificity of *Tg:Pax7-Cre$^{ERT2}$* deletion (Figure S3C). Efficiency of Nfix deletion was also measured by counting the percentage of Pax7$^+$ cells that had excised *Nfix* and was calculated to be 96.2% ± 0.4 (Figure S3D). Notably, tamoxifen treated *Tg:Pax7-Cre$^{ERT2}$:Nfix$^{fl/-}$* mice showed a delayed regeneration when compared to both tamoxifen untreated floxed mice and tamoxifen treated *Nfix$^{+/+}$* mice (Figure 4A). This defective regeneration was evident in tamoxifen treated *Tg:Pax7-Cre$^{ERT2}$:Nfix$^{fl/-}$* mice at 7 and 14 days post-CTX injection where dMHC expression persisted, and H&E sections revealed the continued presence of necrotic and inflammatory areas (Figures 4A and S3E). Further, the analysis of Myogenin clearly showed protracted expression in the tamoxifen treated *Tg:Pax7-Cre$^{ERT2}$:Nfix$^{fl/-}$* mice, confirming the delay in the regenerative process (Figure 4B). Finally, the distribution of the cross sectional area of regenerating myofibers in the three groups supports the delayed regeneration phenotype of tamoxifen treated *Tg:Pax7-Cre$^{ERT2}$:Nfix$^{fl/-}$* mice, mostly evident after 14 days (Figure S3B). These data support the specific function of *Nfix* in SCs for proper timing of Myogenin expression as well as the regeneration process.

## Nfix Regulates Myostatin Expression in Differentiating Myoblasts

In keeping with the observation that *Nfix*-null mice exhibit delayed muscle regeneration, Myostatin expression was upregulated in the absence of Nfix (Figure 3B). Since Myostatin is a TGF-β family member with anti-myogenic properties (Elliott et al., 2012), its upregulation can explain the delayed regeneration observed in mice lacking Nfix. To address this point, we investigated the possibility that Nfix might directly regulate Myostatin expression in differentiating myoblasts. First, we analyzed Myostatin expression in differentiating SC-derived myoblasts. As shown in Figure 5A, Nfix acts as a suppressor of Myostatin in differentiating myoblasts, even in absence of the contribution of the myofiber.

For biochemical analysis, we validated this result using the C2C12 myogenic cell line. C2C12 cells were transduced with a lentiviral vector carrying a small hairpin RNA targeting Nfix (shNfix) or a scrambled sequence as a control (scramble). The transduction effectively resulted in the downregulation of *Nfix* expression in shNfix-treated C2C12, as confirmed by western blot (Figure 5B). Importantly, Myostatin expression was upregulated in Nfix-silenced myotubes starting from day 5, confirming that Nfix was able to downregulate Myostatin expression in differentiating C2C12 myoblasts (Figure 5C).

Nfix can bind with high affinity to the palindromic consensus sequence TTGGC(N5)GCCAA (Kruse and Sippel, 1994), although NFI factors can also bind to hemi-binding sites (a single TTGGC or GCCAA site alone) (Gronostajski, 2000) with a lower affinity. In silico analysis using Genomatix Software allowed us to identify hypothetical Nfix hemi-binding sites in the Myostatin

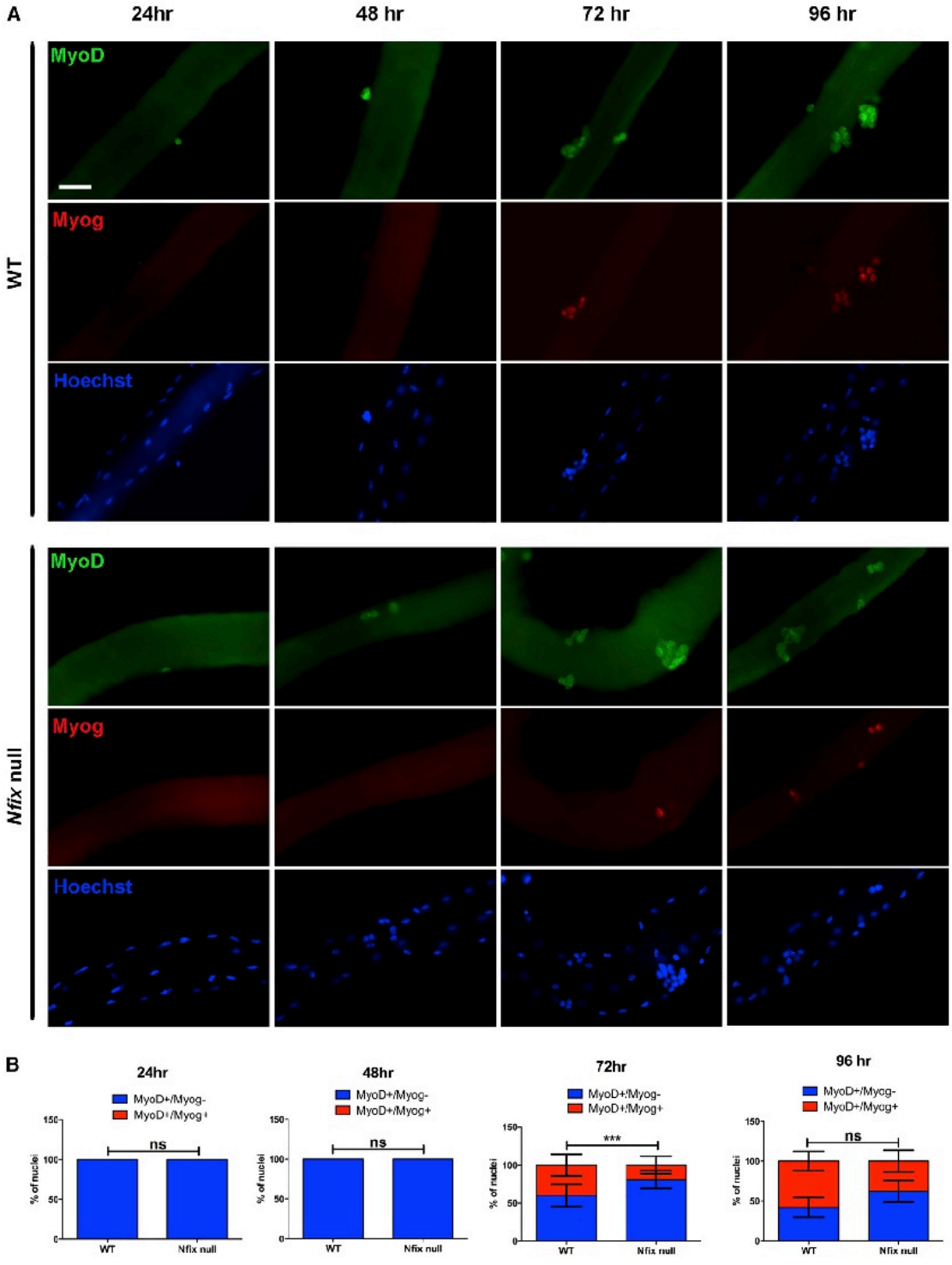


**Figure 2. SCs Lacking Nfix Are Characterized by a Delayed Differentiation**

(A) Immunofluorescence analysis of MyoD (green) and Myogenin (Myog, red) expression on single muscle fibers from WT and *Nfix*-null muscles after 24, 48, 72, and 96 hr in culture. Hoechst was used to stain nuclei (n = 3 WT and 3 *Nfix*-null mice). The scale bar represents 50 μm.

(B) Quantification of $MyoD^+$/$Myogenin^+$ and $MyoD^+$/$Myogenin^-$ SCs associated with WT and *Nfix*-null myofibers at 24, 48, 72, and 96 hr in culture. The quantification is the result of three independent experiments on three WT and three *Nfix*-null mice. The data are presented as mean ± SD (not significant, ns; ***$p < 0.001$ with n = 11 WT myofibers and n = 16 *Nfix*-null myofibers; and two-tailed unpaired t test).

See also Figure S2.

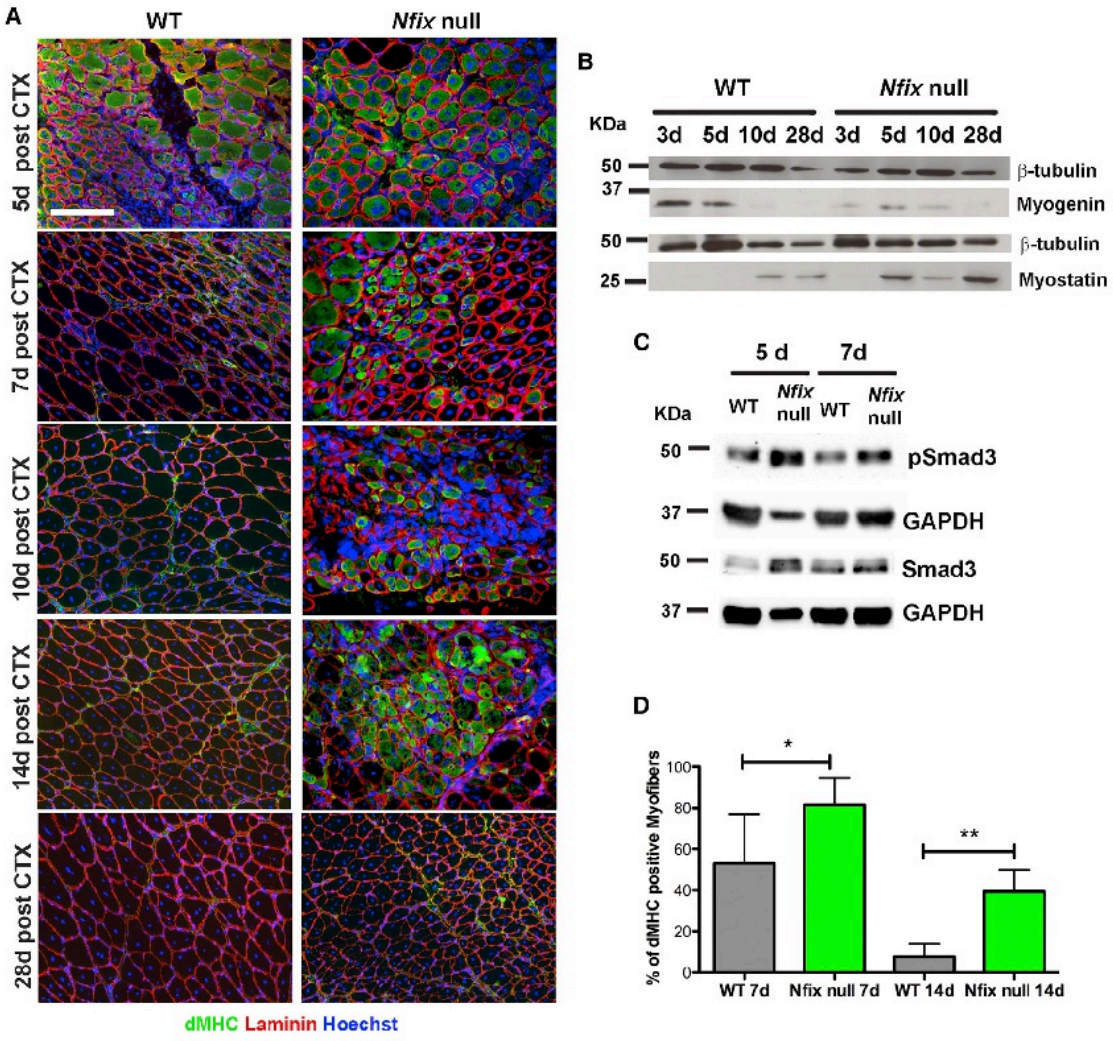


**Figure 3. Absence of Nfix Leads to a Marked Impairment of Muscle Regeneration after Injury**

(A) Immunofluorescence for dMHC (green) on regenerating WT and *Nfix*-null *Tibialis anterior* muscles 5, 7, 10, 14, and 28 days (d) following CTX injection. The laminin is marked in red and Hoechst was used to stain nuclei (n = 3 mice for each group). The scale bar represents 50 μm.

(B) Western blot analysis of Myogenin and Myostatin expression on WT and *Nfix*-null muscles 3, 5, 10, and 28 days (d) following CTX injection. The β-tubulin was used to normalize.

(C) Western blot analysis of pSmad3 and Smad3 expression on WT and *Nfix*-null muscles 5 and 7 days (d) following CTX injection. GAPDH was used to normalize.

(D) Quantification of the percentage of dMHC positive myofibers in WT and *Nfix*-null mice after 7 and 14 days following CTX injection (n = 6 mice for time point 7 and n = 5 mice for time point 14). The data are presented as mean ± SD (*$p < 0.05$; **$p < 0.01$; and two-tailed unpaired t test).

See also Figure S2E.

promoter that were used to design specific primers. Notably, the identified sites are flanked by putative binding sites for MEF-2, which is a known co-factor of Nfix (Messina et al., 2010).

To assess whether Nfix can bind directly and regulate the Myostatin promoter, we performed a chromatin immunoprecipitation (ChIP) assay on differentiating C2C12. Proliferating C2C12 myoblasts were transduced with a HA-tagged Nfix2 lentiviral vector and then ChIP analysis was performed after 4 days in differentiation medium on the identified Nfix binding domains of Myostatin promoter. As expected, Nfix bound to the Nfatc4 promoter as described previously (Messina et al., 2010), and it was also found to directly bind to Myostatin promoter (Figure 5D). To determine how Nfix binding affected Myostatin expression, we transduced wild-type and *Nfix*-null SC-derived myoblasts with a Nfix2-HA lentivirus. A significant decrease in Myostatin expression was noted following *Nfix* overexpression, both in wild-type and in *Nfix*-null myoblasts (Figure 5E), thereby confirming the repressive role of Nfix on *Mstn* expression.

## In Vivo Silencing of Myostatin Rescues the Regeneration Delay in *Nfix*-Null Mice

From the results indicated above, we predicted that regeneration defects observed in *Nfix*-null mice would be rescued by reducing Myostatin expression. Due to lethality of perinatal mice and

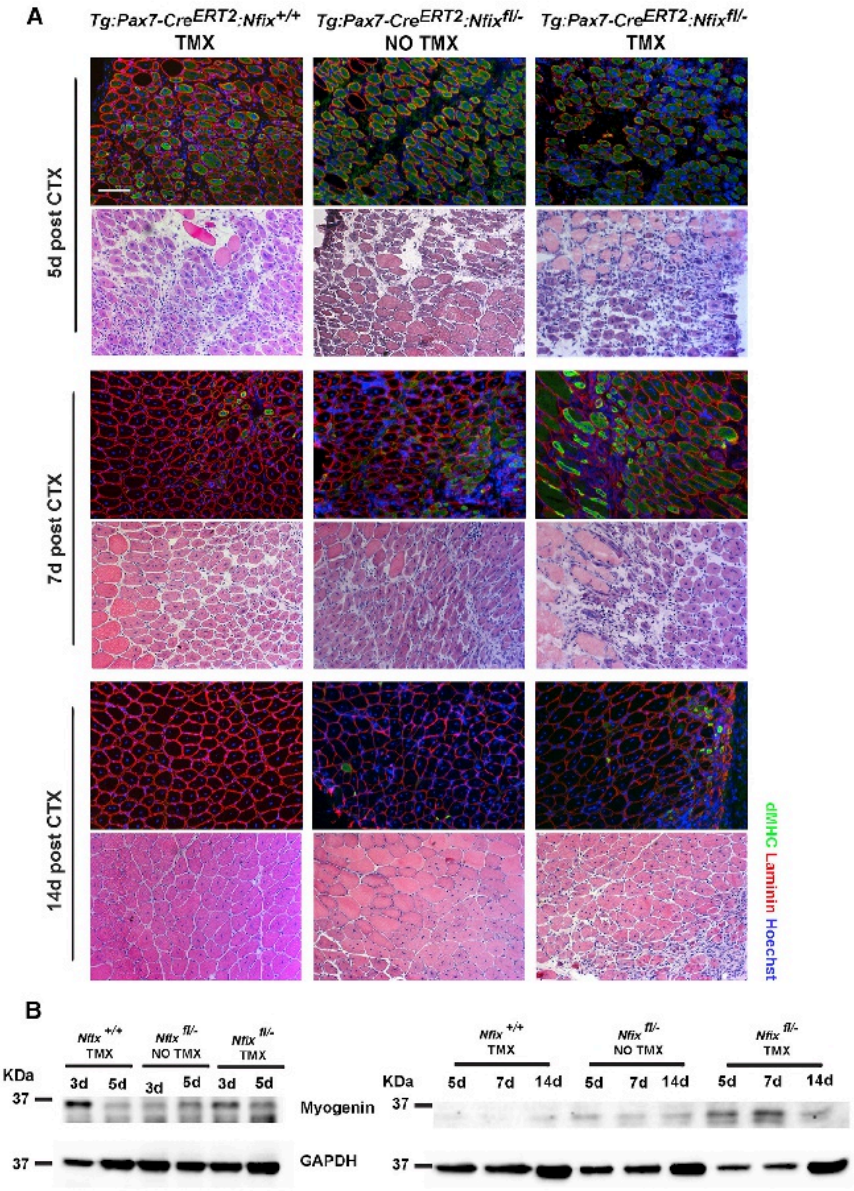


**Figure 4. Absence of Nfix in SCs Determines the Delay in Muscle Regeneration**

(A) H&E staining and immunofluorescence for dMHC (green) on transverse sections of regenerating *Tibialis anterior* muscles from *Tg:Pax7-Cre*$^{ERT2}$*:Nfix*$^{+/+}$ and *Tg:Pax7-Cre*$^{ERT2}$*:Nfix*$^{fl/-}$ mice with (TMX) or without (NO TMX) tamoxifen treatment. The muscles were collected and stained after 5, 7, and 14 days (d) from CTX injection. The laminin is marked in red and Hoechst was used to stain nuclei (n = 3 mice for each group). The scale bar represents 100 μm.

(B) Western blot analysis of Myogenin expression on regenerating muscles from *Tg:Pax7-Cre*$^{ERT2}$*:Nfix*$^{+/+}$ (*Nfix*$^{+/+}$) and *Tg:Pax7-Cre*$^{ERT2}$*:Nfix*$^{fl/-}$ mice (*Nfix*$^{fl/-}$) with (TMX) or without (NO TMX) tamoxifen treatment after 3, 5, 7, and 14 days (d) from CTX injection. Myogenin and GAPDH in the right panel come from two separate gels but using the same samples and protein amount. GAPDH was used to normalize.

See also Figure S3.

difficulties in obtaining viable *Nfix:Mstn* double-null mice, we electroporated wild-type and *Nfix*-null regenerating *Tibialis anterior* muscles with control plasmids (scramble) or plasmids carrying an shRNA targeting *Mstn* (shmstn). Initial studies were carried out to verify the correct downregulation of *Mstn* expression after electroporation of the shmstn plasmid both in entire muscles and in re-isolated myoblasts (Figures S4A and 6C). We then electroporated scramble and shmstn plasmids 4 days after muscle injury, to obtain the maximal downregulation of Myostatin around day 6, which corresponds to the temporal window in which Myostatin was upregulated in *Nfix*-null mice (Figure 3B). Muscles were then isolated and processed at different time points after injury. Remarkably, we obtained a rescue of the regeneration defects of *Nfix*-null mice in muscles treated with the shmstn plasmid, but not with the scramble control vector (Figure 6A). This was particularly evident at 14 days after muscle injury, as shown by analysis of muscle sections stained for dMHC. The differences observed were even more striking in total muscle section reconstructions (Figure S4C). The analysis of the cross sectional area of regenerating myofibers revealed, as expected, a reduced cross sectional area for *Nfix*-null muscles with respect to wild-type. However, the regenerative delay phenotype was rescued upon Myostatin silencing; shmstn treated *Nfix*-null myofibers were comparable in size to scramble-treated wild-type (WT) fibers at the same time points (Figure S4B). This result highlights Myostatin involvement in the regeneration defects of *Nfix*-null mice, although from this experiment we cannot rule out the contribution of Myostatin to *Nfix*-null myofiber size in resting conditions. Strikingly, the regeneration rescue is supported by quantification of dMHC, whose expression was significantly reduced as a consequence of Myostatin silencing in *Nfix*-null mice (Figure 6B).

## DISCUSSION

Developmental and regenerative myogenesis share common and distinct features. Previous work from our group demonstrated that Nfix is responsible for the transcriptional switch from embryonic to fetal myogenesis during prenatal development (Messina et al., 2010). In the present study, we show that *Nfix* is required for maintaining muscle physiology postnatally and for the proper timing of muscle regeneration, where we report a link between Nfix and *Mstn* expression. Notably, the

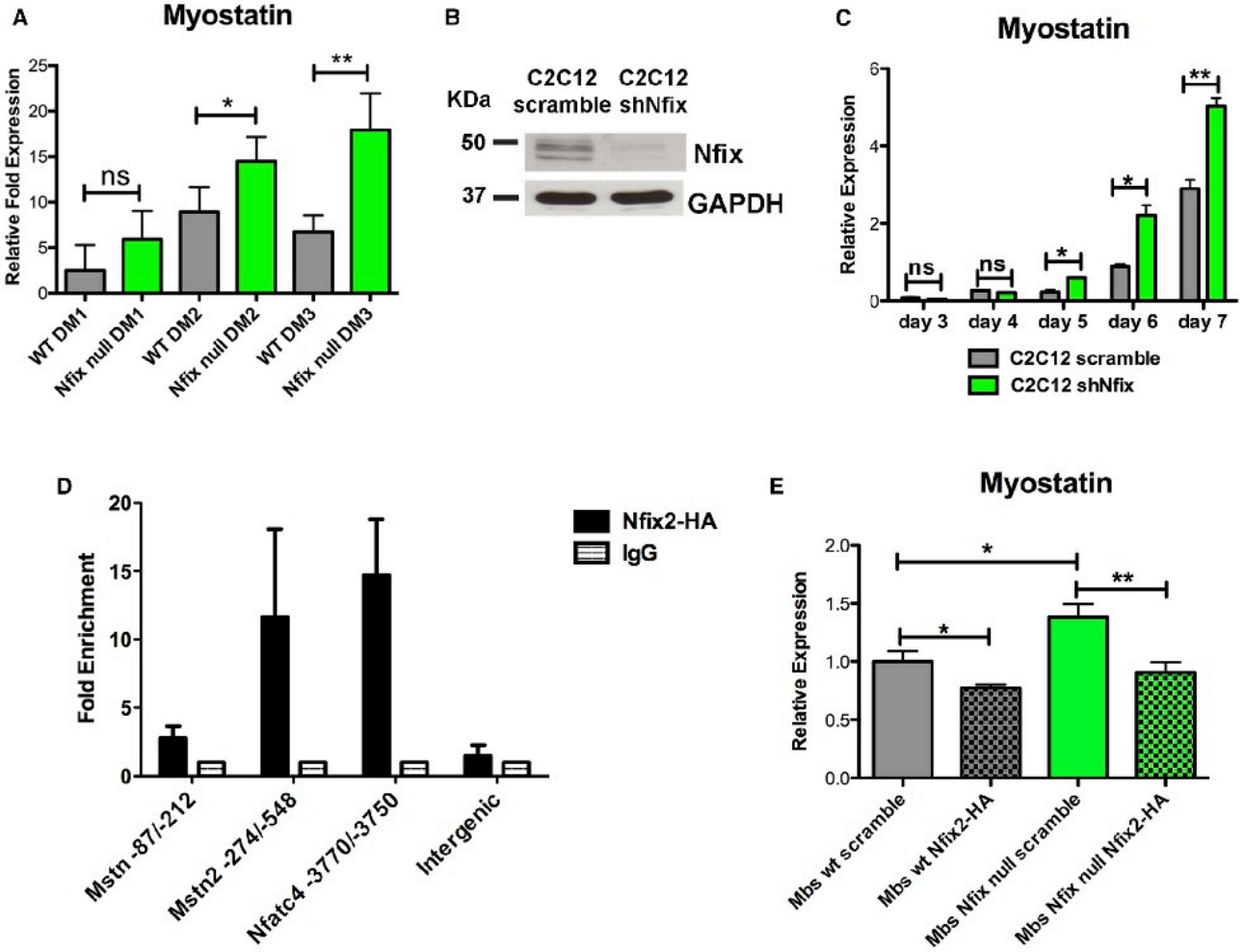


**Figure 5. Nfix Regulates Myostatin Expression in Differentiating Myoblasts through a Direct Binding to its Promoter**

(A) Real-time qPCR showing Myostatin upregulation in differentiating SC-derived myoblasts. The SCs were isolated by FACS and plated in differentiation medium for a time course analysis from 1 to 3 days (DM1, DM2, and DM3) (n = 4 DM1 WT, n = 2 DM1 *Nfix*-null, n = 5 DM2 WT, n = 3 DM2 *Nfix*-null, n = 4 DM3 WT, and n = 4 DM3 *Nfix*-null). The data are presented as mean ± SD (not significant, ns; *p < 0.05; **p < 0.01; and two-tailed unpaired t test).

(B) Western blot analysis of Nfix expression in C2C12 myoblasts transduced with a control vector (C2C12 scramble) or with a vector carrying a shRNA targeting Nfix (C2C12 shNfix). GAPDH was used to normalize.

(C) Real-time qPCR analysis of Myostatin expression in scramble and shNfix C2C12 in a time course from 3 to 7 days in differentiation medium. The values are plotted as relative expression and normalized to GAPDH (n = 3 independent samples for each time point). The data are presented as mean ± SD (not significant, ns; *p < 0.05; **p < 0.01; and two-tailed unpaired t test).

(D) ChIP on differentiated C2C12 transduced with a vector expressing a HA-tagged Nfix2 isoform to test binding to putative Nfix binding sites on Myostatin promoter located at −87/−212 bp and −274/−548 bp from transcription start site. Binding on Nfatc4 promoter and on an intergenic region were used as positive and negative controls, respectively. The data are means of two independent experiments and expressed as fold enrichment (mean ± SD) relative to the IgG signal (n = 3 independent ChIP).

(E) Real-time qPCR for Myostatin in WT and *Nfix*-null SC-derived myoblasts transduced with a control vector (scramble) or with a vector overexpressing the Nfix2 isoform (Nfix2-HA). The values are plotted as relative expression and normalized to GAPDH (n = 3 samples for each group). The data are presented as mean ± SD (*p < 0.05; **p < 0.01; and two-tailed unpaired t test).

absence of Nfix leads to a dramatic delay in muscle regeneration in vivo, and this phenotype can be rescued by suppressing *Mstn* expression.

One of the main features that we observed in *Nfix*-null muscles was an altered muscular physiology characterized by a strikingly reduced muscle fiber size and an overexpression of the slow MyHC isoform. As already observed during prenatal development, the ability of Nfix to modulate slow MyHC expression is maintained after birth. Since Nfix plays important roles in brain and CNS development (Campbell et al., 2008), those phenotypes might directly or indirectly impact on the muscle phenotypes reported here. However, we show that upregulation of slow MyHC in the absence of Nfix is reproducible in SC-derived myotubes in culture, thus suggesting that the phenotype

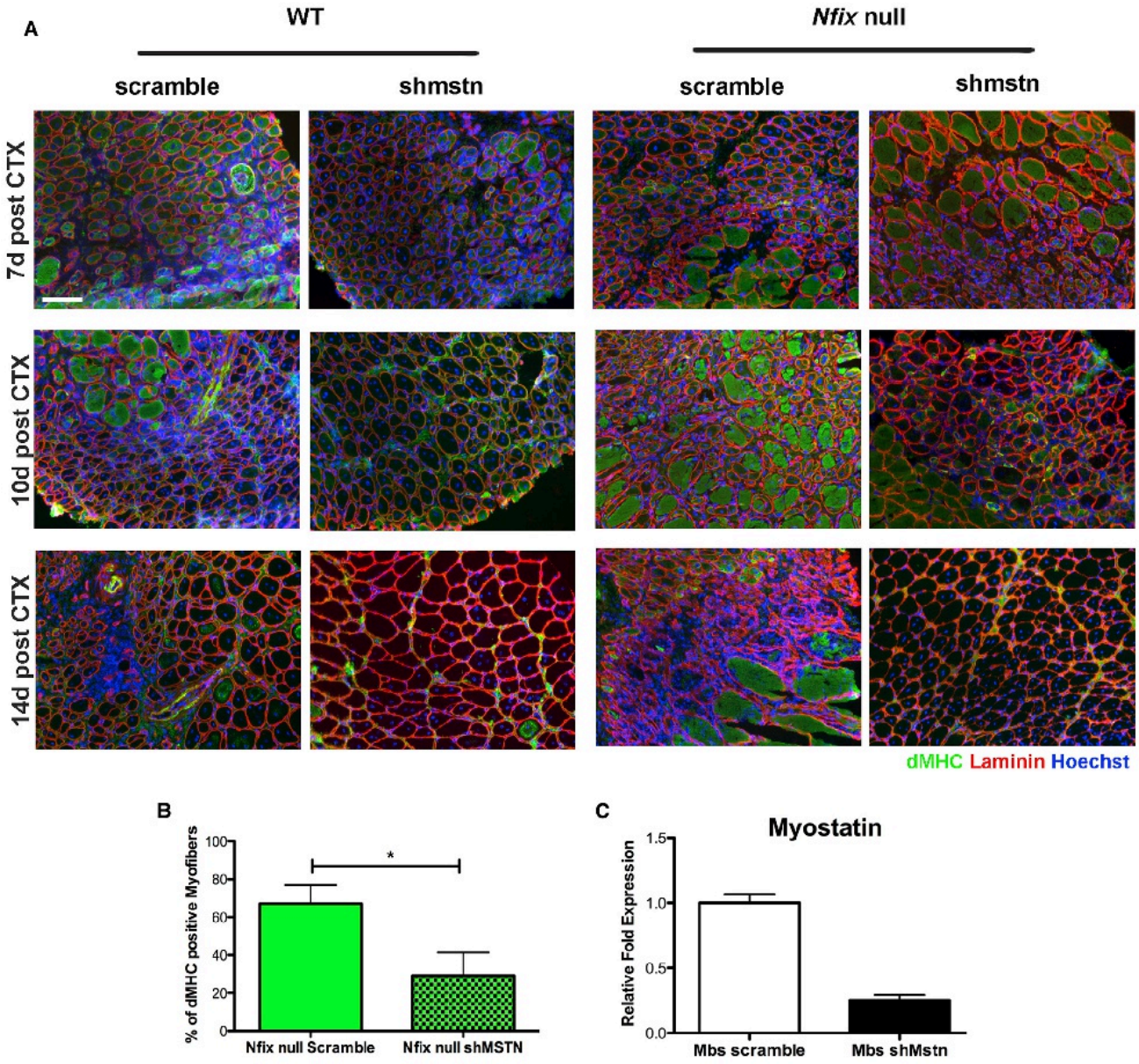


**Figure 6. In Vivo Silencing of Myostatin in Regenerating *Nfix* Null Muscles Rescues their Regeneration Defects**

(A) Immunofluorescence analysis of dMHC expression (green) on regenerating WT and *Nfix*-null *Tibialis anterior* muscles after muscle electroporation with a control plasmid (scramble) or with a plasmid carrying an shRNA targeting Myostatin (shmstn). The muscles were electroporated after 4 days following CTX injection and were collected and stained after 7, 10, and 14 days (d) following CTX injection. The laminin is marked in red and Hoechst was used to stain nuclei (n = 3 mice for each group). The scale bar represents 100 μm.

(B) Quantification of the percentage of dMHC positive myofibers in *Nfix*-null mice electroporated with scramble or shmstn plasmids after 7 and 14 days following CTX injection (n = 5 mice for each group). The data are presented as mean ± SD (*$p < 0.05$ and two-tailed unpaired t test).

(C) Real-time qPCR showing Myostatin expression in myoblasts re-isolated from *Tibialis anterior* electroporated with control (scramble) or shMyostatin (shMstn) plasmids. The myoblasts were isolated the day after in vivo transfection, and cultures were stopped 2 days later to perform qRT-PCR. The data are presented as mean ± SD.

See also Figure S4.

observed is cell-autonomously dependent on *Nfix* function in muscle. Moreover, ChIP experiments on C2C12 confirmed Nfix binding to Nfatc4 promoter, further suggesting that the mechanism of action is conserved between prenatal and postnatal life.

We also noted delayed differentiation of single fiber-associated myogenic cells that is accompanied by the modulation of *Myogenin* expression. This finding is consistent with the marked delay in regeneration observed in *Nfix*-null mice.

Importantly, in addition to the persistent expression of dMyHC and to a delayed expression of *Myogenin* we observed a sustained expression of *Mstn* in injured muscles of *Nfix*-null mice. Myostatin (GDF8) is a potent inhibitor of myogenesis, where a dramatic increase in muscle mass was reported in *Mstn*-null mice (McPherron et al., 1997). However, the mode of action of Myostatin remains under debate for both prenatal and postnatal myogenesis (Manceau et al., 2008). Here, we show that the increased expression of *Mstn* in both *Nfix* silenced differentiating C2C12 cells and SC-derived myoblasts, as also in *Nfix*-null regenerating muscles, correlates with the delayed differentiation in vitro and in injured muscles. Myostatin is known to inhibit myoblast differentiation through inhibition of SC activation and proliferation (McCroskery et al., 2003; Taylor et al., 2001) and through repression of MyoD activity (Langley et al., 2002). Moreover, inhibition of Myostatin is known to accelerate muscle regeneration (McCroskery et al., 2005), thus supporting a causative relationship between the increase in Myostatin levels that we observed in regenerating *Nfix*-null mice and the delayed regeneration that characterizes them. We note that differences between WT and *Nfix*-null mice are apparent in muscles from day 5 after CTX injection, coinciding with the first difference in *Mstn* expression. Moreover, in vivo silencing of *Mstn* in adult *Nfix*-null muscles resulted in recovery of the correct timing of muscle regeneration after injury, confirming the causative relationship between *Mstn* sustained expression and the delayed regeneration observed in mice lacking *Nfix*. Importantly, the delayed regeneration was observed also in tamoxifen treated *Tg:Pax7-Cre$^{ERT2}$:Nfix$^{fl/-}$* mice, supporting the central role played by Nfix in SCs. Accordingly, isolated SC-derived *Nfix*-null myotubes express higher levels of Myostatin during differentiation and this is reversed upon *Nfix* re-expression. We therefore identified a mechanism of action for Nfix by showing that it can act as a direct regulator of *Mstn*. In light of contradictory reports on the mode of action of Myostatin, it is important to underscore the potentially distinct contextual roles of Myostatin (Manceau et al., 2008). Similar to the contextual roles for Notch signaling in adult myogenesis (Mourikis et al., 2012a, 2012b; Rios et al., 2011), recent studies suggest that Myostatin is necessary to regulate to proper balance between proliferation and differentiation of progenitor cells (George et al., 2013; Manceau et al., 2008; McCroskery et al., 2003).

Here, we suggest that *Mstn* regulation is temporally controlled for appropriate muscle differentiation and regeneration. Forced *Mstn* expression or silencing would inevitably led to a complete block in regeneration or to an accelerated differentiation at the expense of the proper muscle physiology.

In summary, this work demonstrates that Nfix acts through an inhibitory mechanism at the *Mstn* promoter in differentiating myoblasts, thereby influencing the commitment of SCs during differentiation and the proper timing of muscle regeneration. The mechanism identified not only broadens our knowledge on the function of Nfix in postnatal skeletal myogenesis, but also contributes to our understanding of molecular mechanisms involved in the regulation of *Mstn*.

## EXPERIMENTAL PROCEDURES

### Animal Models

*Nfix*-null mice were generated crossing heterozygous mice obtained from Prof. Richard M. Gronostajski (University of Buffalo) and were always compared to WT littermates or age-matched WT mice. To increase *Nfix*-null mice survival, their food was supplemented with a soft dough chow (Transgenic Dough Diet, Bioserv) starting from postnatal day (P)21, as described (Campbell et al., 2008). WT mice used as controls were fed with the same diet. *Tg:Pax7-Cre$^{ERT2}$* mice were described previously (Mourikis et al., 2012b). *Nfix$^{fl}$* mice were obtained from Prof. Richard M. Gronostajski (Campbell et al., 2008). Mouse genotyping was performed by PCR (GoTaq DNA Polymerase, Promega) using the primers listed in Table S1. For muscle regeneration, 20 μl of 100 μM CTX from *Naja mossambica* (Sigma-Aldrich) were injected in the *Tibialis anterior* of 2-month-old mice. Induction of *Nfix* deletion in *Tg:Pax7-Cre$^{ERT2}$:Nfix$^{fl/-}$* was performed by multiple tamoxifen injections. Starting from P18, mice received three subcutaneous injections (one every 24 hr for 3 days) of 50 μg tamoxifen (20 mg/ml) per gram of mouse. At 1 week before CTX, mice were subjected to an intraperitoneal injection of 25 mg/ml tamoxifen (250 μγ per gram of mouse). Starting from the day after, mice were fed with a specific tamoxifen enriched or control diet (Harlan). A detailed scheme of tamoxifen treatment is described in Figure S3A.

Mice were kept in pathogen-free conditions and all procedures were conformed to Italian law (D. Lgs n° 2014/26, implementation of the 2010/63/UE) and approved by the University of Milan Animal Welfare Body and by the Italian Minister of Health.

### Measurement of Myofiber Cross Sectional Area

Cross sectional area of the myofibers was calculated on section images obtained from *Tibialis anterior* muscles using ImageJ.

### Cell Culture

C2C12 cells (ATCC) were cultured at 37°C, 5% $CO_2$ in DMEM (Lonza) plus 20% fetal bovine serum (FBS) (Lonza), 2 mM L-Glutamine (Sigma-Aldrich), and 1% Penicillin/Streptomycin (Euroclone). Differentiation was induced plating 1.5 × $10^5$ cells in 35 mm petri dishes with DMEM, 2% horse serum (Lonza), 2 mM L-Glutamine and 1% Penicillin/Streptomycin.

### SC Isolation and Culture

SCs (myoblasts) were isolated from WT and *Nfix*-null mice at P7–P10. Forelimb, hindlimb, and diaphragm muscles were dissected, mechanically cut, and enzymatically digested at 37°C under constant shaking with a solution containing Collagenase I (100 μg/ml, Sigma-Aldrich), Dispase (500 μg/ml, Gibco), and DNaseI (100 μg/ml, Roche) in PBS (Sigma-Aldrich). Undigested tissue was precipitated for 5 min, and the supernatant was centrifuged for 5 min at 1,200 *g*. The cell pellet was resuspended in DMEM plus 10% FBS, 3% chick embryo extract, 2 mM L-Glutamine, 1% Penicillin/Streptomycin and preplated in 150 mm petri dishes for 1 hr. After pre-plating, the non-adherent, myoblast enriched population was collected and plated in collagen coated (Collagen from calf skin, Sigma-Aldrich) 90 mm petri dishes at a density of 15,000 cells per petri. After a few days in proliferation, the myoblasts were eventually plated at high density (250,000 cells in 35 mm dishes) in differentiation medium (DMEM, 5% horse serum, 2 mM L-Glutamine, and 1% Penicillin/Streptomycin).

For cell sorting experiments, tissues were processed similarly, and then cells were blocked with 10% donkey serum (Sigma-Aldrich) in PBS for 15 min at room temperature (RT). The cells were incubated 30 min on ice with primary antibody detecting SM/C-2.6 antigen, biotinylated, 1:200 (Fukada et al., 2004). After two washes, cells were incubated with Streptavidin-APC (BD Pharmingen, 1:500) and CD45-FITC (Rat Anti-Mouse, 30-F11, BD Pharmingen, 1:100), 20 min on ice. The cells were washed again and sorted with a MoFlo XDP cell sorter (Beckman Coulter) based on positivity for SM/C-2.6 antigen and negativity for CD45.

### BrdU Incorporation

For BrdU incorporation, 3 × $10^4$ SC-derived myoblasts were plated in 35 mm petri dishes. The cells were exposed for 1 hr to 50 μm BrdU (Amersham). The

cells were then fixed with 95% EtOH-5% acetic acid (VWR) for 20 min at RT, incubated with PBS-1.5 M HCl (VWR) for 10 min at RT, washed twice with PBS, and permeabilized with 0.2% Triton in PBS. Primary antibody (1:100, anti-Bromo-deoxyuridine clone BU-1, Amersham) was incubated for 1 hr at 4°C. After four washes, secondary antibody (1:500) was incubated with Hoechst for 40 min at RT. The cells were washed twice with PBS before mounting.

### ELISA Assay for Caspase 9 Concentration

Measurement of the apoptosis rate was performed with an ELISA kit for the detection of mouse Caspase-9 concentration (Cusabio Biotech), according to manufacturer's instructions. Data were acquired with a spectrophotometer (wavelength 450 nm, Tecan). Calculation of results was performed using Curve Expert software.

### Single Fiber Isolation and Culture

Single muscle fibers were isolated from gastrocnemius and quadriceps muscles as previously described (Rosenblatt et al., 1995). In brief, muscles were enzymatically dissociated with 0.2% Collagenase I (Sigma-Aldrich) in DMEM for 30 min at 37°C with constant rolling. Single fibers were isolated under a stereomicroscope by gently passing through fire-polished Pasteur pipettes with different sized apertures. Purified single fibers were transferred in new plates with SC growth medium, cultured at 37°C, 5% $CO_2$, and fixed for staining with 4% paraformaldehyde every 24 hr from 0 to 96 hr. EdU incorporation and staining were performed using the Click-iT EdU Alexa Fluor 594 Imaging Kit (Life Technologies), according to manufacturer's instruction.

### Lentiviral Transduction

C2C12 myoblasts were transduced with a lentivirus carrying a scrambled sequence or a shNfix. Transduction was performed in suspension (in DMEM 20% FBS), at a MOI of 100 and in the presence of Polybrene (8 μg/ml, Sigma-Aldrich). After overnight (O/N) incubation, the medium was changed, and cells were treated with puromycin (2 μg/ml, Sigma-Aldrich). SC-derived myoblasts and C2C12 used for ChIP experiments were transduced with a lentiviral vector carrying a control sequence or a Nfix2-HA-tagged isoform, described in Messina et al. (2010).

### Immunofluorescence and Histology

Muscles were isolated from tendon to tendon, rapidly passed in liquid nitrogen-cooled isopentane (VWR) for 1 min, then in liquid nitrogen for 2 min, and left at −80°C until processed. There were 7 μm sections that were cut with a cryostat (Leica) on positively charged glass slides (Superfrost Plus, Thermo Scientific). Muscle sections were stained with H&E (Sigma-Aldrich) according to standard protocols. For immunofluorescence analysis, cells or sections were fixed for 10 min with 4% paraformaldehyde in PBS at 4°C (apart from staining for dMHC that do not require fixation). Samples were then permeabilized with 1% BSA (Sigma-Aldrich)-0.2% Triton X-100 (Sigma-Aldrich) in PBS for 30 min and blocked with 10% goat serum (Sigma-Aldrich) in PBS for 30 min at RT. Primary antibodies were incubated O/N at 4°C in PBS. After two washes with PBS-1% BSA-0.2%Triton, samples were incubated with secondary antibodies (1:500, Jackson Laboratory. Fluorochromes used: 488, 649, 594, and 546) and Hoechst (1:500, Sigma-Aldrich) in PBS for 45 min at RT, washed twice with PBS-0.2% Triton and mounted with Fluorescence Mounting Medium (Dako).

Immunofluorescences on single fibers were performed in suspension. Single myofibers were collected in 1.5 ml tubes and fixed for 10 min with 4% paraformaldehyde in PBS at 4°C. Fixed myofibers were treated with PBS-1% Triton-10% goat serum for 30 min at RT. Primary antibodies were incubated O/N in PBS-1% goat serum. After two washes with a solution containing 1% BSA in PBS, single myofibers were incubated with secondary antibodies and Hoechst in PBS for 1 hr at RT, washed twice with PBS-1% BSA, and mounted on slides.

Images were acquired at RT using a Leica-DMI6000B fluorescence microscope equipped with 10× and 20× magnification objectives. Leica DFC365FX or DFC400 cameras were used for image capture. The Leica Application Suite software was used for acquisition. Single channel pictures were merged using Photoshop. The following primary antibodies and dilutions were used: rabbit anti-Nfix (1:200, Novus Biologicals); chicken anti-laminin (1:500, Abcam); rabbit anti-laminin (1:300, Sigma-Aldrich); mouse anti Pax7 (1:2, DSHB); mouse anti-total MyHC (MF20) (1:2, DSHB); chicken anti-β-gal (1:500, Abcam); mouse anti-dMHC, which detects the Myh3 isoform (1:40, Monosan); rabbit anti-MyoD (C-20) (1:60, Santa Cruz Biotechnology); and mouse anti-Myogenin (1:3, DSHB).

### RNA Extraction, RT-, and Real-Time qPCR

Total RNA from cultured cells was extracted using the NucleoSpin kits RNA XS and II (Macherey-Nagel). Isolation of total RNA from muscles was performed with TRIzol Reagent (Invitrogen) according to the manufacturer's instructions. RNA was quantified using a NanoPhotometer (Implen). There was 1 μg of total RNA for each sample that was retrotranscribed with the iScript Reverse Transcription Supermix for RT-quantitative (q)PCR (Bio-Rad) in a total volume of 20 μl. For qRT PCR, cDNA was diluted 1:10 and 5 μl of the diluted cDNA was loaded in a total volume of 20 μl (iTaq Universal, Bio-Rad). Primers used are listed in Table S2. The relative quantification of gene expression was determined by comparative CT method, and normalized to glyceraldehyde 3-phosphate dehydrogenase (GAPDH).

### ChIP Assay

For ChIP, 3.5 × $10^6$ scramble C2C12 myoblasts per antibody were plated. The cells were maintained in culture for 1 day in DMEM, 20% FBS, and then induced to differentiate with DMEM, 2% horse serum, at a density of 1.5 × $10^6$ cells in 90 mm petri dishes. Crosslink was performed at day 4 in differentiation with 1% formaldehyde (Sigma-Aldrich) in DMEM for 10 min. Crosslink was blocked with 0.125 M Glycine (Sigma-Aldrich) in PBS for 10 min while shaking. After two washes with PBS, cells were scraped with PBS containing protease inhibitors and phenylmethanesulfonyl fluoride (PMSF) and centrifuged for 15 min at 1,500 *g* at 4°C. The cell pellet was dounced 20 times in a 7 ml pestle in swelling buffer, then centrifuged for 10 min at 5,000 *g* at 4°C, and the nuclei pellet was sonicated with a Bioruptor Sonicator (Diagenode) for 15 min, with repeated cycles of 15 s of sonication and 15 s of resting. Samples were finally centrifuged for 10 min at 12,000 *g* at 4°C, and chromatin-enriched supernatant was used in the following passages. Chromatin was pre-cleared for 2 hr with Protein G Sepharose (PrG, 15 μl per sample) (Amersham) and rabbit serum (2.5 μl per sample) and for 2 hr with PrG previously blocked with BSA (10 μg/ml) and Salmon Sperm (1 μg/ml) (Sigma-Aldrich) on a rotating platform at 4°C. Chromatin was than incubated O/N with primary antibodies. The day after, immunocomplexes were precipitated by addition of blocked PrG for 3 hr on rotating platform at 4°C, then centrifuged for 2 min at 12,000 *g* at 4°C. Samples were then repeatedly washed and the antibody-protein-DNA complexes were eluted twice for 10 min at 65°C. Eluted samples were incubated O/N at 65°C with 10 μg RNase (Sigma-Aldrich) and 200 mM NaCl (Sigma-Aldrich) to reverse crosslinks. Finally, DNA was treated with Proteinase K (Sigma-Aldrich) (20 μg per sample) for 3 hr at 50°C and then extracted with phenol-chloroform. Obtained DNA samples were analyzed with qPCR and results were plotted as fold enrichment with respect to the IgG sample. Primers used are listed in Table S3.

There were 5 μg of the following primary antibodies that were used: rabbit anti-HA-probe (Y-11, Santa Cruz Biotechnology); normal rabbit IgG (Santa Cruz Biotechnology).

### Western Blot

Total protein extracts were obtained from cells or homogenized tissues, lysed with RIPA or Tissue extraction buffer plus protease and phosphatase inhibitors for 30 min on ice. Samples were then centrifuged 10 min at 12,000 x *g* at 4°C, and the supernatant transferred into a new tube and quantified using the DC Protein Assay (Bio-Rad). There were 30 μg of total protein extracts that were loaded on a 7%–12% SDS (Sigma-Aldrich) acrylamide gel (Sigma-Aldrich) and blotted to a nitrocellulose membrane (Whatman, Protran Nitrocellulose Transfer Membrane). After 1 hr of blocking in milk, primary antibodies were incubated O/N. Blots were then washed and incubated with secondary antibodies (1:10,000, IgG-HRP, Bio-Rad) for 40 min at RT and washed again. Finally, bands were revealed with ECL detection reagent (Amersham) and exposed to an X-ray film (Hyperfilm ECL, Amersham). In some cases, blots were acquired using the Chemidoc software (Bio-Rad).

The following primary antibodies and dilutions were used: rabbit anti-Nfix (1:5,000, Geneka Biotechnology); mouse anti-β-tubulin (1:5,000, Covance); mouse anti-slow MyHC (Bad5, 1:2, DSHB); mouse anti-total MyHC (MF20, 1:5, DSHB); mouse anti-Myogenin (IF5D, 1:3, DSHB); rabbit anti-Myostatin (1:500, Millipore); mouse anti-GAPDH (1:5,000, Sigma-Aldrich); rabbit anti-Smad3 (1:1,000, Abcam); rabbit anti-pSmad3 (1:1,000, Abcam).

### In Vivo Electroporation

In vivo electroporation was performed 4 days after CTX injection. WT and *Nfix*-null mice were anesthetized and 40 μg of control (scramble, Sigma-Aldrich), or shmstn (Sigma-Aldrich) plasmids were injected in a total volume of 20 μl in *Tibialis anterior* muscles. Muscles were then immediately electroporated using a pulse generator (ECM 830, BTX) equipped with 5 mm needle electrodes to generate 100 V pulses, with a fixed duration of 20 ms and an interval of 200 ms between the pulses.

### Statistical Analysis

All data are expressed as mean ± SD. Data were graphed using GraphPad Prism and analyzed with the two-tailed unpaired Student's t test. *$p < 0.05$; **$p < 0.01$; ***$p < 0.001$; and confidence intervals 95%, alpha level 0.05.

## SUPPLEMENTAL INFORMATION

Supplemental Information includes four figures and three tables and can be found with this article online at http://dx.doi.org/10.1016/j.celrep.2016.02.014.

## AUTHOR CONTRIBUTIONS

Conceptualization, G.R. and G.M.; Methodology, S.A.; Investigation, G.R., S.A., C.B., S.M., and C.V.; Writing – Original Draft, G.R.; Writing – Review & Editing, S.T., G.C., and G.M.; Supervision, G.M.; and Funding Acquisition, G.M.

## ACKNOWLEDGMENTS

We thank G. Maroli for helpful discussion. We are also grateful to M. Magistroni for technical assistance, C. Villa (FRACTAL) for the Cytometry service, P. Mourikis for help with the tamoxifen protocol, F. Relaix and H. Amthor for their help and exchange of animal models, and R. Gronostajski for the kind exchange of information and animal models. G.R. conducted this study as partial fulfillment of her PhD in Cellular and Molecular Biology, San Raffaele University, Milan. This work received funding from the European Community, ERC StG2011 (RegeneratioNfix 280611), and the Italian Ministry of University and Research (MIUR-Futuro in Ricerca 2010).

Received: May 28, 2015
Revised: December 2, 2015
Accepted: January 28, 2016
Published: February 25, 2016

## REFERENCES

Bachurski, C.J., Kelly, S.E., Glasser, S.W., and Currier, T.A. (1997). Nuclear factor I family members regulate the transcription of surfactant protein-C. J. Biol. Chem. *272*, 32759–32766.

Bedford, F.K., Julius, D., and Ingraham, H.A. (1998). Neuronal expression of the 5HT3 serotonin receptor gene requires nuclear factor 1 complexes. J. Neurosci. *18*, 6186–6194.

Biressi, S., Molinaro, M., and Cossu, G. (2007a). Cellular heterogeneity during vertebrate skeletal muscle development. Dev. Biol. *308*, 281–293.

Biressi, S., Tagliafico, E., Lamorte, G., Monteverde, S., Tenedini, E., Roncaglia, E., Ferrari, S., Ferrari, S., Cusella-De Angelis, M.G., Tajbakhsh, S., and Cossu, G. (2007b). Intrinsic phenotypic diversity of embryonic and fetal myoblasts is revealed by genome-wide gene expression analysis on purified cells. Dev. Biol. *304*, 633–651.

Bogdanovich, S., Krag, T.O., Barton, E.R., Morris, L.D., Whittemore, L.A., Ahima, R.S., and Khurana, T.S. (2002). Functional improvement of dystrophic muscle by myostatin blockade. Nature *420*, 418–421.

Campbell, C.E., Piper, M., Plachez, C., Yeh, Y.T., Baizer, J.S., Osinski, J.M., Litwack, E.D., Richards, L.J., and Gronostajski, R.M. (2008). The transcription factor Nfix is essential for normal brain development. BMC Dev. Biol. *8*, 52.

Collins, C.A., Olsen, I., Zammit, P.S., Heslop, L., Petrie, A., Partridge, T.A., and Morgan, J.E. (2005). Stem cell function, self-renewal, and behavioral heterogeneity of cells from the adult muscle satellite cell niche. Cell *122*, 289–301.

Darville, M.I., Antoine, I.V., and Rousseau, G.G. (1992). Characterization of an enhancer upstream from the muscle-type promoter of a gene encoding 6-phosphofructo-2-kinase/fructose-2,6-bisphosphatase. Nucleic Acids Res. *20*, 3575–3583.

Driller, K., Pagenstecher, A., Uhl, M., Omran, H., Berlis, A., Gründer, A., and Sippel, A.E. (2007). Nuclear factor I X deficiency causes brain malformation and severe skeletal defects. Mol. Cell. Biol. *27*, 3855–3867.

Edmondson, D.G., Cheng, T.C., Cserjesi, P., Chakraborty, T., and Olson, E.N. (1992). Analysis of the myogenin promoter reveals an indirect pathway for positive autoregulation mediated by the muscle-specific enhancer factor MEF-2. Mol. Cell. Biol. *12*, 3665–3677.

Elliott, B., Renshaw, D., Getting, S., and Mackenzie, R. (2012). The central role of myostatin in skeletal muscle and whole body homeostasis. Acta Physiol. (Oxf.) *205*, 324–340.

Fukada, S., Higuchi, S., Segawa, M., Koda, K., Yamamoto, Y., Tsujikawa, K., Kohama, Y., Uezumi, A., Imamura, M., Miyagoe-Suzuki, Y., et al. (2004). Purification and cell-surface marker characterization of quiescent satellite cells from murine skeletal muscle by a novel monoclonal antibody. Exp. Cell Res. *296*, 245–255.

Funk, W.D., and Wright, W.E. (1992). Cyclic amplification and selection of targets for multicomponent complexes: myogenin interacts with factors recognizing binding sites for basic helix-loop-helix, nuclear factor 1, myocyte-specific enhancer-binding factor 2, and COMP1 factor. Proc. Natl. Acad. Sci. USA *89*, 9484–9488.

George, R.M., Biressi, S., Beres, B.J., Rogers, E., Mulia, A.K., Allen, R.E., Rawls, A., Rando, T.A., and Wilson-Rawls, J. (2013). Numb-deficient satellite cells have regeneration and proliferation defects. Proc. Natl. Acad. Sci. USA *110*, 18549–18554.

Gronostajski, R.M. (2000). Roles of the NFI/CTF gene family in transcription and development. Gene *249*, 31–45.

Hutcheson, D.A., Zhao, J., Merrell, A., Haldar, M., and Kardon, G. (2009). Embryonic and fetal limb myogenic cells are derived from developmentally distinct progenitors and have different requirements for beta-catenin. Genes Dev. *23*, 997–1013.

Jackson, D.A., Rowader, K.E., Stevens, K., Jiang, C., Milos, P., and Zaret, K.S. (1993). Modulation of liver-specific transcription by interactions between hepatocyte nuclear factor 3 and nuclear factor 1 binding DNA in close apposition. Mol. Cell. Biol. *13*, 2401–2410.

Johanson, M., Meents, H., Ragge, K., Buchberger, A., Arnold, H.H., and Sandmöller, A. (1999). Transcriptional activation of the myogenin gene by MEF2-mediated recruitment of myf5 is inhibited by adenovirus E1A protein. Biochem. Biophys. Res. Commun. *265*, 222–232.

Kruse, U., and Sippel, A.E. (1994). The genes for transcription factor nuclear factor I give rise to corresponding splice variants between vertebrate species. J. Mol. Biol. *238*, 860–865.

Langley, B., Thomas, M., Bishop, A., Sharma, M., Gilmour, S., and Kambadur, R. (2002). Myostatin inhibits myoblast differentiation by down-regulating MyoD expression. J. Biol. Chem. *277*, 49831–49840.

Lepper, C., Partridge, T.A., and Fan, C.M. (2011). An absolute requirement for Pax7-positive satellite cells in acute injury-induced skeletal muscle regeneration. Development *138*, 3639–3646.

Manceau, M., Gros, J., Savage, K., Thomé, V., McPherron, A., Paterson, B., and Marcelle, C. (2008). Myostatin promotes the terminal differentiation of embryonic muscle progenitors. Genes Dev. *22*, 668–681.

Mauro, A. (1961). Satellite cell of skeletal muscle fibers. J. Biophys. Biochem. Cytol. *9*, 493–495.

McCarthy, J.J., Mula, J., Miyazaki, M., Erfani, R., Garrison, K., Farooqui, A.B., Srikuea, R., Lawson, B.A., Grimes, B., Keller, C., et al. (2011). Effective fiber hypertrophy in satellite cell-depleted skeletal muscle. Development *138*, 3657–3666.

McCroskery, S., Thomas, M., Maxwell, L., Sharma, M., and Kambadur, R. (2003). Myostatin negatively regulates satellite cell activation and self-renewal. J. Cell Biol. *162*, 1135–1147.

McCroskery, S., Thomas, M., Platt, L., Hennebry, A., Nishimura, T., McLeay, L., Sharma, M., and Kambadur, R. (2005). Improved muscle healing through enhanced regeneration and reduced fibrosis in myostatin-null mice. J. Cell Sci. *118*, 3531–3541.

McPherron, A.C., and Lee, S.J. (1997). Double muscling in cattle due to mutations in the myostatin gene. Proc. Natl. Acad. Sci. USA *94*, 12457–12461.

McPherron, A.C., Lawler, A.M., and Lee, S.J. (1997). Regulation of skeletal muscle mass in mice by a new TGF-beta superfamily member. Nature *387*, 83–90.

Messina, G., Biressi, S., Monteverde, S., Magli, A., Cassano, M., Perani, L., Roncaglia, E., Tagliafico, E., Starnes, L., Campbell, C.E., et al. (2010). Nfix regulates fetal-specific transcription in developing skeletal muscle. Cell *140*, 554–566.

Mourikis, P., Gopalakrishnan, S., Sambasivan, R., and Tajbakhsh, S. (2012a). Cell-autonomous Notch activity maintains the temporal specification potential of skeletal muscle stem cells. Development *139*, 4536–4548.

Mourikis, P., Sambasivan, R., Castel, D., Rocheteau, P., Bizzarro, V., and Tajbakhsh, S. (2012b). A critical requirement for notch signaling in maintenance of the quiescent skeletal muscle stem cell state. Stem Cells *30*, 243–252.

Murphy, M.M., Lawson, J.A., Mathew, S.J., Hutcheson, D.A., and Kardon, G. (2011). Satellite cells, connective tissue fibroblasts and their interactions are crucial for muscle regeneration. Development *138*, 3625–3637.

Pistocchi, A., Gaudenzi, G., Foglia, E., Monteverde, S., Moreno-Fortuny, A., Pianca, A., Cossu, G., Cotelli, F., and Messina, G. (2013). Conserved and divergent functions of Nfix in skeletal muscle development during vertebrate evolution. Development *140*, 1528–1536.

Relaix, F., and Zammit, P.S. (2012). Satellite cells are essential for skeletal muscle regeneration: the cell on the edge returns centre stage. Development *139*, 2845–2856.

Rios, A.C., Serralbo, O., Salgado, D., and Marcelle, C. (2011). Neural crest regulates myogenesis through the transient activation of NOTCH. Nature *473*, 532–535.

Rosenblatt, J.D., Lunt, A.I., Parry, D.J., and Partridge, T.A. (1995). Culturing satellite cells from living single muscle fiber explants. In Vitro Cell. Dev. Biol. Anim. *31*, 773–779.

Sambasivan, R., Yao, R., Kissenpfennig, A., Van Wittenberghe, L., Paldi, A., Gayraud-Morel, B., Guenou, H., Malissen, B., Tajbakhsh, S., and Galy, A. (2011). Pax7-expressing satellite cells are indispensable for adult skeletal muscle regeneration. Development *138*, 3647–3656.

Sartore, S., Gorza, L., and Schiaffino, S. (1982). Fetal myosin heavy chains in regenerating muscle. Nature *298*, 294–296.

Schiaffino, S., Gorza, L., Dones, I., Cornelio, F., and Sartore, S. (1986). Fetal myosin immunoreactivity in human dystrophic muscle. Muscle Nerve *9*, 51–58.

Schuelke, M., Wagner, K.R., Stolz, L.E., Hübner, C., Riebel, T., Kömen, W., Braun, T., Tobin, J.F., and Lee, S.J. (2004). Myostatin mutation associated with gross muscle hypertrophy in a child. N. Engl. J. Med. *350*, 2682–2688.

Spitz, F., Salminen, M., Demignon, J., Kahn, A., Daegelen, D., and Maire, P. (1997). A combination of MEF3 and NFI proteins activates transcription in a subset of fast-twitch muscles. Mol. Cell. Biol. *17*, 656–666.

Szabó, P., Moitra, J., Rencendorj, A., Rákhely, G., Rauch, T., and Kiss, I. (1995). Identification of a nuclear factor-I family protein-binding site in the silencer region of the cartilage matrix protein gene. J. Biol. Chem. *270*, 10212–10221.

Taylor, W.E., Bhasin, S., Artaza, J., Byhower, F., Azam, M., Willard, D.H., Jr., Kull, F.C., Jr., and Gonzalez-Cadavid, N. (2001). Myostatin inhibits cell proliferation and protein synthesis in C2C12 muscle cells. Am. J. Physiol. Endocrinol. Metab. *280*, E221–E228.

Thomas, M., Langley, B., Berry, C., Sharma, M., Kirk, S., Bass, J., and Kambadur, R. (2000). Myostatin, a negative regulator of muscle growth, functions by inhibiting myoblast proliferation. J. Biol. Chem. *275*, 40235–40243.

Xu, H., Uno, J.K., Inouye, M., Collins, J.F., and Ghishan, F.K. (2005). NF1 transcriptional factor(s) is required for basal promoter activation of the human intestinal NaPi-IIb cotransporter gene. Am. J. Physiol. Gastrointest. Liver Physiol. *288*, G175–G181.

**Cell Reports, Volume *14***

## Supplemental Information

# Nfix Regulates Temporal Progression of Muscle Regeneration through Modulation of Myostatin Expression

**Giuliana Rossi, Stefania Antonini, Chiara Bonfanti, Stefania Monteverde, Chiara Vezzali, Shahragim Tajbakhsh, Giulio Cossu, and Graziella Messina**

**Supplemental Information**

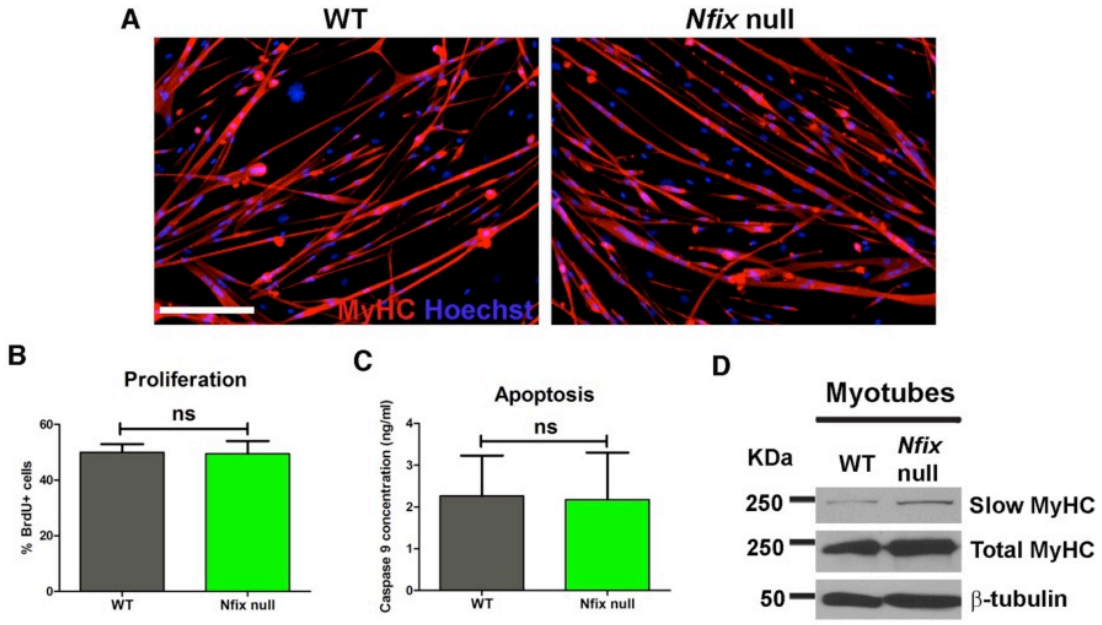


**Fig.S1. Isolated satellite cells in culture correctly differentiate in absence of Nfix, while expressing higher levels of slow MyHC, Related to Fig.1.**

**(A)** Immunofluorescence analysis of total MyHC expression (red) on wild-type and *Nfix* null satellite cell-derived myotubes after 48 h in differentiation medium. Hoechst was used to stain nuclei. n=3 independent myoblast preparations. Scale bar represents 50μm.

**(B)** Quantification of the percentage of wild-type and *Nfix* null BrdU incorporating myoblasts after 1h of exposure to 50μM BrdU. The experiment was performed in duplicate (n=2 independent myoblast preparations) in proliferation conditions. Data are presented as mean ± SD. ns: not significant, two-tailed unpaired *t* Test.

**(C)** ELISA assay measuring caspase 9 concentration as a marker of apoptosis. The test was performed on protein extracts from wild-type and *Nfix* null proliferating myoblasts. Data are presented as mean ± SD. ns: not significant, two-tailed unpaired *t* Test. n=2 assays performed on independent myoblast preparations.

**(D)** Western blot analysis of slow and total MyHC expression on wild-type and *Nfix* null satellite cell-derived myotubes after 48 h in differentiation medium. β-tubulin was used to normalize the amount of loaded proteins.

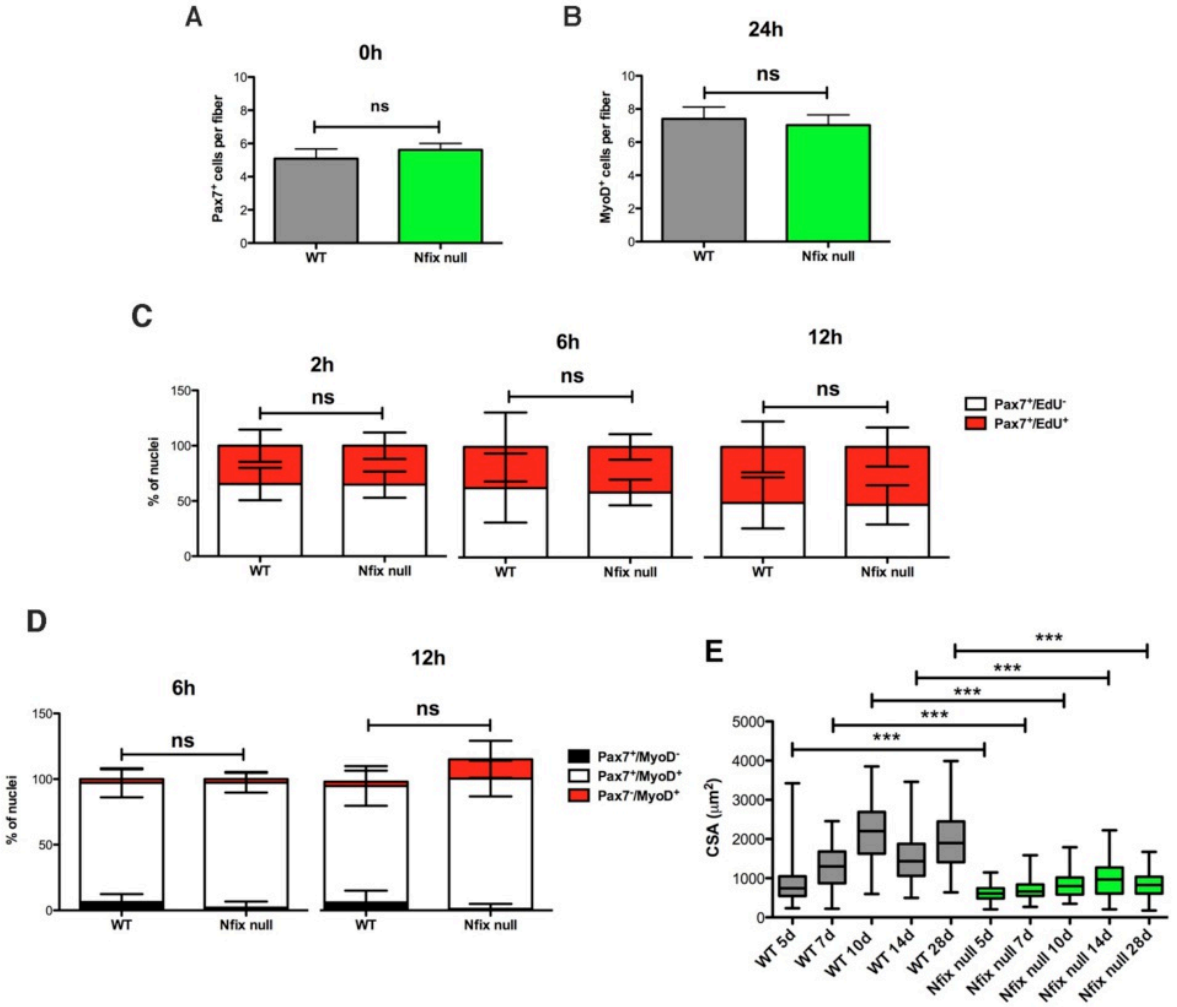


**Fig.S2. Number and proliferation of satellite cells associated to myofibers does not change in the absence of Nfix, Related to Figs.2 and 3.**

**(A)** Quantification of $Pax7^+$ satellite cells associated to freshly isolated wild-type and *Nfix* null myofibers. (n=35 WT and 41 *Nfix* null myofibers). Data are presented as mean ± SD. ns: not significant, two-tailed unpaired *t* Test.

**(B)** Quantification of $MyoD^+$ satellite cells associated to wild-type and *Nfix* null myofibers after 24 hours in culture. (n=32 WT and 34 *Nfix* null myofibers). Data are presented as mean ± SD. ns: not significant, two-tailed unpaired *t* Test.

**(C)** Quantification of the percentage of proliferating ($EdU^+$) wild-type and *Nfix* null satellite cells after 2 (n=18 WT and 14 *Nfix* null myofibers), 6 (n=7 WT and 15 *Nfix* null myofibers), and 12 hours (n=8 WT and 16 *Nfix* null myofibers) (h) in culture. Data are presented as mean ± SD. ns: not significant, two-tailed unpaired *t* Test.

**(D)** Quantification of the percentage of satellite cells expressing MyoD and Pax7 after 6 (n=9 WT and 22 *Nfix* null myofibers) and 12 hours (n=10 WT and 24 *Nfix* null myofibers) in culture. Data are presented as mean ± SD. ns: not significant, two-tailed unpaired *t* Test.

**(E)** Measurement of the myofiber cross sectional area distribution in WT and *Nfix* null regenerating muscles at different time points from injury. n=225 myofibers. Data are presented as mean±whiskers from min to max. ***P < 0.001; two-tailed unpaired t Test.

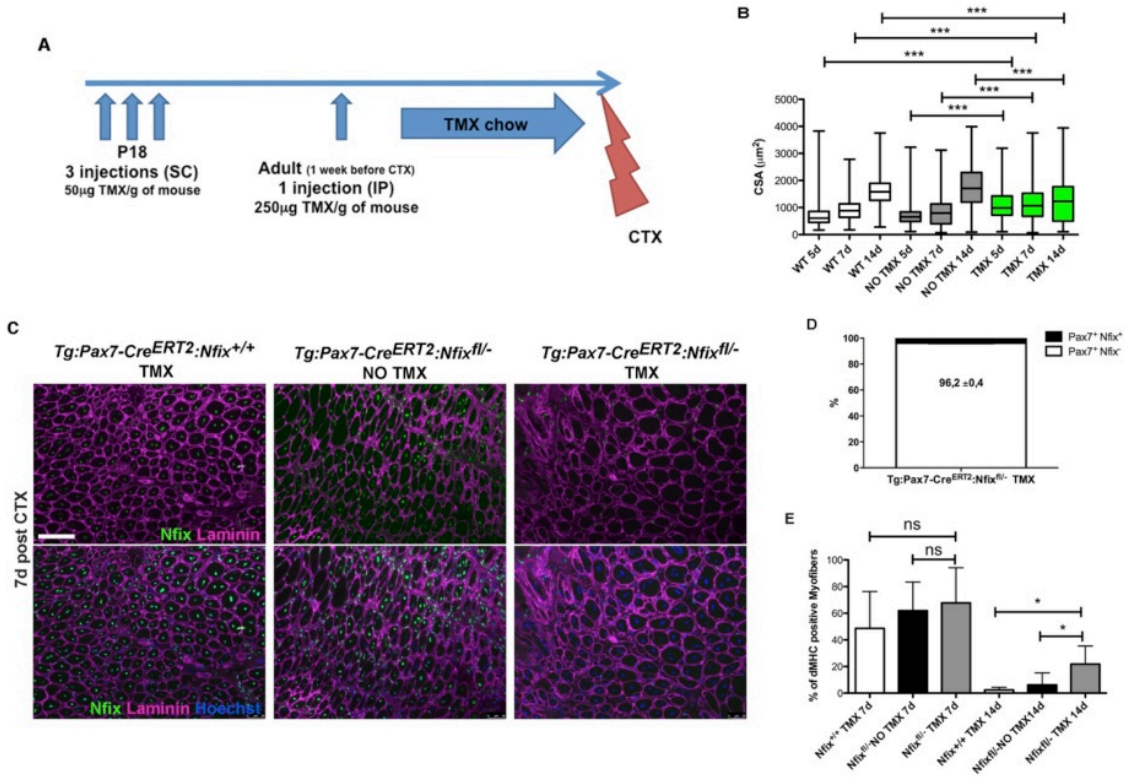


**Fig.S3. Tamoxifen treatment of *Tg:Pax7-Cre$^{ERT2}$:Nfix$^{fl/-}$* mice determines Nfix excision in satellite cells, Related to Fig.4.**

**(A)** Scheme representing the protocol used for tamoxifen treatment (TMX) and cardiotoxin (CTX) injection. SC, subcutaneous. IP, intraperitoneal.

**(B)** Measurement of the myofiber cross sectional area distribution in regenerating muscles of *Tg:Pax7-Cre$^{ERT2}$:Nfix$^{+/+}$* (indicated as WT) and *Tg:Pax7-Cre$^{ERT2}$:Nfix$^{fl/-}$* mice with (TMX) or without (NO TMX) tamoxifen at different time points from injury. n=750 myofibers. Data are presented as mean±whiskers from min to max. ***P < 0.001; two-tailed unpaired *t* Test.

**(C)** Immunofluorescence analysis of Nfix expression (green) in *Tg:Pax7-Cre$^{ERT2}$:Nfix$^{+/+}$* and *Tg:Pax7-Cre$^{ERT2}$:Nfix$^{fl/-}$* mice with (TMX) or without (NO TMX) tamoxifen treatment 7 days (d) after cardiotoxin injection. Laminin, purple; Hoechst, nuclei. n=3 mice for each group. Scale bar represents 100µm.

**(D)** Graphical representation of the percentage of Nfix excision in tamoxifen treated *Tg:Pax7-Cre$^{ERT2}$:Nfix$^{fl/-}$* mice. Quantification was obtained counting the percentage of cells expressing Pax7 and Nfix in muscle sections. n=2 mice. Data are presented as mean ± SD.

**(E)** Quantification of the percentage of dMHC positive myofibers in *Tg:Pax7-Cre$^{ERT2}$:Nfix$^{+/+}$* and *Tg:Pax7-Cre$^{ERT2}$:Nfix$^{fl/-}$* mice with (TMX) or without (NO TMX) tamoxifen treatment 7 and 14 days following cardiotoxin injection. For time point 7, n=5 *Tg:Pax7-Cre$^{ERT2}$:Nfix$^{+/+}$*, n=8 *Tg:Pax7-Cre$^{ERT2}$:Nfix$^{fl/-}$* NO TMX mice, n=6 *Tg:Pax7-Cre$^{ERT2}$:Nfix$^{fl/-}$* TMX mice. For time point 14, n=5 *Tg:Pax7-Cre$^{ERT2}$:Nfix$^{+/+}$*, n=6 *Tg:Pax7-Cre$^{ERT2}$:Nfix$^{fl/-}$* NO TMX mice, n=6 *Tg:Pax7-Cre$^{ERT2}$:Nfix$^{fl/-}$* TMX mice. Data are presented as mean ± SD. ns: not significant, *P <0,05, two-tailed unpaired *t* Test.

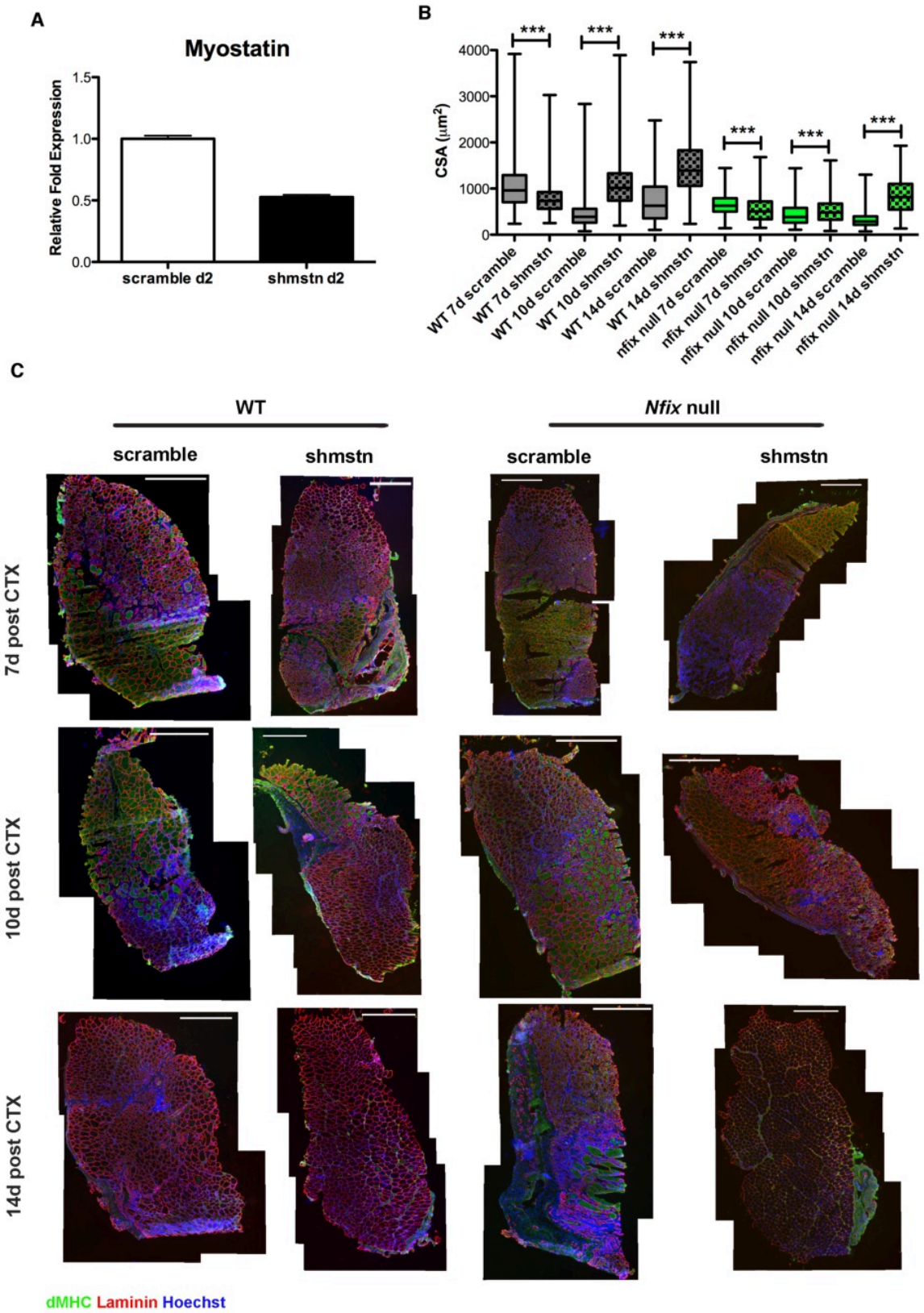
A
Myostatin
Relative Fold Expression
1.5
1.0
0.5
0.0
scramble d2
shmstn d2
B
CSA (μm²)
4000
3000
2000
1000
0
***
WT 7d scramble
WT 7d shmstn
WT 10d scramble
WT 10d shmstn
WT 14d scramble
WT 14d shmstn
nfix null 7d scramble
nfix null 7d shmstn
nfix null 10d scramble
nfix null 10d shmstn
nfix null 14d scramble
nfix null 14d shmstn
C
WT
Nfix null
scramble
shmstn
scramble
shmstn
7d post CTX
10d post CTX
14d post CTX
dMHC Laminin Hoechst

**Fig.S4. *In vivo* silencing of Myostatin rescues the regeneration defects of *Nfix* null muscles, Related to Fig.6.**

**(A)** Real-Time qPCR showing Myostatin expression in *Tibialis anterior* muscles at 2 days (d) after electroporation with control (scramble) or shMyostatin (shmstn) plasmids. Data are presented as mean ± SD.

**(B)** Measurement of the myofiber cross sectional area distribution in WT and *Nfix* null regenerating muscles electroporated with scramble or shmstn plasmids. n=475 myofibers. Data are presented as mean±whiskers from min to max.***P < 0.001; two-tailed unpaired *t* Test.

**(C)** Immunofluorescence analysis of developmental MyHC expression (dMHC, green) on regenerating wild-type and *Nfix* null *Tibialis Anterior* m uscle sections after muscle electroporation with a control plasmid (scramble) or with a plasmid carrying an shRNA targeting myostatin (shmstn). Muscle sections were collected and stained 7, 10 and 14 days (d) after cardiotoxin (CTX) injection. Muscles were electroporated 4 days (d) after cardiotoxin injection. Laminin, red; Hoechst, nuclei. Images represent photomerge reconstruction of the entire muscle section shown in Fig.6. Scale bar represents 500μm.

**Table S1. Related to Experimental Procedures. List of primers used for mouse genotyping**

| Primer Name | Sequence |
|---|---|
| **Nfix I1F5** | ATGGACATGTCATGGGTGCGACAG |
| **Nfix I2R2-CEC** | AAGCCCCTCAGCTCTAGCACAGAG |
| **Nfix I1R1** | AACCAGAGGCACGAGAGCTTGTC |
| ***Pax7-Cre*$^{ERT2}$ for** | CCACACCTCCCCCTGAACCTGAAACATAAA |
| ***Pax7-Cre*$^{ERT2}$ rev** | GAATTCCCCGGGGAGTCGCATCCGCGG |

**Table S2. Related to Experimental Procedures. List of primers used for qRT-PCR**

| Primer Name | Sequence |
|---|---|
| **Myostatin for** | AAGATGACGATTATGACGCTACC |
| **Myostatin rev** | CCGCTTGCATTAGAAAGTCAGA |
| **GAPDH for** | AGGTCGGTGTGAACGGATTTG |
| **GAPDH rev** | TGTAGACCATGTAGTTGAGGTCA |

**Table S3. Related to Experimental Procedures. List of primers used for ChiP**

| Primer Name | Sequence |
|---|---|
| **Myostatin promoter (415-539)for** | TTGTGGAGCAGGAGCCAATC |
| **Myostatin promoter (415-539)rev** | GTACCGTCCGAGAGACAACC |
| **Myostatin promoter (116-369)for** | GTAACAAAACAGCACTCCAAGTC |
| **Myostatin promoter (116-369)rev** | CCCTGTCTGTCACAAGTCACC |
| **Nfatc4 promoter for** | GGCGCTTAACCCTTTAGGTG |
| **Nfatc4 promoter rev** | CAAGACAGGGGAGCAGTCAC |
| **Intergenic region for** | GACCTGCCTGTTCCTTCTTG |
| **Intergenic region rev** | GTTACCCAGCACTGCAAAGG |

# PART III

# MANUSCRIPT IN PREPARATION

## Mesoangioblasts engraft lung and intestinal epithelium upon systemic transplantation in CF mouse models rescuing CFTR function

Chiara Vezzali[1], C. Bonfanti[1], S. Antonini[1], C. Barone[2], D. de Stefano[3], L. Maiuri[3], M. Egan[2], E. Bruscia[2] and Graziella Messina[1]

*[1]University of Milan, Dept of BioSciences, Milan, Italy, [2]Yale University, School of Medicine, New Haven (CT), USA, [3]Ospedale San Raffaele, Milan, Italy*

### Abstract

Cystic Fibrosis (CF) is caused by mutations in the *CFTR* gene. Lung disease, characterized by airway obstruction, inflammation and chronic bacterial infection, is the leading cause of death in CF patients. At variance with some pharmacological approaches, no efficacious gene and cell therapy have been proved to date. Mesoangioblasts (MABs) are small vessel associated progenitor cells able to differentiate into different mesoderm cell types, cross the vessel wall upon intra-arterial injection and rescue skeletal muscle dystrophy in mice and dogs. Moreover, a recent clinical trial in human patients affected by Duchenne Muscular Dystrophy (DMD) definitely confirmed their transplantation as feasible and safe. During studies on MABs isolated from adult mouse skeletal muscle (mMABs) we observed that, when systemically transplanted in healthy wild type mouse model, mMABs surprisingly engraft lung, tracheal and intestinal epithelium up to one month from a single transplantation. Due to this striking evidence, together with MAB capability to express CFTR, we are proposing a possible use of MABs as a therapeutic tool for CF disease. In this work we demonstrated that mMABs engraft the respiratory and intestinal epithelium in CF mice up to six months from their single transplantation, rescuing CFTR-dependent chloride current. Strikingly, engrafted mMABs express epithelial markers, showing an unexpected ability to differentiate into epithelial cells, thus contributing to airways and intestine homeostasis and biology. Taken together, this work demonstrates that MABs are an eligible therapeutic tool for a cell-based therapy of CF.

### Introduction

Cystic Fibrosis is a recessive genetic disease caused by mutations of the *cystic fibrosis transmembrane conductance regulator* (*CFTR*) gene, which encodes for a cAMP-dependent chloride channel. These mutations lead to the loss of CFTR-dependent chloride transport on the

apical membrane of epithelial cells (Welsh 2001), causing a multi-organ disease affecting lung, pancreas, intestine, liver and reproductive tract (Davis 2006). The most common lethal consequence of CFTR mutations is a lung disease that evolves from small-airway obstruction with mucus plugging, airway inflammation and intermittent infection, into chronic bacterial infection, bronchiectasis and ultimately death.

Since the *CFTR* gene was cloned in 1989 (Riordan et al. 1989; Berger 1991) there has been high motivation aiming to develop strategies, such as gene therapy (Amaral 2011) and drug discovery (Boyle et al. 2014; Rowe 2012), for restoring the defective protein. Besides the symptomatic therapeutic approaches that target cellular events downstream the CFTR failure (Belcher & Vij 2010; Ratjen & Grasemann 2012; Waters & Smyth 2015), other strategies focused on the basic CFTR defect have emerged (Lukacs & Verkman 2012; De Stefano et al. 2014). However, over 20 years later, effective treatments for CF have not been proved for the majority of CF patients. Because of the significant obstacles that have limited the effectiveness of these approaches, lung transplantation still remains the only option for patients with progressive decline of lung function.

Advances in the understanding and application of stem cell therapies have generated hope that, by the use of this new potential tool, it will be possible to provide therapeutic treatments for CF, where current therapies are still inadequate. Although initial studies suggested engraftment of exogenously administered stem cells in the lung, this is now generally felt to be a rare occurrence of uncertain physiologic significance (Sueblinvong and Weiss 2010; Weiss et al. 2013; Kotton et al. 2005; Murphy and Atala 2013). However, it has been proved that any benefit that might arise from these cells would probably be due to paracrine effects, including stimulation of angiogenesis and modulation of local inflammatory and immune responses in mouse lung disease models (Lama et al. 2007). Recently, it has been shown that preconditioning the pulmonary niche with naphthalene injury and sub-lethal radiation, allows engraftment of mouse embryonic lung cells up to sixteen weeks after transplantation (Rosen et al. 2015), even if the use of embryonic stem cells still remains debated.

Our laboratory worked for several years on mesoangioblasts (MABs), blood vessel-associated progenitor cells that can differentiate into different mesoderm cell types (Minasi et al. 2002). MABs have been isolated and characterized from embryonic and adult tissues (Minasi et al. 2002; Dellavalle 2007; Messina & Cossu 2009; Tonlorenzi et al. 2007; Bonfanti et al. 2015), demonstrating to be able to proliferate in culture and most importantly, to cross the vessel wall upon intra-arterial administration. When delivered in the arterial circulation, MABs cross the blood vessel wall and participate to skeletal muscle regeneration, ameliorating signs of Muscular Dystrophies (MDs) in different pre-clinical animal models (Sampaolesi et al. 2003; Sampaolesi et al. 2006;

Díaz-Manera et al. 2010; Tedesco et al. 2011). For these reasons they have been used in a trial in human patients that definitely demonstrated that intra-arterial transplantation of donor MABs in humans is feasible and safe (Cossu et al. 2015). During studies on MABs isolated from adult mouse skeletal muscle (mMABs) (Diaz-Manera et al. 2010) we observed that, when systemically transplanted in healthy, wild type mouse model (C57BL/6), mMABs surprisingly engraft lung, tracheal and intestinal epithelium up to one month from a single transplantation trough the caudal vein. Due to this striking evidence, included MAB capability to express CFTR, we proposed to investigate on a possible use of MABs as a therapeutic tool for CF disease. The ability of MABs to cross the vessel wall and their systemic delivery confer them an advantage as therapeutic donor cells compared with other stem populations that need to be delivered directly into the airways, facing significant physical/immunological obstacles. In this work we presented strong evidence that the transplantation of mMABs in two different CF mouse models leads to a rescue of CF phenotype. We demonstrated that mMABs engraft the respiratory and the intestinal epithelium in CF mice up to six months from their single transplantation, leading to a functional rescue of CFTR-dependent chloride current. Notably, once engrafted the epithelium, mMABs express typical epithelial markers, revealing an unexpected and powerful relevant ability of MABs to differentiate into epithelial cells, thus contributing to lung and intestine homeostasis and biology.
Overall, these data demonstrate that MABs are eligible for a cell-based therapy of CF.

## Methods

### Mice

The *F508del CFTR* mice (van Doorninck et al. 1995; Clarke et al. 1992; Wilke et al. 2011) were obtained from Bob Scholte, Erasmus MC Rotterdam, The Netherlands. The C57Bl/6, 129/FVB and *F508del CFTR* mice studied were housed at the mouse facility of the University of Milan. Mice were kept in pathogen-free conditions and all procedures were conformed to Italian law (D. Lgs n° 2014/26, implementation of the 2010/63/UE) and approved by the University of Milan Animal Welfare Body and by the Italian Minister of Health. The C57Bl/6 and 129/FVB were fed with regular food. In order to prevent intestinal obstruction *F508del CFTR* mice received a SRM-A diet (AB Diets, Animal Nutrition) and acidified water of pH 2.4-2.7 (tape water with HCl 1/2,000) as recommended (Legssyer et al. 2006). The CFTR *knock-out* (*KOCftr*$^{tm1UNC}$) (Snouwaert et al. 1992) mice were bred in the Yale University Animal Facility and genotyped with standard protocol. To allow *KOCftr*$^{tm1UNC}$ mice to reach adulthood, they were fed with 9F food (Tekland) and the drinking water was supplemented with 17.5 g/250 ml of Colyte (Schwarz Pharma) (Eckman et al. 1995).

*KOCftr*$^{tm1UNC}$ mice that underwent Mesoangioblast transplantation were fed with a liquid diet of Peptamen (Nestle clinical nutritional product). All procedures were performed in compliance with relevant laws and institutional guidelines and were approved by the Yale University Institutional Animal Care and Use Committee. The mice used were completely backcrossed to the C57Bl/6 (*KOCftr*$^{tm1UNC}$) or 129/FVB (*F508del CFTR*) backgrounds. Wild type (wt) mice were generated from the same colonies and used as controls.

**Cell cultures, mesoangioblast transduction and transplantation**

Adult mouse mesoangioblasts (named mMABs, mMABs #2, mMABs #3) were isolated from 5-week-old C57BL/6 mice as previously described (Tonlorenzi et al. 2007). These cells were maintained in Dulbecco's Modified Eagle's Medium (DMEM, Sigma) containing 20% Fetal Bovine Serum (FBS, Gibco), 2 mM L-glutamine (EuroClone), 100 IU/ml penicillin and 100 mg/ml streptomycin (Euroclone).

For the *in vitro* epithelial differentiation, mMABs were cultured in Small Airway Grow Medium (SAGM, Lonza) with 5% FBS for 8 days, and in Human Bronchial/tracheal epithelial cells differentiation medium (HBTEC, LifeLine) with 5% FBS for 15 days, changing the medium every other day in both cases.

C2C12 murine myoblasts (ATCC) were grown in DMEM/20% FBS/2 mM L-glutamine/100 IU/ml penicillin and 100 mg/ml streptomycin (defined as growth medium, GM). Muscle differentiation was induced, after 24 h in GM, by incubating cells in DMEM supplemented with 2% Horse Serum (HS, defined as differentiation medium, DM).

Murine lung epithelial (MLE)-12 cell (purchased from ATCC) were cultured in HITES medium composed by: DMEM/Ham's F-12 (ATCC) (1:1) supplemented with 2% FBS, 2 mM L-glutamine, 0,005 mg/ml Insulin, 0,1 mg/ml Transferrin, 30 nM Sodium Selenite, 10 nM Hydrocortisone, 10 nM b-estradiol, 10 mM Hepes (all from Sigma).

To realize air liquid interface (ALI) culture, mMABs were co-cultured with primary nasal epithelial cells deriving from *KOCftr*$^{tm1UNC}$ mice. Epithelia were removed from the nasal cavity and processed as described (Grubb et al. 2006). On day 2 post-seeding on a 6.5 mm T-Col Transwell (Corning Costar), all apical liquid was removed and replaced with 0,2 ml of fresh MTEC complete culture medium (described below). The basolateral liquid was also removed and 1,2 ml of fresh medium was added basolaterally. The cultures were fed in this way every other day. Once the cells have reached 70% of confluence (approximately after 5-7 days), 10^3 GFP-mMABs were added to each culture. Almost after 2 weeks, when the cells were confluent and made tight junctions, the medium on top started to dry up, as a result of absorption of the apical liquid. From this point onward, no

liquid was left on the apical surface and the cultures were fed only on the bottom. After almost 12 days the medium was switched with HBTEC differentiation medium for at least 4 weeks before ready to use. The MTEC complete culture medium was composed of 50% Ham's F-12 (Gibco) and 50% DMEM, to which the following ingredients were added (all concentrations given as final medium concentration): 10%FBS, 10 µg/ml insulin (Roche), 1 µM hydrocortisone, 30 nM triiodothyronine, 0,1 ng/ml cholera toxin, 5 µg/ml transferrin (all from Sigma), 3.75 µg/ml endothelial cell growth supplement, 25 ng/ml epidermal growth factor, and 15 µg/ml bovine pituitary extract (all from BD).

To the aim of the transplantation experiments, mMABs were tranduced with third generation lentiviral vectors expressing nuclear LacZ or GFP at the multiplicity of infection of 100, after previous incubation with 8 µg/ml Polybrene (Sigma) as previously described (Bonfanti et al. 2015).

mMAB systemic delivery through the caudal vein was performed as follows: *F508del CFTR*, *KOCftr*$^{tm1UNC}$ and wt littermate mice were treated in the site of injection with a topic anesthetic (EMLA, made by lidocain and prilocaine) and 30x10^4 nLacZ/GFP-mMABs diluted in 100 µl of phosphate-buffered saline (PBS) and injected into the caudal vein. Animals were sacrificed at the different time points analysed and the organs collected and processed, according to the different types of analysis.

**Tumorigenesis assay**

CD1 nude mice were treated in the site of injection with a topic anesthetic (EMLA, made by lidocain and prilocaine) and injected subcutaneously with 2x10^6 nLacZ-mMABs or nLacZ-S180 tumorigenic cells (n=6 for each group) diluted in 150 µl of PBS. The onset of the tumors was then monitored.

**Immunofluorescence and histology**

The analysed organs were washed twice with PBS and fixed with 4% paraformaldehyde at 4°C for 10 min and included in paraffin. Serial 7-µm-thick sections were cut with a Leica microtome (Leica Microsystems).

Samples were also embedded in OCT (Killik, Bio-Optica) and frozen in liquid nitrogen cooled isopentane (VWR) and serial 7-µm-thick sections cut with a Leica cryostat (Leica Microsystems).

Tissue sections or cells were fixed with 4% paraformaldehyde at 4°C for 10 min, washed in PBS and permeabilized with 0.2% Triton X-100 (Sigma), 1% bovine serum albumin (BSA, Sigma) in PBS for 30 min at RT, then blocked with 10% goat/donkey serum for 30 min at RT. Samples were incubated overnight at 4°C with the following primary antibodies: rabbit anti-GFP 1:500

(Invitrogen), mouse anti-E-cadherin 1:50 (BD), goat anti-CC10 1:50 (Santa Cruz), mouse anti-CK5 1:200 (Thermo), goat anti-CK6 1:50 (Santa Cruz), goat anti-SP-C 1:50 (Santa Cruz), mouse anti-Acetilated Tubulin 1:200 (Abcam).

After incubation, samples were washed with 0.2% Triton X-100, 1% BSA in PBS and then incubated with the secondary antibodies 1:500 (Jackson Lab) together with 4',6-diamidino-2-phenylindole (DAPI) 1:500 (Sigma) for 45 min at RT in 0.2% Triton X-100 in PBS. After two washes, dishes or slides were mounted using fluorescent mounting medium (Dako) and watched under fluorescent microscope (Leica-DMI6000B) or confocal microscope (Leica Microsystems), obtaining orthogonal projection analysis.

Tissue sections were also stained with Carmallume and Eosin (Sigma) and X-gal (Invitrogen) according to standard protocols. To distinguish in situ hystochemical detection the activity of β-gal of donor cells from that of endogenous mammalian β-gal, the X-gal staining was performed under alkaline condition as previously described (Bell et al. 2005; Weiss et al. 2008)

**HS-YFP assay for CFTR activity**

mMABs were transfected with the Lipofectamine LTX transfection reagent (Invitrogen) according to standard protocols. The plasmids used were the pcDNA3.1CFTR (*wild type CFTR, wt*) and pcDNA3.1ΔF508CFTR (*F508del CFTR*) (kindly provided by L. Maiuri) (Moyer et al. 1998; Luciani et al. 2010).

Measurements of CFTR activity were carried out on MABs transiently transfected with the plasmids cited before and the halide-sensitive (HS) YFP 48 h after cells plating on microplates. At the time of the assay, cells were washed with PBS and stimulated for 30 min with forskolin (20 μM; for cells transfected with *wt CFTR* together with HS-YFP or HS-YFP alone) or forskolin plus genistein (50 μM; for cells transfected with *F508del CFTR* together with HS-YFP). Then, cells were transferred to a fluorescence microscope equipped with a CCD camera (Nikon) for CFTR activity determination. The microscope was equipped with high-quality excitation and emission filters for YFP. Each assay consisted of a continuous 40 s fluorescence reading with 7 s before and 33 s after injection of an iodide-containing solution (PBS with $Cl^-$ replaced by $I^-$; final $I^-$ concentration in the well: 100 mM). Data were normalized to the initial background-subtracted fluorescence. To determine fluorescence quenching rate (QR) associated with $I^-$ influx, the final 33 s of the data for each well were fitted with an exponential function to extrapolate initial slope (dF/dt).

**Isolation of nasal epithelial cells and cytospin**

Epithelia from GFP-mMAB-injected *KOCftr*$^{tm1UNC}$ mice were removed from the nasal cavity and dissociated in single cells as described (Grubb et al. 2006). Cells were then resuspended in 5% BSA in PBS, filtered in a 70 µm cell strainer and counted. 10^5 cells were diluted in 150 µl of 5% BSA in PBS and cytospun for the following immunofluorescence analysis.

**Quantitative PCR with reverse transcription**

Total RNA was isolated using NucleoSpin RNA XS/L Kit (Macheray-Nagel) and retro-transcribed to cDNA with the iScript Reverse Transcription Supermix (Bio-Rad), according to the manufacturer's protocol. Each cDNA sample was amplified in triplicate using the iTaq Universal SYBR Green Supermix or the SSo Advanced SYBR Green Supermix (both from Bio-Rad). The primers used are listed in the Supplementary Table S1. For any sample the expression level, normalized to the housekeeping gene encoding GAPDH, was determined with the comparative threshold cycle (Ct) method.

***In vivo* NPD measurement**

The nasal potential difference (NPD) was measured as described (Egan et al., 2004) with perfusion of 3 solutions: (1) Kreb's solution, (2) Kreb's solution/$10^{-4}$M amiloride (Sigma), (3) $Cl^-$-free bicarbonate Kreb's solution/$10^{-4}$M amiloride/$10^{-5}$M forskolin (FSK, Sigma)/$10^{-5}$M 3-isobutyl-1methylxantine (IBMX, Sigma). The NPD was sensed with a 3M KCl-agar bridge inserted 0.3 cm into one nostril of the C57BL/6 wt and *KOCftr*$^{tm1UNC}$ mice untreated and GFP-mMAB-injected and connected through an Ag-AgCl electrode to a digital voltmeter. The measurement was performed 3 times on each mouse. One measurement was obtained before mMAB injection and 2 measurements were obtained post-transplantation at the different time points analyzed.

**Ussing Chamber analysis**

Short-circuit current *in vitro* analysis was performed as described (Grubb & Boucher 1999; Bruscia et al. 2006). The distal colon was removed, cut longitudinally, washed of any intestinal contents, and mounted in the Ussing chambers with an aperture size of 0.3 $cm^2$ (Physiologic Instruments). Analyses were performed under open-circuit conditions and tissues were pulsed with 1 µA current for 1s every 60s. During all experiments, solutions were continuously gassed with 95% $O_2$/5% $CO_2$ and warmed to 37°C. Data were recorded continuously using the Acquire and Analyze software program (Physiologic Instruments). Kreb's bicarbonate Ringer's solution (KBR) and a $Cl^-$-free Ringer's solution containing 5 mM barium hydroxide were used. Amiloride and FSK were added to

the $Cl^-$-free Ringer's solution at final concentrations of $10^{-4}$ M and $10^{-5}$ M, respectively. After the tissue reached maximum response to FSK (8–10 min), 20 μM $CFTR_{inh}$-172 was added bilaterally. At the end of the measurement, Kreb's bicarbonate Ringer's solution was added to verify the integrity of the tissues, measuring again their baseline after the assay, thus validating the data obtained. All drugs and chemicals are from Sigma Chemical Co. and J. T. Baker. From the change in the transepithelial voltage, the resistance and equivalent short-circuit current were calculated with Ohm's law.

**Preparation of single cell suspensions and Flow Cytometry**

Lungs were separated and lobes processed as described (Wang et al. 2012). Single cell suspensions were resuspended in DMEM/20% FBS/20 mM Hepes (Sigma)/5 mM EDTA (Ambion). GFP-mMABs and lungs of untreated mice were used as positive and negative controls respectively. Engrafted GFP positive (GFP+) and negative (GFP-) mMABs fractions were obtained by fluorescence-activated cell sorting (FACS) using FACSAria cell sorter (BD). Cells were cytospun for the following immunofluorescence analysis and collected for qRT-PCR.

## Results

### mMABs engraft lung, tracheal and intestinal epithelium in C57BL/6 wild type mice

To investigate and characterize the potential mMAB engraftment as a possible tool for a targeted cell therapy, we injected 30x10^4 mMABs, previously tranduced with a lentiviral vector expressing nuclear LacZ (nLacZ-mMABs), in the caudal vein of wild type (wt) mice. After mMAB injection in healthy C57BL/6 mice (n=3 for each time point), we examined if their engraftment in multiple organs would persist even after 2 months. Strikingly, we noticed that mMABs engraft lung, tracheal and intestinal epithelium up to two months from their single transplantation (Fig. 1A and B). As shown in Fig. 1, lung, tracheal and intestinal epithelium derived from nLacZ-mMAB-injected mice clearly reveals the presence of donor β-gal-positive nuclei in the stratified epithelium, whose architecture still remains preserved. As control, we performed the same analysis on C57BL/6 not transplanted mice (n=3 for each time point) and we never found LacZ-positive staining. Moreover, to investigate the possible tumorigenic potential of mMABs we performed a subcutaneous tumor assay in CD1 nude mice, by injecting 2x10^6 nLacZ-mMABs (n=6) and we compared their tumor forming ability with that of nLacZ-S180 sarcoma cell line (n=6). Eight months after transplantation we observed that none of the mice injected with nLacZ-mMABs displayed micro and or macroscopic tumor masses, while all CD1 nude mice injected with S180 cells showed tumor masses, already detectable one week after transplantation. This result clearly demonstrates the safety of mMABs and further confirmed data already published by others (Sampaolesi et al. 2003; Sampaolesi et al. 2006; Díaz-Manera et al. 2010; Tedesco et al. 2011; Tedesco et al. 2012; Domi et al. 2015).

These evidences unequivocally demonstrate the ability of mMABs to properly engraft and integrate in the lung, tracheal and intestinal epithelia of C57BL/6 wt mice.

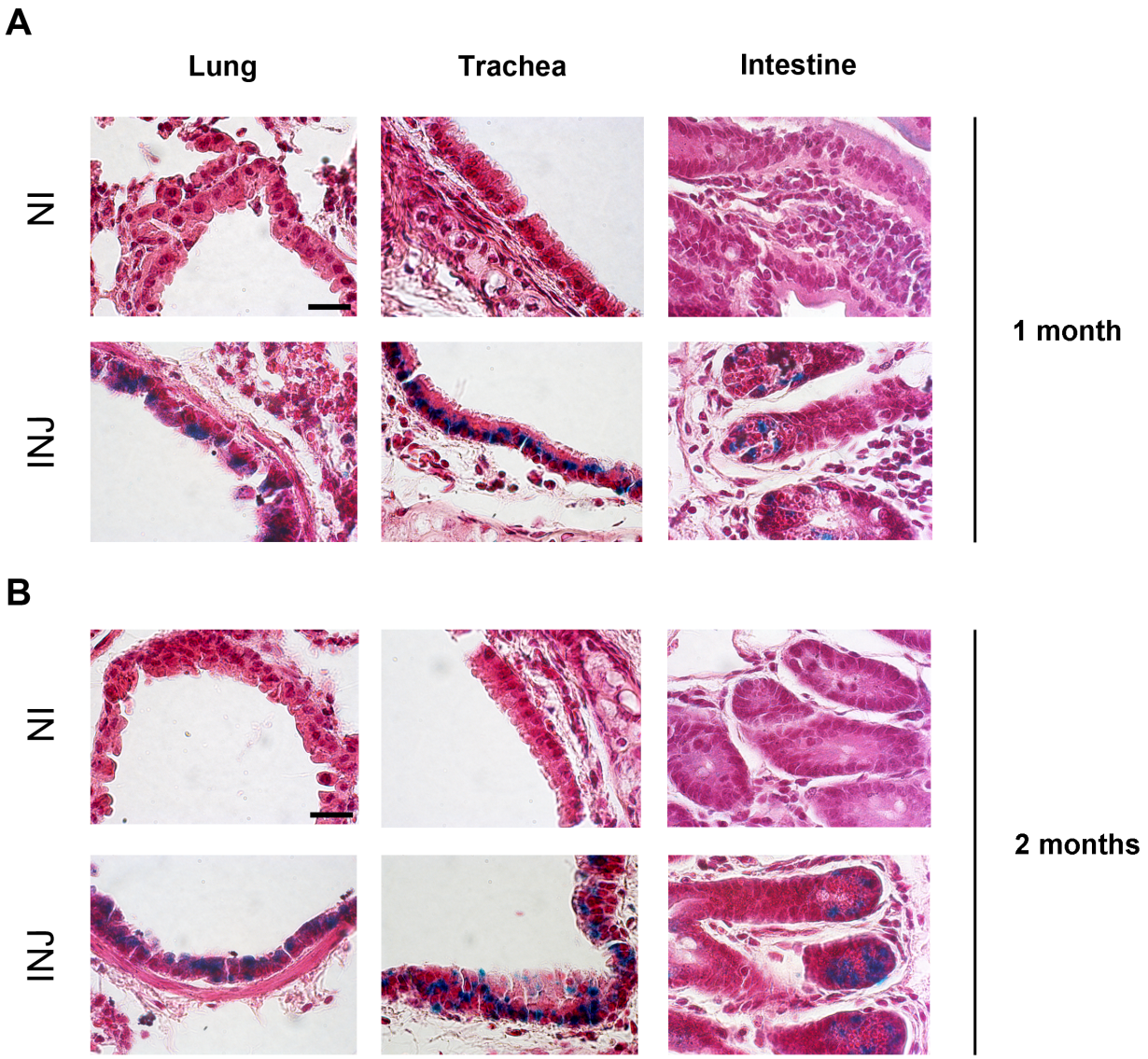


**Figure 1: nLacZ-mMABs, after systemic transplantation, engraft lung, tracheal and intestinal epithelium in C57BL/6 wt mice.** Carmallume/Eosin and X-Gal staining on serial transverse sections of lung lobes, trachea and intestine of transplanted (INJ) and not-transplanted (NI) C57BL/6 wt mice at 1 month (**A**) and 2 months (**B**) from nLacZ-mMAB systemic transplantation. X-gal was used to identify transplanted nLacZ-mMABs (blue). Scale bar 20 μm.

**mMABs can express functional CFTR channel**

After demonstrating the substantial mMAB engraftment in the proximal and distal airway epithelia, these latter known to be strongly protected by physical and immunological barriers, we decided to investigate CFTR expression in mMABs, in order to develop an innovative cell-based therapy for CF. To this aim, we evaluated CFTR expression in mMABs in terms of gene expression and activity

*in vitro*. Regarding CFTR expression, we first measured CFTR transcript levels by qRT-PCR, which demonstrates the presence of CFTR mRNA in mMABs *in vitro,* compared to *CFTR ko* nasal epithelial cells (Fig. 2A). Once demonstrated the gene expression of *CFTR* in mMABs we also started to investigate its functional activity, *in vitro*. In fact, to verify whether mMABs have the proper cellular mechanisms necessary to express a correctly localized and functional CFTR channel, we compared CFTR-dependent halide expression in ctl versus mMABS transiently transfected with two plasmids, the first carrying the *wt CFTR* and the second the *F508del* mutated form (*F508del*), together with a halide-sensitive YFP (HS-YFP) variant. In the YFP based microfluorimetric assay, a quantitative procedure that exploits halide-sensitivity of YFP variants, we analyzed CFTR-mediated halide transport (Pedemonte et al. 2005). Cells transfected with *F508del* mutant were tested under control condition or following 24h-treatment with a well established corrector of *F508del* CFTR misfolding, the VX-809 compound (1 M) (Van Goor et al. 2011). At the time of the assay, cells were acutely stimulated with forskolin (20 M) alone (mMABs transfected with the empty vector and *wt CFTR*) or forskolin plus genistein (50 M; for cells expressing *F508del* CFTR). CFTR activity for each condition was determined by measuring the rate of cell fluorescence quenching after addition of the iodide-rich solution. Fig. 2B reports original traces recorded from mMABs. Quantification of CFTR activity in the various cell populations is shown in Fig. 2C. In particular, mMABs display no endogenous CFTR activity, while cells transfected with *wt CFTR* have significantly higher quenching rate values, suggesting that mMABs can express a functional channel. As expected, cells transfected with the *F508del* mutant do not have functional activity, showing that mMABs are a very stringent cell model with very low levels of expression of the *F508del CFTR*. However, when treated for 24h with the corrector VX-809, *F508del* mMABs show a significantly increased anion transport.

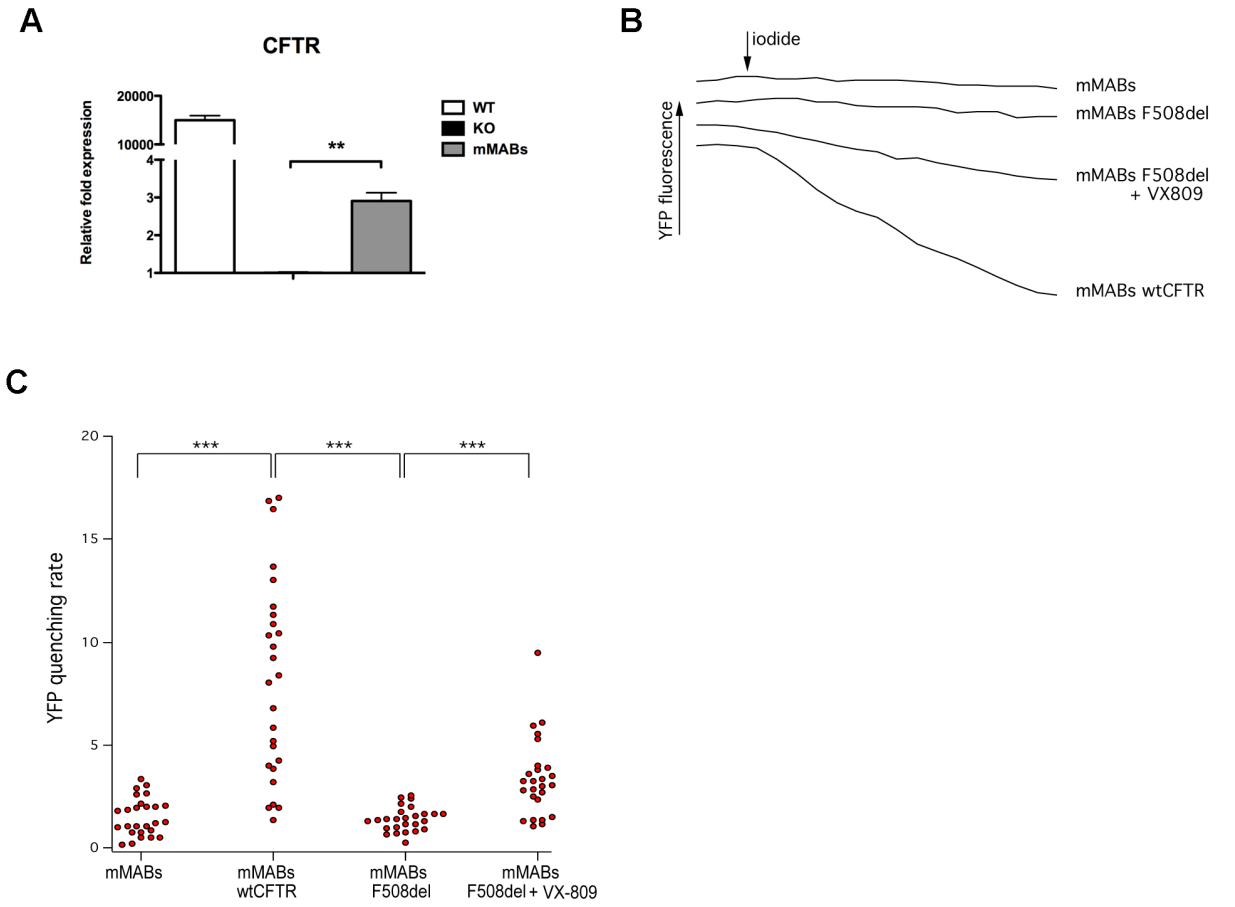


**Figure 2: mMABs can express functional CFTR channel.** (**A**) CFTR transcript levels evaluated by qRT-PCR in nasal epithelial cells from noses of wt, *CFTR ko* mice and mMABs. Values are plotted as relative fold expression and normalized to GAPDH expression. Each assay was performed in triplicate. All data are represented as means +/- S.D.,**P<0.005, unpaired t Test. (**B**, **C**) Graphs show YFP quenching rate data in mMABs transiently transfected with two plasmids, one encoding for the halide-sensitive YFP and the other one being an empty vector (control), wt or *F508del CFTR*. Cells transfected with *F508del* mutant were assayed under control condition or following 24h-treatment with corrector VX-809 (1µM). At the time of the assay, cells were acutely stimulated with forskolin (20µM) alone (ctl and wt CFTR cells) or forskolin plus genistein (50µM; for F508de CFTR cells). (**B**) Representative traces showing YFP quenching induced by the addition of an iodide-rich solution. Rate of YFP quenching is proportional to CFTR activity. (**C**) Rate of YFP quenching in single cells. Data collected from 26 cells examined *per* population. Comparison of values was performed using the non-parametric Kruskal-Wallis ANOVA test, followed by the Mann-Whitney U test and Bonferroni's correction; ***P<0.001.

**mMABs efficiently engraft overtime the epithelium of airways and intestine of the *F508del CFTR* mouse model**

We then proceeded to verify the potential of mMAB transplantation in the mouse model of CF *F508del CFTR* and whether this engraftment would persist overtime. This model was used because it carries the same mutation (belonging to class II) that affects almost the 70% of human patients (van Doorninck et al. 1995). Due to its misfold, *F508del* CFTR does not reach the plasma membrane, is prematurely degraded, and loses its essential ion channel activity thus provoking local inflammation, increased susceptibility to respiratory bacterial infections and progressive pulmonary and digestive insufficiency (O'Sullivan & Freedman 2009; Ratjen 2009). It has been deeply demonstrated that these mice display basal inflammation and a prolonged and exuberant inflammatory response to bacteria and bacterial products characterized by massive migration of neutrophils in the lung, increased secretion of pro-inflammatory cytokines, and higher rates of mortality at steady-state and after an inflammatory challenge (Luciani et al. 2012). This suggests that this CF mouse model represents a valuable tool for studying certain aspects of CF lung disease, albeit not reproducing all aspects of the pathology (e.g. chronic bacterial lung colonization, viscous mucus) (van Doorninck et al. 1995; Clarke et al. 1992; Wilke et al. 2011).

To this aim mMABs have been transduced with a lentiviral vector carrying the GFP marker and 30x10^4 GFP-mMABs were systemically transplanted, through the caudal vein, in *F508del CFTR* mice (n=3 for each condition, transplanted and not-transplanted). Mice were sacrificed at 2 weeks, 1, 2, 4 and 6 months after transplantation. As shown in Fig. 3, GFP-mMABs properly engraft the E-cadherin-positive epithelium in the lung, trachea and intestine up to 6 months from their single transplantation. At the same time points we also evaluated engrafted mMAB proliferation by analyzing the expression of the proliferative marker Ki67, revealing that very few mMABs proliferate once localized in the host epithelia (data not shown).

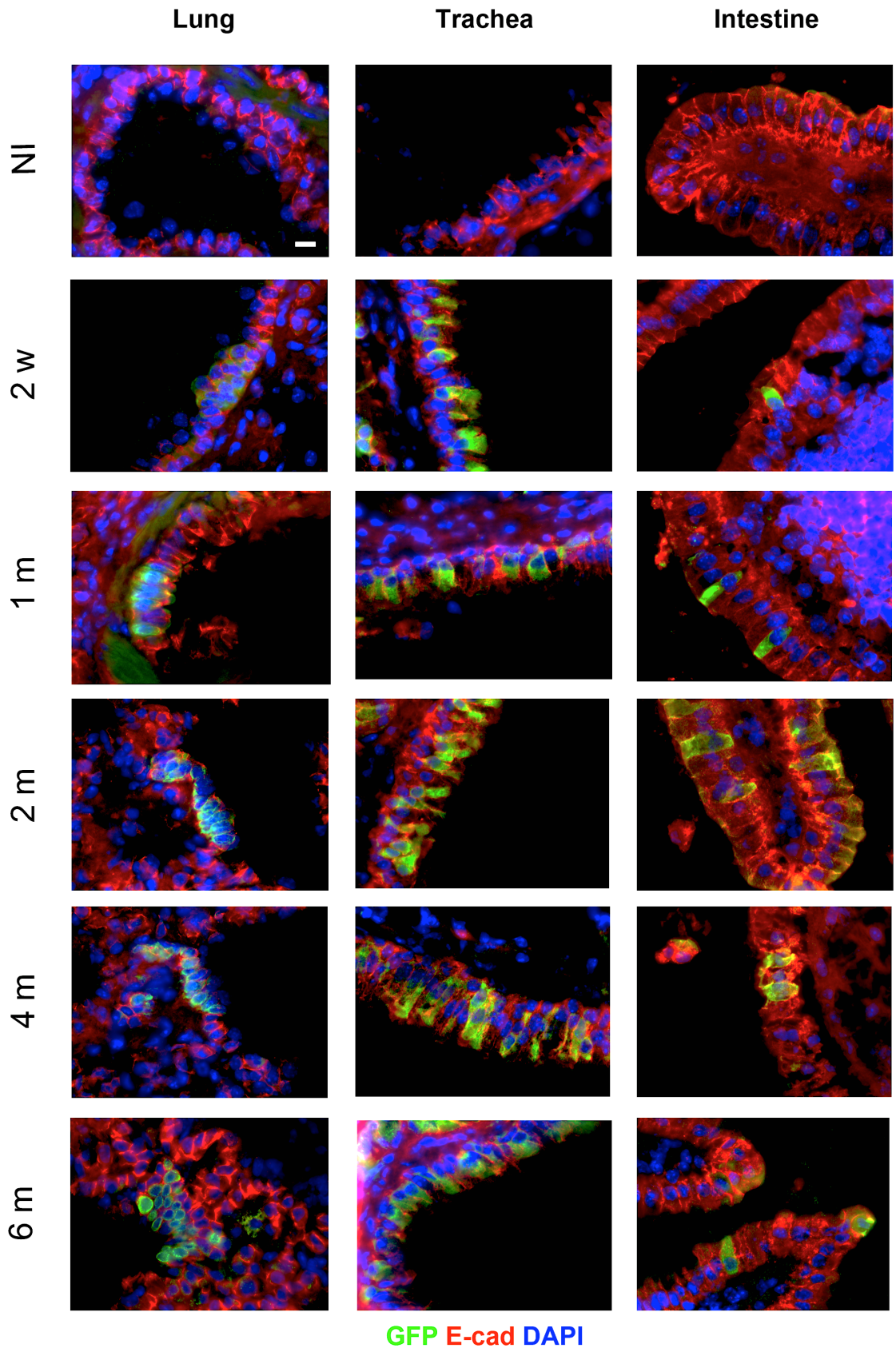
Lung
Trachea
Intestine
NI
2 w
1 m
2 m
4 m
6 m
GFP E-cad DAPI

**Figure 3: GFP-mMABs, after systemic transplantation, engraft lung, tracheal and intestinal epithelium in *F508del CFTR* mice.** Immunofluorescence staining for GFP on serial transverse sections of lung lobes, trachea and intestine of transplanted and not-transplanted (NI) *F508del CFTR* mice (GFP, green; E-cad, red; nuclei, dapi). These results have been reproduced by three independent experiments carried on 3 not-injected (NI) and 3 transplanted mice each at different time points: 2 weeks (2w), 1, 2, 4, 6 months (1m, 2m, 4m, 6m). Scale bar 10 μm.

To further confirm our previous results we replicated the same experiments by injecting different polyclonal classes of mesoangioblasts, named mMABs #2 and #3. To this aim, we repeated the *in vivo* experiments, by injecting 30x10^4 GFP- #2 / #3 mMABs in the caudal vein of *F508del CFTR* mice and we analyzed the engraftment of the donor GFP-cells after 1 month from the transplantation in the lung, tracheal and intestinal epithelium. Both #2 and #3 MABs engraft the E-cadherin positive epithelia of the considered organs (Supplementary Fig. 1), demonstrating that mMAB epithelial engraftment is an intrinsic and specific property of mMABs, regardless of a particular cell preparation.

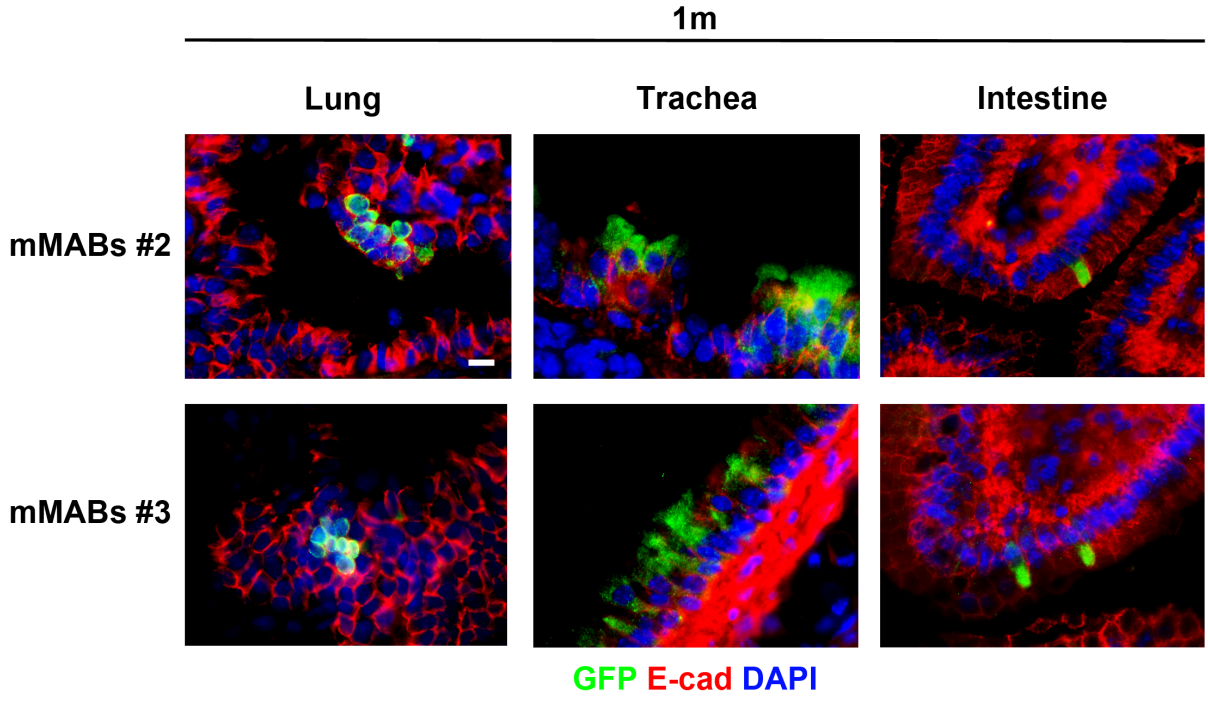


**Supplementary Figure 1: The engraftment in the respiratory and intestinal epithelia is an intrinsic property of mMABs.** Immunofluorescence staining for GFP on serial transverse sections of lung lobes, trachea and intestine of transplanted *F508del CFTR* mice (GFP, green; E-cad, red;

nuclei, dapi). These results have been reproduced by three independent experiments; mice were sacrificed 1 month (1m) after mMAB transplantation. Scale bar 10 μm.

**mMABs rescue CFTR activity in *CFTR ko* mouse model**

To test whether mMABs could even restore CFTR-dependent chloride secretion *in vivo* once engrafted in the epithelia, they were transplanted in homozygous CFTR knockout mice (*KOCftr*$^{tm1UNC}$ mice, *CFTR ko;* Snouwaert et al. 1992). *CFTR ko* mice do not express any CFTR protein and they recapitulate the electrophysiological abnormalities observed in individuals affected by CF, such as $Na^+$ hyperabsorption and lack of cAMP-dependent $Cl^-$ secretions in their intestine and respiratory epithelia (Clarke et al. 1992; Grubb et al. 2002; Fischer et al. 2002). For all these reasons these mice represent the most valuable model for assessing a potential rescue of functional CFTR after mMAB transplantation. In this study, wt and *KOCftr*$^{tm1UNC}$ mice were transplanted *via* caudal vein with 30x10^4 GFP-mMABs. First we evaluated mMABs engraftment in *CFTR ko* mice, analyzing the presence of the donor-engrafted GFP-cells in the lung epithelium. We found GFP-mMABs engrafted in the E-cadherin-positive epithelium of transplanted lungs at 2 weeks and 4 months from cell transplantation (Fig. 4A).

In view of measuring the nasal potential difference across the nasal epithelium in *CFTR ko* mMAB-injected mice, we firstly proceeded by evaluating mMAB engraftment in that tissue.

We then isolated epithelial cells from the nasal cavity of *CFTR ko* mice, untreated and injected with GFP-mMABs after 4 months from transplantation and we found GFP-positive cells in the nasal epithelium of transplanted mice. Strikingly, we also observed that engrafted GFP-mMABs express the epithelial marker E-cadherin (Fig. 4B, right panel, green arrow). To further confirm the colonization of GFP-positive mMABs, we measured, by qRT-PCR, the transcript levels of GFP (Fig. 4C) and CFTR (Fig. 4D) from the nasal epithelial cells of wt and *CFTR ko* mice, untreated and injected with GFP-mMABs after 2 weeks and 4 months from transplantation. As shown in Fig. 4C, the transcript levels of GFP are statistically significant higher in transplanted mice, both wt and *CFTR ko*, respect to the untreated ones. Moreover, the level of CFTR mRNA was increased, definitively confirming the occurred engraftment (Fig. 4D).

To evaluate the rescue of CFTR activity we then measured, at the same time points, the potential difference across the nasal epithelia (nasal potential difference, NPD). In this assay, the removal of luminal $Cl^-$ and the subsequent exposure to CFTR stimulators such forskolin (FSK) and 3-isobutyl-1methylxantine (IBMX) induced a hyperpolarization (more negative potential difference) in wt

animals, which is not substantially altered in wt animals injected with mMABs (n = 6) compared to wt untreated mice (n = 9) (-2.67 ± 0.7 mV vs. -3.82± 1.1 mV, *P* = 0.19) (Supplementary Fig. 2A; Fig. 4E). On the contrary, the change in NPD in response to $Cl^-$-free bicarbonate Kreb's solution/amiloride/FSK/IBMX (ΔNPD) is statistically significant different between *CFTR ko* untreated mice (n = 15) and transplanted ones, after 2 weeks (n = 9) and also after 4 months (n = 10) (KO NI, ΔNPD = 2.78 ± 0.6 mV; KO INJ 2w, ΔNPD = -0.77 ± 0.7 mV, *P* = 0.0008; KO INJ 4m, ΔNPD = -0.11 ± 0.9 mV, *P* = 0.0067) (Supplementary Fig. 2A; Fig. 4E). *CFTR ko* transplanted mice have a more negative PD indeed, in response to $Cl^-$-free bicarbonate Kreb's solution/amiloride/FSK/IBMX compared to *CFTR ko* untreated mice, suggesting some CFTR-dependent chloride secretion. Furthermore, in order to definitively remove any variability given by the *in vivo* assay, we measured the ΔNPD in the same mice before and after the transplantation of mMABs. We observed that the average value of the ΔNPD measured after mMAB injection is statistically significant more negative if compared to the measurements performed on the same *CFTR ko* mice before the transplantation (Supplementary Fig. 2B).

Finally, CFTR function was also measured *ex vivo* after 4 months from mMAB transplantation by the Ussing chamber assay, the gold standard method to test CFTR activity. We therefore examined the change in $I_{sc}$ ($\Delta I_{sc}/cm^2$) by Ussing chamber analysis on the distal colon of all mice studied, first in response to apical $0Cl^-$ and then to FSK. After FSK stimulation, the wt group (n = 6) has a $\Delta I_{sc}$ of 40.7± 3.7 μA/$cm^2$ which is not essentially different from transplanted wt mice (n = 3) with a $\Delta I_{sc}$ of 37.6 ± 0.3 μA/$cm^2$ (*P* = 0.22) as expected. The FSK-derived $\Delta I_{sc}/cm^2$ in the distal colon of *CFTR ko* not injected mice (n = 5) and that of mMAB-transplanted ones (n = 11) is -3.2 ± 1.7 and 2.2 ± 1.6 μA/$cm^2$ respectively. Strikingly, we observed a statistical significant difference in terms of the change in $I_{sc}$ in mMAB-transplanted *CFTR ko* mice, if compared to untreated ones (*P* = 0,02) (Fig. 4F). Overall, these results unequivocally confirm mMAB ability to functionally rescue the CFTR-dependent chloride secretion in the most severe mouse model of CF.

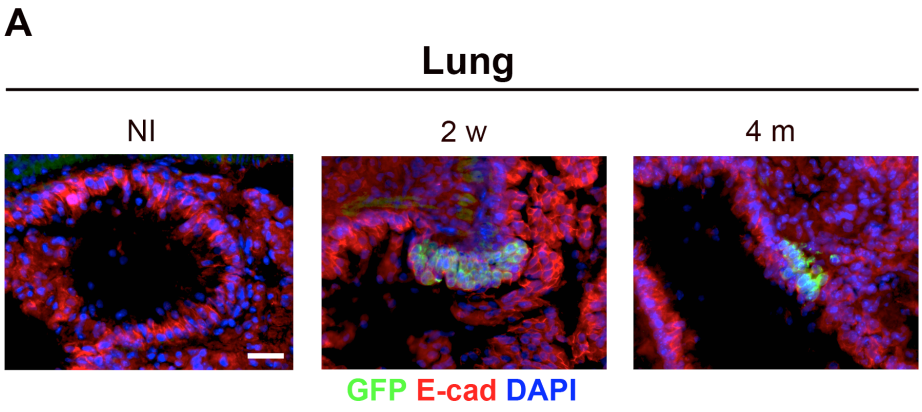
A
Lung
NI
2 w
4 m
GFP E-cad DAPI

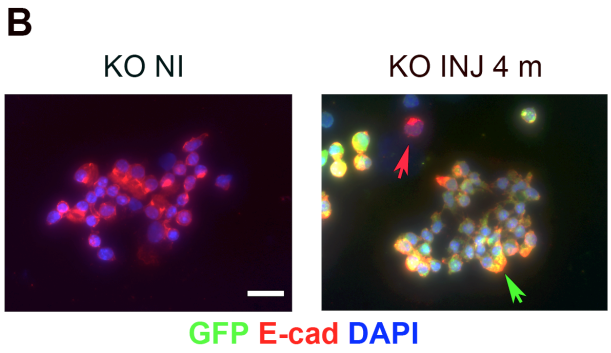
B
KO NI
KO INJ 4 m
GFP E-cad DAPI

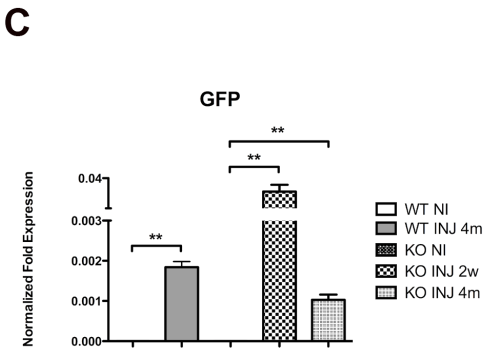
C
GFP
Normalized Fold Expression
0.04
0.003
0.002
0.001
0.000
**
**
**
WT NI
WT INJ 4m
KO NI
KO INJ 2w
KO INJ 4m

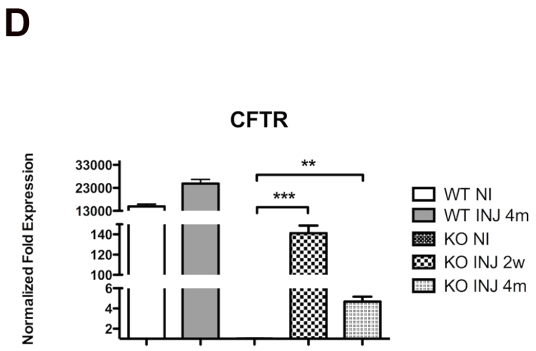
D
CFTR
Normalized Fold Expression
33000
23000
13000
140
120
100
6
4
2
**
***
WT NI
WT INJ 4m
KO NI
KO INJ 2w
KO INJ 4m

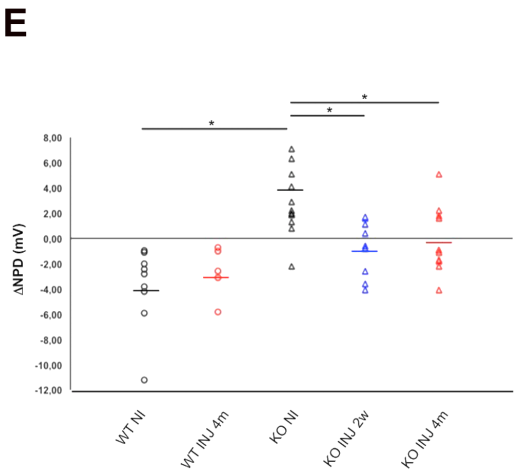
E
ΔNPD (mV)
8,00
6,00
4,00
2,00
0,00
-2,00
-4,00
-6,00
-8,00
-10,00
-12,00
*
*
*
WT NI
WT INJ 4m
KO NI
KO INJ 2w
KO INJ 4m

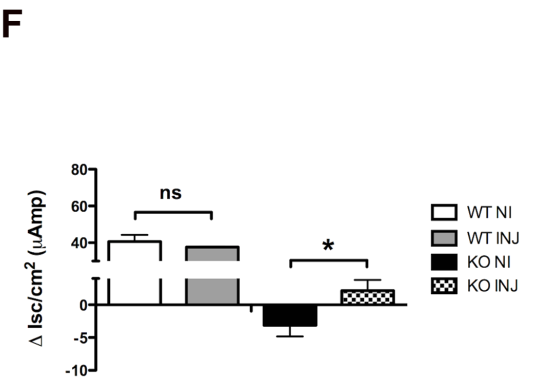
F
Δ Isc/cm² (μAmp)
80
60
40
0
-5
-10
ns
*
WT NI
WT INJ
KO NI
KO INJ

**Figure 4: mMABs engraft the lung and nasal epithelia of *CFTR ko* mice and contribute to the rescue of CFTR activity.** (**A**) Immunofluorescence staining for GFP on serial transverse sections of lung lobes of transplanted and not-transplanted (NI) *CFTR ko* mice (GFP, green; E-cad, red; nuclei, dapi). These results have been reproduced by three independent experiments carried on 3 not-injected (NI) and 3 transplanted mice each at different time points: 2 weeks (2w) and 4 months (4m). Scale bar 10 μm. (**B**) Representative images showing nasal epithelial cells isolated from *CFTR ko* mice untreated (KO NI) and injected with GFP-mMABs at 4 months after transplantation (KO INJ 4m). *CFTR ko* mice have GFP-mMABs-derived nasal cells (GFP, green) that also express E-cadherin (red). Red arrow represents a GFP negative/E-cadherin positive epithelial cell; green arrow represents a GFP-mMAB donor cell expressing E-cadherin. Scale bar 25 μm. (**C**, **D**) GFP and CFTR transcript levels evaluated by qRT-PCR in nasal epithelial cells from noses of wt and *CFTR ko* mice, untreated and injected with GFP-mMABs after 2w and 4m from transplantation. Values are plotted as relative fold expression and normalized to GAPDH expression. Each assay was performed in triplicate. All data are represented as means +/- S.D., ***P < 0.0005, **P < 0.005, unpaired t Test. (**E**) Scatter plots of the ΔNPD from wt and *CFTR ko* mice untreated and injected with GFP-mMABs after 2w and 4m from transplantation. The NPD measurements were performed in not injected wt animals (WT NI), wt mice injected with GFP-mMABs at 4m from transplantation (WT INJ 4m), *CFTR ko* not injected mice (KO NI) and *CFTR ko* mice injected with GFP-mMABs at 2w (KO INJ 2w) and 4m (KO INJ 4m) from transplantation. Horizontal bars indicate the ΔNPD average for each group. Statistical analysis was conducted using one-sided two-sample t-tests. *: $P = 0.00005$ (WT NI vs. KO NI); $P = 0.0008$ (KO NI vs. KO INJ 2w); $P = 0.0067$ (KO NI vs. KO INJ 4m). (**F**) Distal colon ΔIsc/cm$^2$ in response to forskolin for WT NI, WT INJ, KO NI, KO INJ mice. The value for each mouse represents the ΔIsc (mean of three readings for each solution) *: $P = 0.0245$ (KO NI vs. KO INJ); ns= not significant (WT NI vs. WT INJ).

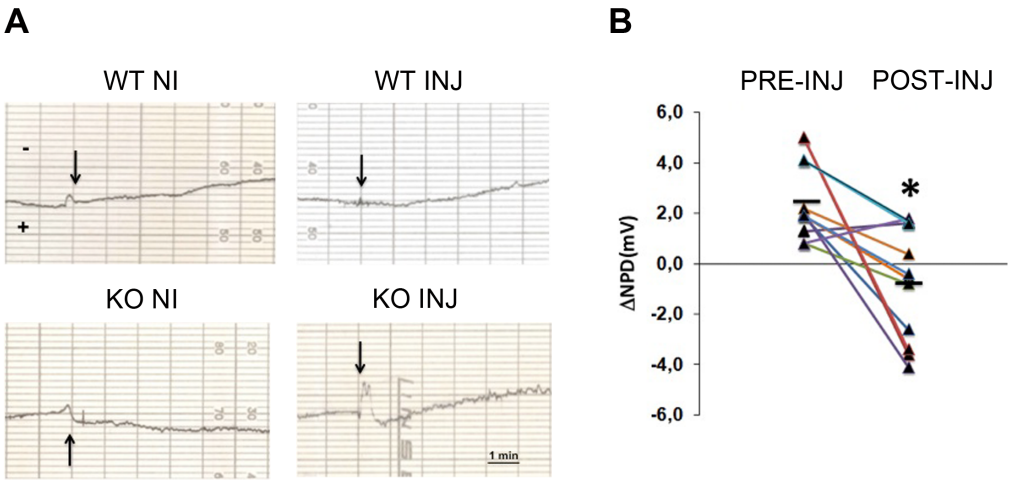


**Supplementary figure 2: *CFTR ko* mMAB-transplanted mice respond to CFTR stimulation.** (**A**) Original NPD recordings for representative wt and *CFTR ko* mice, untreated (WT NI, KO NI) and injected with GFP-mMABs (WT INJ, KO INJ). Each rectangle of the chart paper represents time (1 min) horizontally and PD (1mV) vertically. The arrows indicate the switch from Kreb's solution/amiloride to $Cl^-$-free bicarbonate Kreb's solution/amiloride/FSK/IBMX (which activates CFTR and induces chloride transport). The DELTA PD (ΔPD) is calculated as the difference in mV between the second and the first solution. (**B**) Scatter plots of the ΔNPD from the same *CFTR ko* mice before (PRE-INJ) and after mMAB transplantation (POST-INJ). Horizontal bars indicate the DNPD average for each group. Statistical analysis was conducted using one-sided two-sample t-tests. *: $P$ =0.0018.

**mMABs differentiate in epithelial cells once engrafted in the lung**

Since the results shown clearly demonstrate that mMABs engraft lung and intestinal epithelia overtime, we investigated their ability to differentiate in epithelial cells and, alternately, their contribution to the stem cell niches, an issue never investigated so far. We hypothesized that the epithelial environment could drive mMABs towards an epithelial fate, since they showed a good tropism to epithelial tissues. We faced this aim by different *in/ex vivo* and *in vitro* approaches. Firstly, we re-isolated GFP-mMABs from 5 months injected *F508del CFTR* lungs (n = 5) by FACS. We obtained a 97% of mMABs purity after re-isolation, data also confirmed by both immunofluorescence (Fig. 5A) and qRT-PCR for GFP (Fig. 5B). Interestingly, re-isolated GFP-mMABs express higher levels of mRNA of the epithelial marker E-cadherin and of SCGB1a1, if compared to not transplanted mMABs (Fig. 5C, D). In particular, *SCGB1a1* encodes for a well

known and studied secretoglobin firstly called Clara cell secretory protein (CCSP/CC10), expressed by noncilated bronchiolar club (Clara) cells lining the distal bronchiolar epithelium (BRANDT et al. 1985; LUND et al. 1985; Singh et al. 1985; Singh & Katyal 1997) that in the adult murine lung constitute the majority of the bronchiolar epithelium (around 64% of the volume) and have a role of progenitors/stem cells (Plopper 1983; Karnati & Baumgart-Vogt 2008; Karnati et al. 2016). Moreover, we confirmed by immunofluorescence that mMABs are not only engrafted in the CC10-positive terminal bronchiolar epithelium of transplanted *F508del CFTR* mice after 6 months of engraftment, but that they simultaneously express this marker (Supplementary Fig. 3A). We further demonstrated, by immunofluorescence, that donor engrafted mMABs after 6 months also express the epithelial markers Cytokeratin 6 and Cytokeratin 5, but it seems they do not differentiate in SPC+ alveolar epithelial type II cells or Acetylated α-Tubulin+ ciliated cells (Supplementary Fig. 3B, C, D, E).

Injected mMABs, once reached the colonization site, also express E-cadherin. The analysis of transplanted epithelia, performed by confocal microscopy, showed in the orthogonal projection that engrafted GFP-mMABs at 2 months already express E-cadherin, once localized in the lung and in the trachea of injected *F508del CFTR* mice, suggesting their plasticity to differentiate in epithelial-like cells once engrafted in the airways (Fig. 5E, red arrows)

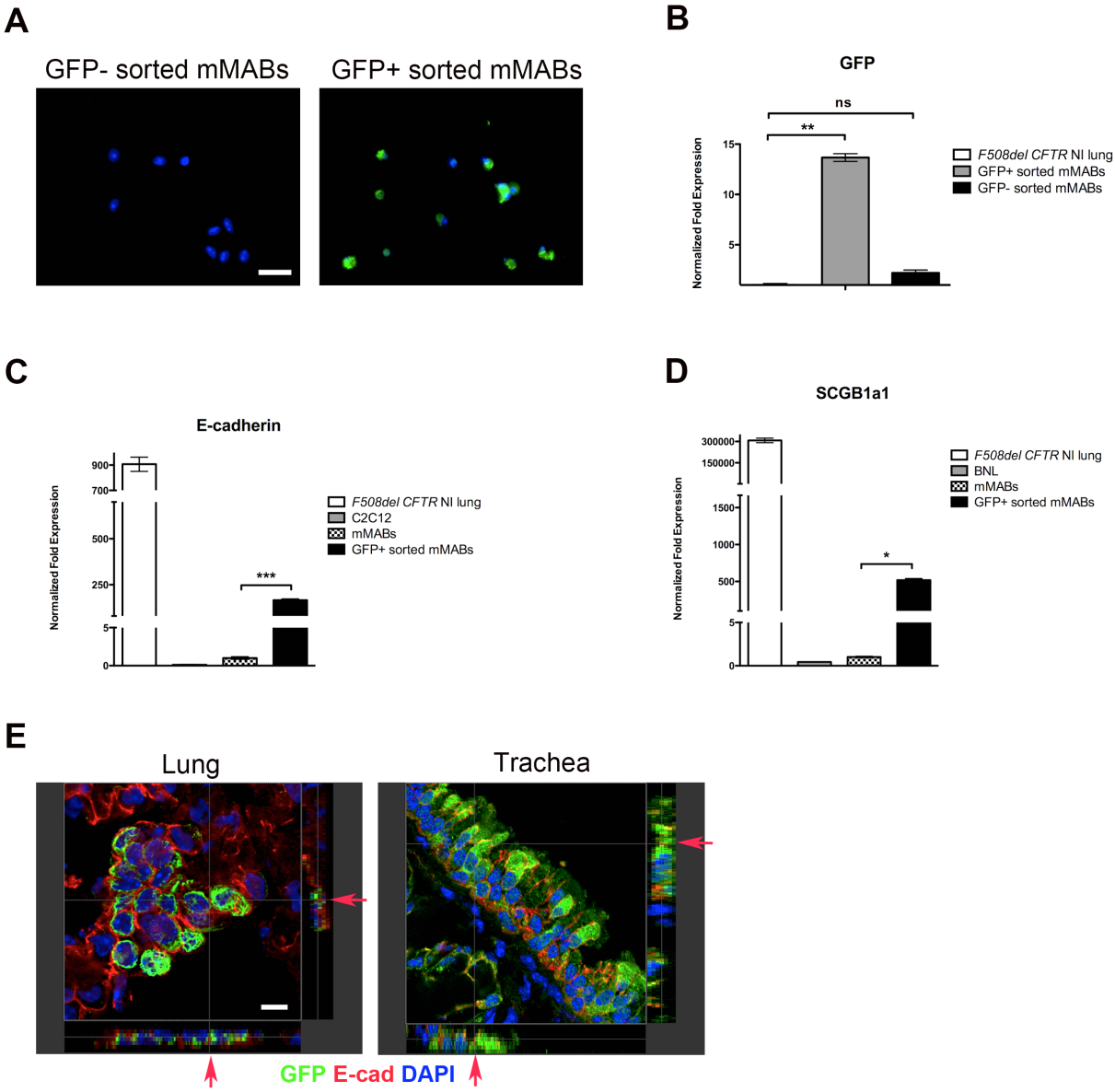


**Figure 5: mMAB plasticity towards epithelial differentiation, once engrafted in the airways.**

(**A**) Immunofluorescence staining for GFP showing re-isolated GFP negative (GFP- sorted mMABs) and positive (GFP+ sorted mMABs) mMABs from injected *F508del CFTR* lungs (GFP, green; nuclei, dapi). Scale bar 25 µm. (**B**) GFP transcript levels evaluated by qRT-PCR in GFP + and – sorted mMABs. *F508del CFTR* NI lungs were used as negative control. Each assay was performed in triplicate. Values are plotted as relative fold expression and normalized to GAPDH expression. All data are represented as means +/- S.D., **P < 0.005, ns= not significant, unpaired t Test. E-cadherin (**C**) and SCGB1a1 (**D**) levels evaluated in re-isolated GFP + sorted mMABs. Proliferating mMABs, C2C12 murine myoblasts and BNL murine liver epithelial cells were used as negative controls, respectively for E-cadherin and SCGB1a1. Values are plotted as relative fold expression

and normalized to GAPDH expression. Each assay was performed in triplicate. All data are represented as means +/- S.D., ***P < 0.0005, *P < 0.05, unpaired t Test. (**E**) Orthogonal projection analysis of immunofluorescences showing lung and trachea of GFP-mMAB-transplanted *F508del CFTR* mice (GFP, green; E-cadherin, red; nuclei, dapi). The representative images show GFP-positive donor cells expressing E-cadherin, as indicated on the axis where the signals are projected (red arrows). Scale bar 10 µm.

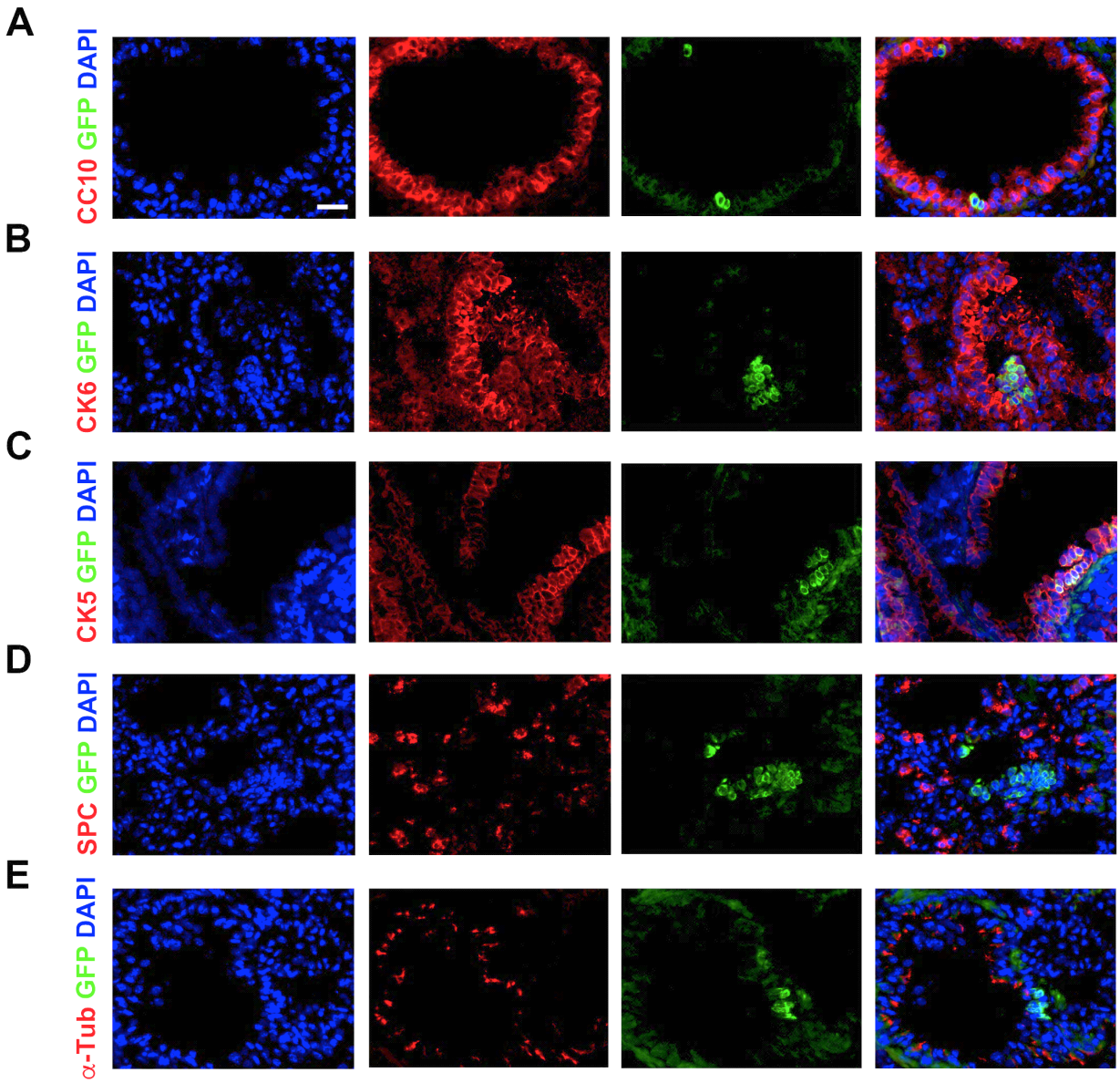


**Supplementary figure 3: Lung-engrafted mMABs express some typical epithelial markers.** Immunofluorescence staining for CC10 (**A**), CK6 (**B**), CK5 (**C**), SPC (**D**) and Acetylated α-Tubulin (α-Tub) (**E**) on serial transverse sections of lung lobes of transplanted *F508del CFTR* mice (GFP, green; lung epithelial markers, red; nuclei, dapi). These results have been reproduced

by three independent experiments; mice were sacrificed 6 months after mMAB transplantation. Scale bar 25 μm.

**mMABs, under specific stimuli, express different epithelial markers *in vitro***

To induce mMAB differentiation in epithelial cells we tested different conditions *in vitro* trying to mimic, as much as possible, the physiological, complex environment present *in vivo*. First we cultured mMABs with Human Bronchial/Tracheal Epithelial Cells (HBTEC) differentiation medium, optimized for the mucociliar differentiation of tracheal and bronchial epithelial cells, until reaching cell confluence and then we evaluated the expression of E-cadherin. As shown in Fig. 6B, the mRNA levels of E-cadherin increase in mMABs cultured with HBTEC medium in time, compared to mMABs cultured with the standard medium. This result was then confirmed at protein level by Immunofluorescence staining. In detail, we observed how some mMABs, after 15 days in culture with HBTEC medium, start to express E-cadherin, although not completely correctly localized (Fig. 6A). In the second approach, we cultured mMABs with Small Airway Grow Medium (SAGM) until the confluence was reached. The SAGM medium is a specific cell medium used for culturing alveolar cells (Ali et al. 2002). In this culture condition, mMABs express high levels of E-cadherin, properly localized in correspondence of the adherens junctions (Fig. 6C). We also analyzed by qRT-PCR the transcript levels of some epithelial and mesenchymal markers. As shown in Fig. 6D we found a statistical significant increase of the epithelial marker E-cadherin and that of the metalloproteinase Adam10, involved in E-cadherin's physiological turnover. In parallel, we evaluated whether the increase of the expression of epithelial markers is accompanied by the decrease of specific mesenchymal markers such as Fibronectin and Vimentin. qRT-PCR revealed a statistical significant decrease of mesenchymal markers in mMABs cultured in SAGM medium respect to the control mMABs cultured with the conventional medium. Moreover, to investigate whether the use of a specific medium for the culture of epithelial cells was sufficient to drive mMABs towards a Mesenchymal to Epithelial Transition (MET), we also examined the mRNA levels of the Epithelial to Mesenchymal Transition (EMT) transcription factors, together with other well-known markers involved in this process. As shown in Fig. 6D the transcript levels of Snail and N-cadherin are statistically significant decreased, compared to mMABs cultured in standard conditions. Finally, to confirm the loss of intrinsic muscular differentiation features of mMABs, we analyzed the expression of myogenic markers such as MyoD and Myogenin, responsible with the other Myogenic Regulatory Factors, of the differentiation of myogenic progenitors (Black & Olson 1998). Interestingly, mMABs cultured in SAGM medium display statistically significant lower mRNA levels of MyoD and Myogenin compared to mMABs cultured with conventional medium.

As last *in vitro* approach, we cultured mMABs in air liquid interface (ALI) condition, which is considered the best way to mimic in culture the physiological *in vivo* respiratory environment (Jong et al. 1993; Grubb et al. 2006). To do that we co-cultured in ALI condition mMABs together with primary nasal epithelial cells extracted from *CFTR ko* mice and we analyzed E-cadherin expression by confocal microscope with a further orthogonal projection analysis. As shown in Fig. 6E, we observed that GFP-mMABs express properly localized E-cadherin in the cell surface membrane (red arrow). Taken together, all the *in vitro* data obtained confirm that mMAB have a sufficient plasticity to change their intrinsic differentiation fate towards an epithelial differentiation.

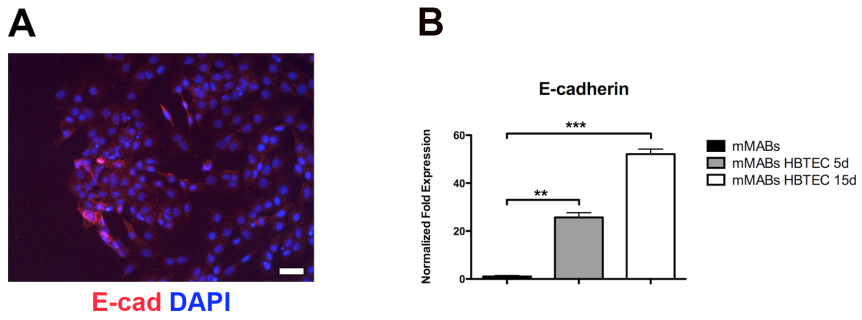
A
B
E-cadherin
Normalized Fold Expression
mMABs
mMABs HBTEC 5d
mMABs HBTEC 15d
E-cad DAPI

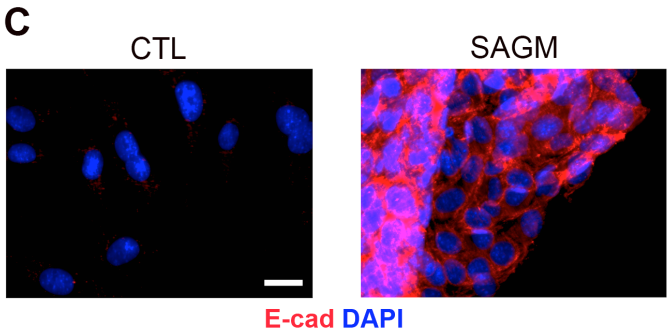
C
CTL
SAGM
E-cad DAPI

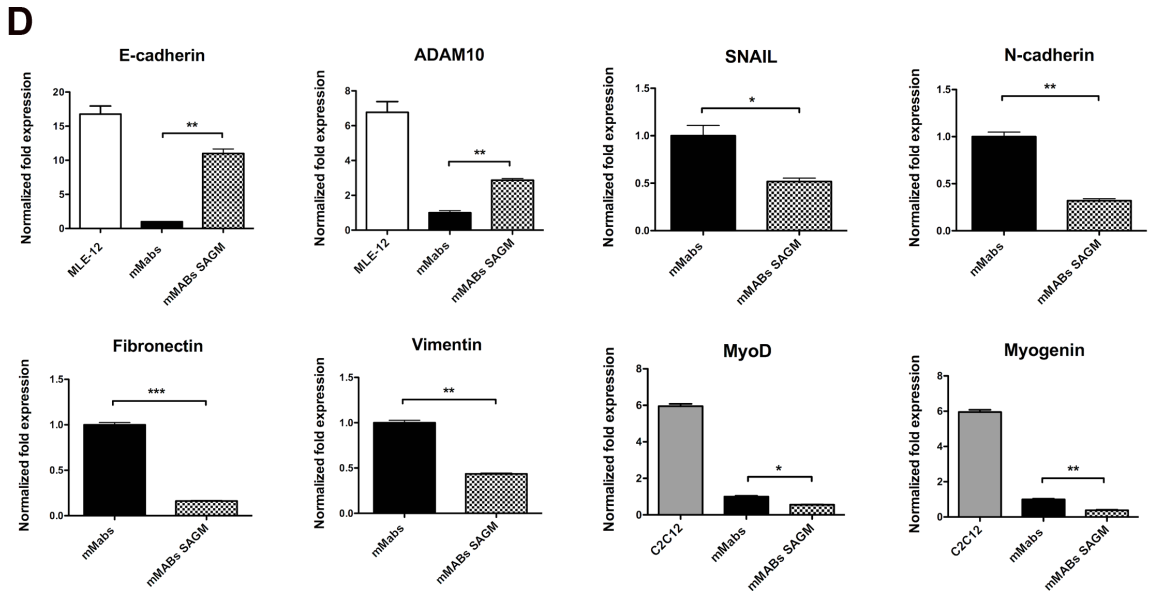
D
E-cadherin
ADAM10
SNAIL
N-cadherin
Fibronectin
Vimentin
MyoD
Myogenin
Normalized fold expression
MLE-12
mMabs
mMABs SAGM
C2C12

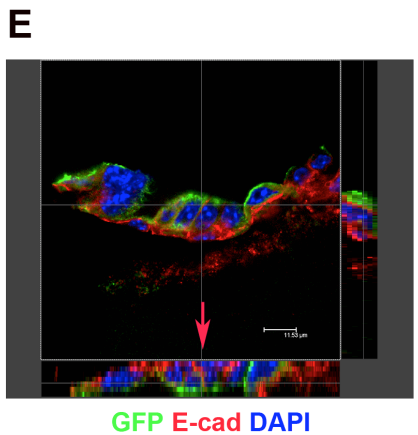
E
GFP E-cad DAPI

**Figure 6: mMABs differentiate in epithelial-like cells *in vitro*.** (**A**) Representative Immunofluorescence showing mMABs, cultured in HBTEC medium, that start to express E-cadherin (red). Scale bar 25 μm. (**B**) E-cadherin transcript levels evaluated by qRT-PCR in mMABs cultured in conventional medium (mMABs) and in HBTEC medium for 5 (mMABs HBTEC 5d) and 15 days (mMABs HBTEC 15d). Values are plotted as relative fold expression and normalized to GAPDH expression. Each assay was performed in triplicate. All data are represented as means +/- S.D., ***P < 0.0005, **P < 0.005, unpaired t Test. (**C**) Representative Immunofluorescence staining for E-cadherin (red) showing mMABs cultured in conventional medium (CTL) that do not express E-cadherin, compared to mMABs cultured in SAGM medium (SAGM) that express good levels of the protein which is also correctly localized. (**D**) E-cadherin, Adam10, Snail, N-cadherin, Fibronectin, Vimentin, MyoD and Myogenin transcript levels evaluated by qRT-PCR in mMABs cultured in conventional medium (mMABs) and in SAGM medium (mMABs SAGM). Murine Lung Epithelial cells (MLE-12) were used as positive control for the epithelial markers, whereas Murine Myoblasts C2C12 were used as positive controls for the myogenic ones. Values are plotted as relative fold expression and normalized to GAPDH expression. Each assay was performed in triplicate. All data are represented as means +/- S.D., ***P < 0.0005, **P < 0.005, *P < 0.05, unpaired t Test. (**E**) Orthogonal projection analysis of immunofluorescences showing GFP-mMABs co-cultured in ALI condition with primary nasal epithelial cells deriving from *CFTR ko* mice (GFP, green; E-cadherin, red; nuclei, dapi). The representative images show GFP-positive cells expressing E-cadherin, as indicated on the axis where the signals are projected (red arrow). Scale bar 11.53 μm.

**Discussion**

Mesoangioblasts are vessel-associated progenitor cells that can be induced to differentiate into different mesodermal derivatives (Cossu & Bianco 2003; Minasi et al. 2002). In the last decade, MABs have been isolated from different species and at different developmental phases (from embryonic to adult, including even iPS cells) (Minasi et al. 2002; Diaz-Manera et al. 2010; Sampaolesi et al. 2006; Dellavalle et al. 2007; Tedesco et al. 2012). Wide studies have demonstrated that, following systemic delivery, MABs can differentiate into skeletal muscle and cross the vessel wall to target the damaged muscles (Sampaolesi et al. 2003; Diaz-Manera et al. 2010; Sampaolesi et al. 2006; Dellavalle et al. 2007). Thanks to these exceptional features, hMABs have been indeed used in a trial in DMD human patients that definitely demonstrated that intra-arterial transplantation of donor MABs in humans is feasible and safe (Cossu et al. 2015).

During our studies on MABs, we observed that mMAB, when systemically transplanted in healthy

wild type mice, engraft lung, tracheal and intestinal epithelium up to one month from their transplantation. This unexpected substantial engraftment represented the starting point to consider these cells as a potential tool for a cell-based therapy for Cystic Fibrosis, which indeed mainly affects the airway and intestinal tracts. Between the different tested approaches to cure CF, cell therapy still did not give good results; the reasons rely in the low engraftment of donor cells, in the small percentage of cells differentiated in airway epithelia and in the even less percentage of CFTR expression (Murphy and Atala 2013; Weiss 2014; Sueblinvong & Weiss 2010). We report here that mMABs engraft the respiratory and intestinal tracts in wild type mice up to two months from their single transplantation. The substantial engraftment does not affect the structure, morphology or functionality of the target organs, while on the contrary corroborates mMAB tropism towards the epithelia, even in absence of an inflammatory or damaged status, as in this case in healthy wild type mice. Furthermore, the consolidated demonstration that MABs are not tumorigenic is of fundamental importance for a therapeutic use of these cells.

Moreover, we observed the presence of CFTR mRNA and that the over-expression of the *wt CFTR* form shows high CFTR activity during *in vitro* studies, thus demonstrating that mMABs have the proper cellular mechanisms necessary to express a correctly localized and functional CFTR channel. Actually, the prove that mMABs can express a functional endogenous CFTR channel was obtained *in vivo*, by transplanting them in the *CFTR ko* mouse model (*KOCftr*$^{tm1UNC}$ mice*;* Snouwaert et al. 1992; Clarke et al. 1992; Grubb et al., 2002; Fischer et al., 2002). We indeed observed that, once engrafted in the nasal and intestinal epithelia of *CFTR ko* mice, mMABs lead to a significant rescue of CFTR-dependent chloride secretions, as measured in electrophysiological assays. This evidence is striking, since it has been evaluated that the level of normal CFTR message necessary to provide normal airway/lung function is estimated to be around 8% (Chu et al. 1992; Johnson et al. 1992; Dorin 1996).

Notably, mMABs engraft the airway epithelium in *CFTR ko* mice up to four months and in the CF mouse model *F508del CFTR* up to six months from their single transplantation. This data is extremely important, since the stem cells tested so far did not show comparable results in terms of time lasting and extent of engraftment (Murphy and Atala 2013; Weiss 2014). Moreover, the demonstration that other populations of mMABs share the same features prove that mMAB epithelial engraftment is an intrinsic and specific property of mMABs, regardless of a particular mMAB cell preparation.

These evidences led us to speculate about the possibility, never investigated so far, that MABs might participate to the engrafted epithelium and/or to its stem cell niche. This could explain MAB

plasticity that would make them an eligible tool for two completely different pathologies such as the Muscular Dystrophies and CF.

Our present results indicate that donor-derived mMABs express the typical epithelial marker E-cadherin and, surprisingly, the univocal marker of club cells CC10. This evidence is particularly interesting, together with the observation that donor-derived mMABs do not express markers of highly specialized and differentiated respiratory epithelial cells, such as alveolar epithelial type II cells or ciliated cells and that their proliferation once engrafted is quite rare (adult lung cells are indeed almost quiescent). We indeed hypothesized that mMABs, once reached the lung, contribute to its homeostasis and stem cell niche, trans-differentiating in epithelial progenitors. In this context, this aspect represents an incredible advantage in a cell therapy approach, since these cells would not only reconstitute CFTR activity, but also contribute to the epithelial homeostasis. More experiments, such as MAB serial transplantation in CF or in lung-injured mice, will be necessary to fully address this point.

Finally, we also investigated on the possible mechanisms through which mMABs could be committed towards an epithelial differentiation *in vitro*. Culturing mMABs with Small Airway Grow Medium (SAGM), specific for alveolar cells (Ali et al. 2002), provokes an increase of the expression of epithelial markers (E-cadherin and its metalloproteinase Adam10) together with a decrease of mesenchymal (Fibronectin and Vimentin) and myogenic ones (MyoD and Myogenin). We therefore hypothesized that the differentiation of mMABs into epithelial cells could be driven by the reverse of the Epithelial to Mesenchymal Transition, the Mesenchymal to Epithelial Transition process. Although many signaling pathways for EMT have been identified, the signals involved in the activation of MET have not been well characterized so far (Craene & Berx 2012); nevertheless it has been demonstrated that MET is strictly associated to the loss of migratory capacity and acquisition of adhesive properties (Li et al. 2011). All these evidences correlate with our present results, together with the decrease of the expression of the EMT-transcription factor Snail and the marker N-cadherin in mMABs cultured in SAGM. Our data let suppose that mMABs, if properly conditioned, could undergo a MET, thus changing their original fate.

In conclusion, this body of evidence represents a major advance over any other cell-based therapeutic strategy for CF. MAB homing towards the epithelium of the main compromised organs in CF, their persistence over time and their capability to rescue CFTR function make these cells eligible for a cell based therapy of CF. This experimental strategy will lead to future clinical translation: the results obtained from this work will indeed represent the first step towards a pre-clinical study in more severe models such as the CF pigs (Rogers et al. 2008) and have the potential

to direct future research into therapeutic concrete goals. Notably, this study may also generate a conceptual insight highly relevant in the cell-based therapy field, not only limited to CF.

| Gene | Forward Primer | Reverse Primer | Ta |
|---|---|---|---|
| ADAM10 | GTGCCGGGATGATTCTGACTG | CACAGGTGCACTCCTCCAAGT | 64.3°C |
| CFTR | CAG TGG AAG AGT TTC ATT CTG | GCA AAC TTG GTG ATG TCCTG | 62.3°C |
| E-cadherin | CAGCCTTCTTTTCGGAAG | GGTAGACAGCTCCCTATGACG | 63 °C |
| N-cadherin | GGCTTGGCGCTCTTTATCC | ACAGGATCGTGGGTGCAG | 62.6°C |
| Fibronectin | AGTCGGTAGCCTGCTATACGG | CTGGGGTCACGTACCTCTTC | 62.6°C |
| GFP | GTGGCACTTTTCGGGGAAAT | CCGGCGTCAATACGGGATAA | 60 °C |
| Myogenin | GACATCCCCCTATTTCTACCA | GTCCCCAGTCCCTTTTCTTC | 60 °C |
| MyoD | ACGGCTCTCTCTTGCTCCTTT | GTAGGGAAGTGTGCGTGCT | 58 °C |
| SCGB1a1 | CAGGATGCCACATAACCAG | TCACTGTGGTCATGCTGTCC | 59 °C |
| TNF-α | CCACCACGCTCTTCTGTCTA | AGGGTCTGGGCCATAGAACT | 56 °C |
| SNAIL | CCACTGCAACCGTGCTTTT | CACATCCGAGTGGGTTTGG | 57 °C |
| TPJ1 | GGTCTTCTCGAGTTGGTGGTC | CTGTCCAGCTCTTCTCTCCAC | 64.3°C |
| Vimentin | AGTACCGGAGACAGGTGCAGT | GGTGACGAGCCATCTCTTCCT | 62.6°C |
| GAPDH | TGTAGACCATGTAGTTGAGGTCA | GGTGACGAGCCATCTCTTCCT | 62.6°C |

**Supplementary Table S1: Primers used for mRNA expression analysis with quantitative Real Time PCR (*Mus musculus*).**

## Bibliography


Ali, N.N. et al., 2002. Derivation of type II alveolar epithelial cells from murine embryonic stem cells. *Tissue Eng*, 8(4), pp.541–550.

Amaral, M.D., 2011. Targeting CFTR: how to treat cystic fibrosis by CFTR-repairing therapies. *Current drug targets*, 12(5), pp.683–693.

Belcher, C.N. & Vij, N., 2010. Protein Processing and Inflammatory Signaling in Cystic Fibrosis: Challenges and Therapeutic Strategies. , 10(1), pp.82–94.

Bell, P. et al., 2005. An optimized protocol for detection of E. coli b-galactosidase in lung tissue following gene transfer. *Histochemistry and Cell Biology*, 124(1), pp.77–85.

Black, B.L. & Olson, E.N., 1998. Transcriptional Control of Muscle Development By Myocyte Enhancer Factor-2 (Mef2) Proteins. *Annu. Rev. Cell Dev. Biol*, 14, pp.167–96.

Bonfanti, C. et al., 2015. PW1/Peg3 expression regulates key properties that determine mesoangioblast stem cell competence. *Nature communications*, 6(May 2014), p.6364.

Boyle, M.P. et al., 2014. A CFTR corrector (lumacaftor) and a CFTR potentiator (ivacaftor) for treatment of patients with cystic fibrosis who have a phe508del CFTR mutation: A phase 2 randomised controlled trial. *The Lancet Respiratory Medicine*, 2(7), pp.527–538.

BRANDT, I. et al., 1985. TARGET CELLS FOR THE POLYCHLORINATED BIS(METHYLSULFONYL)-2,2',5,5'-TETRACHLOROBIPHENYL IN LUNG AND KIDNEY. , pp.490–496.

Bruscia, E.M. et al., 2006. Assessment of cystic fibrosis transmembrane conductance regulator (CFTR) activity in CFTR-null mice after bone marrow transplantation. *Proc.Natl.Acad.Sci.U.S.A.*, 103(8), pp.2965–2970.

Chu, C.S. et al., 1992. Extensive posttranscriptional deletion of the coding sequences for part of nucleotide-binding fold 1 in respiratory epithelial mRNA transcripts of the cystic fibrosis transmembrane conductance regulator gene is not associated with the clinical manifestati. *The Journal of clinical investigation*, 90(3), pp.785–90.

Clarke, L.L. et al., 1992. Defective Epithelial Chloride Transport in a Gene-Targeted Mouse Model of Cystic Fibrosis. *Science*, 257(5073), pp.1125–1128.

Cossu, G. et al., 2015. Intra-arterial transplantation of HLA-matched donor mesoangioblasts in Duchenne muscular dystrophy. *EMBO molecular medicine*, 7(12), pp.1513–28.

Cossu, G. & Bianco, P., 2003. Mesoangioblasts - Vascular progenitors for extravascular mesodermal tissues. *Current Opinion in Genetics and Development*, 13(5), pp.537–542.

Craene, B. & Berx, G., 2012. Regulatory networks defining EMT during cancer initiation and progression. *Nature reviews. Cancer*, 13(2), pp.97–110.

Davis, P.B., 2006. Cystic fibrosis since 1938. *American Journal of Respiratory and Critical Care Medicine*, 173(5), pp.475–482.

Dellavalle, A., 2007. Pericytes of human skeletal muscle are myogenic precursors distinct from satellite cells. , 9(3), pp.1–20.

Díaz-Manera, J. et al., 2010. Partial dysferlin reconstitution by adult murine mesoangioblasts is sufficient for full functional recovery in a murine model of dysferlinopathy. *Cell death & disease*, 1, p.e61.

Domi, T. et al., 2015. Mesoangioblast delivery of miniagrin ameliorates murine model of merosin-deficient congenital muscular dystrophy type 1A. *Skeletal muscle*, 5, p.30.

Dorin, J.R. et al., 1996. A demonstration using mouse models that successful gene therapy for cystic fibrosis requires only partial gene correction. *Gene Ther*, 3(9), pp. 797-801.

van Doorninck, J.H. et al., 1995. A mouse model for the cystic fibrosis delta F508 mutation. *The EMBO journal*, 14(18), pp.4403–4411.

Eckman, E. a et al., 1995. Dietary changes improve survival of CFTR S489X homozygous mutant mouse. *The American journal of physiology*, 269(5 Pt 1), pp.L625–30.

Fischer H., 2002. Electrophysiological approach to studying CFTR. *Methods Mol Med*., 70, pp. 49-65.

Van Goor, F. et al., 2011. Correction of the F508del-CFTR protein processing defect in vitro by the investigational drug VX-809. *Proceedings of the National Academy of Sciences of the United States of America*, 108(46), pp.18843–8.

Grubb, B.R., 2002. Bioelectric measurement of CFTR function in mice. *Methods Mol Med*., 70, pp. 525-535.

Grubb, B.R. et al., 2006. Culture of murine nasal epithelia: model for cystic fibrosis. *American journal of physiology. Lung cellular and molecular physiology*, 290(2), pp.L270–L277.

Grubb, B.R. & Boucher, R.C., 1999. Pathophysiology of gene-targeted mouse models for cystic fibrosis. *Physiological reviews*, 79(1), pp.S193–S214.

Johnson, L.G. et al., 1992. Efficiency of gene transfer for restoration of normal airway epithelial function in cystic fibrosis. *Nature genetics*, 2(1), pp.21–25.

Jong, P.M. De et al., 1993. Ciliogenesis in Human Bronchial Epithelial Cells Cultured at the Air-Liquid Interface.

Karnati, S. et al., 2016. Postnatal development of the bronchiolar club cells of distal airways in the mouse lung: stereological and molecular biological studies. *Cell and Tissue Research*.

Karnati, S. & Baumgart-Vogt, E., 2008. Peroxisomes in mouse and human lung: Their involvement in pulmonary lipid metabolism. *Histochemistry and Cell Biology*, 130(4), pp.719–740.

Kotton, D.N., Fabian, A.J. & Mulligan, R.C., 2005. Rapid Communication. *Cellular & Molecular Biology (Oxford)*.

Lama, V.N. et al., 2007. Evidence for tissue-resident mesenchymal stem cells in human adult lung from studies of transplanted allografts. *Journal of Clinical Investigation*, 117(4), pp.989–996.

Legssyer, R. et al., 2006. Azithromycin reduces spontaneous and induced inflammation in DeltaF508 cystic fibrosis mice. *Respiratory research*, 7, p.134.

Li, B. et al., 2011. Evidence for mesenchymal-epithelial transition associated with mouse hepatic stem cell differentiation. *PLoS ONE*, 6(2).

Luciani, A. et al., 2010. Defective CFTR induces aggresome formation and lung inflammation in cystic fibrosis through ROS-mediated autophagy inhibition. *Nat Cell Biol*, 12(9), pp.863–875.

Luciani, A. et al., 2012. Targeting autophagy as a novel strategy for facilitating the therapeutic action of potentiators on Delta F508 cystic fibrosis transmembrane conductance regulator. *Autophagy*, 8(11), pp.1657–1672.

Lukacs, G. & Verkman, A.S., 2012. CFTR: folding, misfolding and correcting the ΔF508 conformational defect. *Trends Mol Med*, 18(2), pp.81–91.

LUND, J. et al., 1985. Target Cells for the Polychlorinated Biphenyl Metabolite Bis ( methylsulfonyl ) -2 Characterization of High Affinity Binding Rat and Mouse Lung Cytosol. *MOLECULAR PHARMACOLOGY*, pp.314–323.

Messina, G. & Cossu, G., 2009. The origin of embryonic and fetal myoblasts: a role of Pax3 and Pax7. *Genes and Development*, 23(8), pp.902–905.

Minasi, M.G. et al., 2002. The meso-angioblast: a multipotent, self-renewing cell that originates from the dorsal aorta and differentiates into most mesodermal tissues. *Development (Cambridge, England)*, 129(11), pp.2773–2783.

Moyer, B.D. et al., 1998. Membrane trafficking of the cystic fibrosis gene product, cystic fibrosis transmembrane conductance regulator, tagged with green fluorescent protein in madin-darby canine kidney cells. *J.Biol.Chem.*, 273(34), pp.21759–21768.

Murphy, S. V. & Atala, A. 2013. Cell therapy for cystic fibrosis. *Journal of Tissue Engineering and Regenerative Medicine,* pp.1-14.

O'Sullivan, B.P. & Freedman, S.D., 2009. Cystic fibrosis. *The Lancet*, 373(9678), pp.1891–1904.

Pedemonte, N. et al., 2005. Small Molecule. *Journal Of clinical investigation*, 115(9).

Plopper, G.C., 1983. Comparative morphologic features of bronchiolar epithelial cells. The Clara cell. *Am. Rev. Respir. Dis.*, 128(August), pp.S37–S41.

Ratjen, F. & Grasemann, H., 2012. New therapies in cystic fibrosis.

Ratjen, F.A., 2009. Cystic fibrosis: pathogenesis and future treatment strategies. *Respiratory Care*, 54(5), pp.595–605.

Riordan, J. et al., 1989. Identification of the cystic fibrosis gene: cloning and characterization of complementary DNA. *Science (New York, N.Y.)*, 245(4922), pp.1066–1073.

Rogers, C.S. et al., 2008. Disruption of the CFTR gene produces a model of cystic fibrosis in newborn pigs. *Science*, 321(5897), pp.1837–41.

Rosen, C. et al., 2015. Preconditioning allows engraftment of mouse and human embryonic lung cells, enabling lung repair in mice. *Nature medicine*, 21(8), pp.869–79.

Sampaolesi, M. et al., 2003. Cell therapy of alpha-sarcoglycan null dystrophic mice through intra-arterial delivery of mesoangioblasts. *Science*, 301(5632), pp.487–492.

Sampaolesi, M. et al., 2006. Mesoangioblast stem cells ameliorate muscle function in dystrophic dogs. *Nature*, 444(7119), pp.574–579.

Sean V. Murphy and Anthony Atala, 2013. Cell therapy for cystic fibrosis Sean. *Journal of tissue*

*engineering and regenerative medicine*.
Singh, G. et al., 1985. Secretory Proteins of the Lung in Rodents. , pp.564–568.
Singh, G. & Katyal, S.L., 1997. Clara Cells and Clara Cell 10 kD Protein (CC10). *American Journal of Respiratory Cell and Molecular Biology*.
Snouwaert, J.N. et al., 1992. An animal model for cystic fibrosis made by gene targeting. , 257(5073), pp.1083–1088.
De Stefano, D. et al., 2014. Restoration of CFTR function in patients with cystic fibrosis carrying the F508del-CFTR mutation. *Autophagy*, 10(11), pp.2053–2074.
Sueblinvong, V. & Weiss, D.J., 2010. Stem cells and cell therapy approaches in lung biology and diseases. *Translational research : the journal of laboratory and clinical medicine*, 156(3), pp.188–205.
Tedesco, F.S. et al., 2011. Stem cell-mediated transfer of a human artificial chromosome ameliorates muscular dystrophy. *Science translational medicine*, 3(96), p.96ra78.
Tedesco, F.S. et al., 2012. Transplantation of genetically corrected human iPSC-derived progenitors in mice with limb-girdle muscular dystrophy. *Science translational medicine*, 4(140), pp.140ra89–140ra89.
Tonlorenzi, R. et al., 2007. Isolation and characterization of mesoangioblasts from mouse, dog, and human tissues. *Current protocols in stem cell biology*, Chapter 2(December), p.Unit 2B.1.
Wang, X.Y. et al., 2012. Novel method for isolation of murine clara cell secretory protein-expressing cells with traces of stemness. *PLoS ONE*, 7(8), pp.1–10.
Waters, V. & Smyth, A., 2015. Cystic fibrosis microbiology: Advances in antimicrobial therapy. *Journal of Cystic Fibrosis*, 14(5), pp.551–560.
Welsh, M.J. et al., 2001. Cystic Fibrosis. In the metabolic and Molecular Bases of Inherited Disease. pp. 5121-88
Weiss, D.J., 2008. *In Situ* Histochemical Detection of *β*-Galactosidase Activity in Lung: Assessment of X-Gal Reagent in Distinguishing *lacZ* Gene Expression and Endogenous *β*-Galactosidase Activity. *Human Gene Therapy*. 8(13), pp. 1545-1554.
Weiss, D.J., 2014. Current Status of Stem Cells and Regenerative Medicine in Lung Biology and Diseases. *Journal of tissue engineering and regenerative medicine*, pp.16–25.
Weiss, D.J. et al., 2013. Stem cells and cell therapies in lung biology and diseases: Conference report. *Annals of the American Thoracic Society*, 10(5), pp.25–44.
Wilke, M. et al., 2011. Mouse models of cystic fibrosis: Phenotypic analysis and research applications. *Journal of Cystic Fibrosis*, 10(SUPPL. 2), pp.S152–S171.

# ADDITIONAL FIGURES

**Figures related to Main Results section (Part I) not included in the manuscript in preparation**

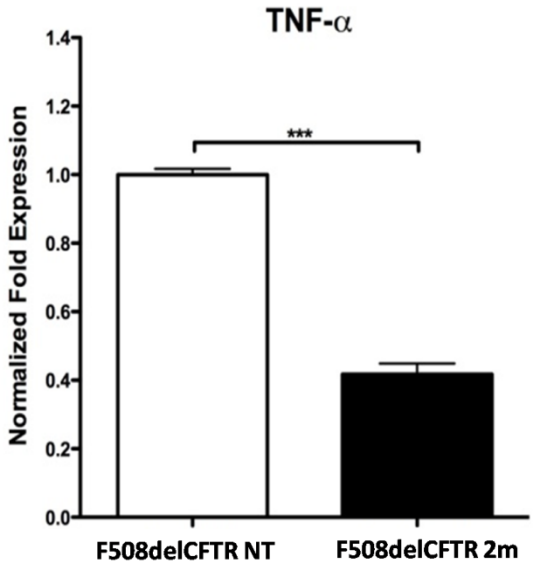


**Transplanted mMABs in *F508del CFTR* mice significantly decrease the inflammatory marker TNF-α.** TNF-α evaluated in lung tissues at 2 months (2M) after mMAB transplantation. TNF-α transcript levels were quantified by qRT-PCR. Values are plotted as relative fold expression and normalized to GAPDH expression. NT, not transplanted. Each assay was performed in triplicate. All data are represented as means +/- S.D., ***P < 0.0005, unpaired t Test.

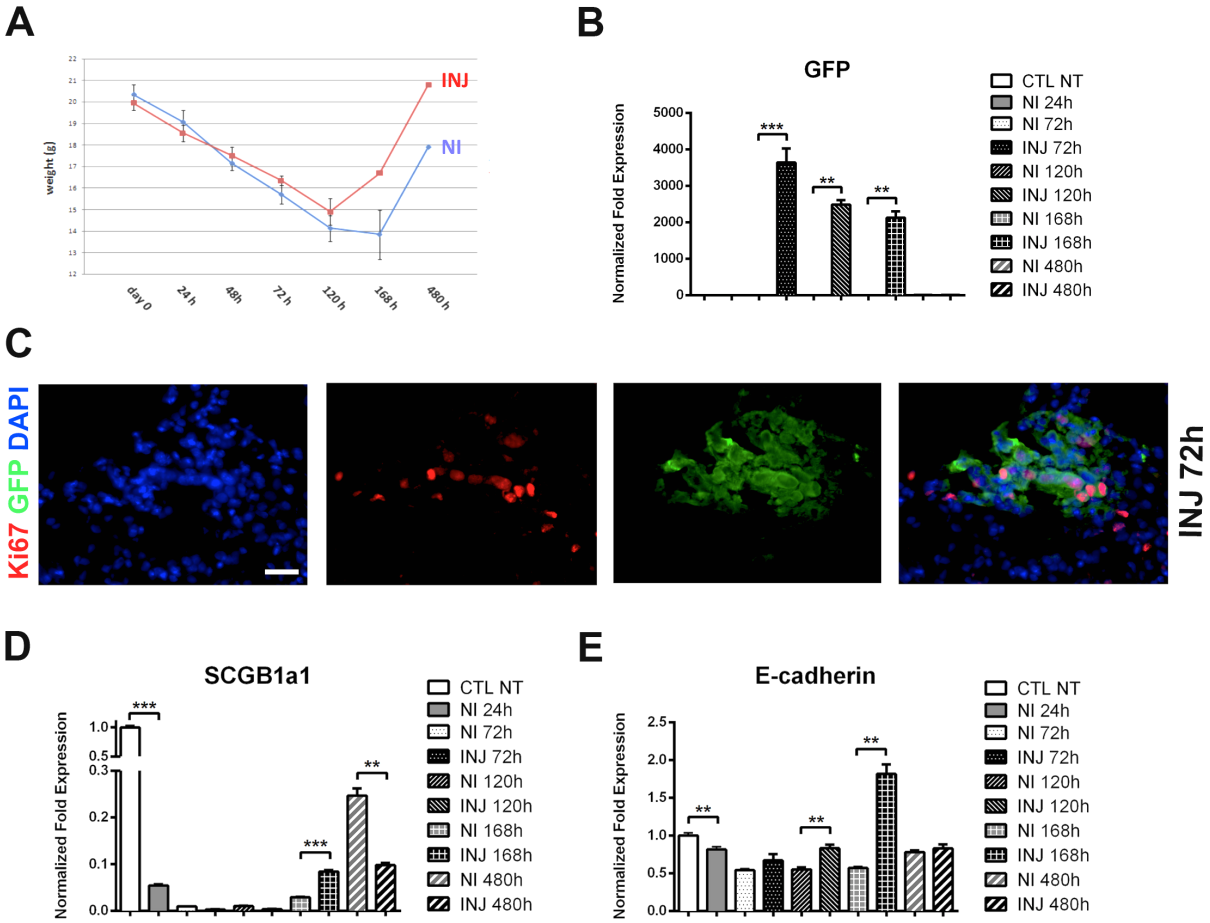


**mMABs contribute to lung homeostasis after acute lung injury.** (**A**) Graph showing the weight (g) during time of naphthalene-treated mice not injected (NI) and injected with GFP-mMABs (INJ). (**B**) GFP transcript levels evaluated by qRT-PCR in lungs of naphthalene-treated mice not injected (NI) and injected with GFP-mMABs (INJ) at the different time points analysed. Lungs of not treated mice were used as negative control (CTL NT). Each assay was performed in triplicate. Values are plotted as relative fold expression and normalized to GAPDH expression. All data are represented as means +/- S.D., ***P < 0.0005, **P < 0.005, unpaired t Test.

(**C**) Immunofluorescence staining for Ki67 and GFP on serial transverse sections of lung lobes of naphthalene-treated mice transplanted with GFP-mMABs after 72 hours (INJ 72h) (GFP, green; Ki67, red; nuclei, dapi). Scale bar 25 µm. SCGB1a1 (**D**) and E-cadherin (**E**) levels evaluated in lungs of naphthalene-treated mice not injected (NI) and injected with GFP-mMABs (INJ) at the different time points analysed. Lungs of not treated mice were used as negative control (CTL NT). Values are plotted as relative fold expression and normalized to GAPDH expression. Each assay was performed in triplicate. All data are represented as means +/- S.D., ***P < 0.0005, **P < 0.005, unpaired t Test.

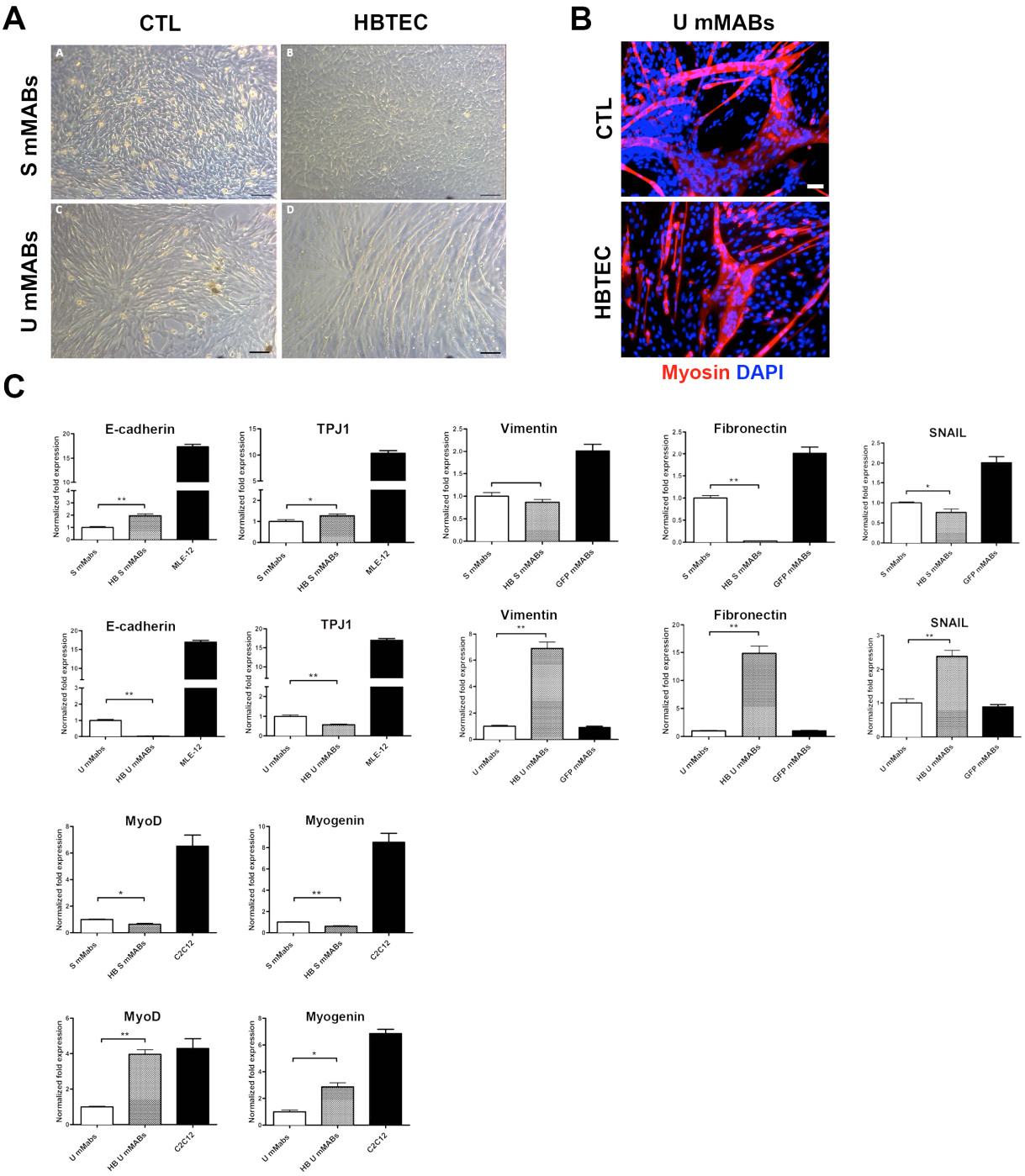


**Clones of mMABs display different potential of epithelial commitment.** (**A**) Phase-contrast morphology of mMABs S and U cultured in conventional (CTL) and HBTEC medium. Scale bar 100 µm. (**B**) Immunofluorescence staining for sarcomeric Myosin on mMABs U cultured in conventional (CTL) and HBTEC medium. (Myosin, red; nuclei, dapi). Scale bar 50 µm. (**C**) E-cadherin, TPJ1, Vimentin, Fibronectin, Snail, MyoD and Myogenin transcript levels evaluated by qRT-PCR in mMABs S and U cultured in conventional medium (S/U mMABs) and in HBTEC medium (HB S/U mMABs). Murine Lung Epithelial cells (MLE-12) were used as positive control

for the epithelial markers, whereas Murine Myoblasts C2C12 were used as positive controls for the myogenic ones. Values are plotted as relative fold expression and normalized to GAPDH expression. Each assay was performed in triplicate. All data are represented as means +/- S.D., **P < 0.005, *P < 0.05, unpaired t Test.